Caloric restriction and the nutrient-sensing protein kinase TOR1 alter the pattern of protein phosphorylation in quiescent and non-quiescent cells of *Saccharomyces cerevisiae*

Darya Mitrofanova

A Thesis
in
The Department
of
Biology

Presented in Partial Fulfillment of the Requirements
for the Degree of Master of Science (Biology) at
Concordia University
Montreal, Quebec, Canada

August 2019

CONCORDIA UNIVERSITY
School of Graduate Studies

This is to certify that the thesis prepared

By: **Darya Mitrofanova**

Entitled: **Caloric restriction and the nutrient-sensing protein kinase TOR1 alter the pattern of protein phosphorylation in quiescent and non-quiescent cells of *Saccharomyces cerevisiae***

and submitted in partial fulfillment of the requirements for the degree of

Master of Science (Biology)

complies with the regulations of the University and meets the accepted standards with respect to originality and quality.

Signed by the final Examining Committee:

_____Chair

Dr. Alisa Piekny

_____Examiner

Dr. Alisa Piekny

_____Examiner

Dr. Madoka Gray-Mitsumune

_____External Examiner

Dr. Donald Gray Stirling

_____Supervisor

Dr. Vladimir Titorenko

Approved by _____

Chair of Department or Graduate Program Director

Date: _____ _____

Dean of Faculty of Arts and Science

ABSTRACT

Caloric restriction and the nutrient-sensing protein kinase TOR1 alter the pattern of protein phosphorylation in quiescent and non-quiescent cells of *Saccharomyces cerevisiae*

Darya Mitrofanova, M.Sc.

The application of yeast as a model organism for studying eukaryotic pathways, notably mechanisms and processes of chronological aging, has been recognized for decades. In fact, several signalling pathways of longevity regulation are conserved across phyla; humans (and other mammals) have orthologs and homologs of yeast proteins integrated into these pathways. One of such pathways is the TOR pathway that responds to nutrient levels, notably via TORC1 (a complex with protein kinase activity; contains TOR1 as a core protein). My thesis taps into both of those advantageous properties of *Saccharomyces cerevisiae*: its ease of culturing for chronological aging studies, and well annotated proteome. I study the chronologically aging quiescent and non-quiescent cell populations under caloric restriction or not using wild-type or *tor1* single gene deletion mutant strains. I use quantitative phosphoproteomics – by means of mass spectrometry – to assess the differences and similarities between different cell populations. Caloric restriction has previously been shown to extend the chronological lifespan of yeast and other organisms. Reduced TOR1 activity (such as via inhibitors or by gene deletion) is also shown to extend yeast chronological lifespan in literature. Quiescence, an ability of a nutrient-limited post-mitotic cell to re-enter the cell cycle when the nutrient supply is restored, is also a lifespan-extending process. Combining these factors, I compared the phosphoproteomes of quiescent and non-quiescent yeast cells limited or not limited in calorie supply and having or lacking the TOR1 protein. I found that both the diet and the state of quiescence have significant effect on the phosphorylation of proteins. Moreover, I found that a single-gene-deletion mutation that eliminates the TOR1 protein has a significant impact on both the state of quiescence and the cell phosphoproteome.

Acknowledgements

I am deeply grateful to my supervisor, Dr. Vladimir Titorenko, for his guidance and generous learning opportunities. I am honoured that my committee members, Dr. Madoka Gray-Mitsumune and Dr. Alisa Piekny, provide their expertise in the evaluation of my thesis. I thank my external examiner, Dr. Donald Gray Stirling for his insights.

I would like to thank my mentor in phosphoproteomics, Dr. Anthony Arlia-Ciommo, who patiently guided my learning process.

I am grateful to the members of the Center for Biological Applications of Mass Spectrometry (CBAMS) – specifically: Dr. Heng Jiang for his utmost valuable teachings, training, and advice on producing quality mass spectrometry data.

I am grateful to all the graduate students, past and present, for their help and discussions. Particularly, thank you, Jennifer Anne Baratang Junio, for your continued support and positivity.

I thank the undergraduate students who directly and/or indirectly contributed to the advancement of my project; namely: Fadi Touma, Nazifa Ali, Amneet Sanhu, Olivia Drummond, and Vlada Lesnic (Vanier College).

I also thank the students in Dr. Brett lab for the occasional sharing of equipment; it is much appreciated.

I am grateful for the funding provided through and by Concordia University, including the Hydro-Québec Master Admission Scholarship, grants by Natural Sciences and Engineering Research Council of Canada (NSERC), as well as teaching assistant opportunities within the Biology Department.

TABLE OF CONTENTS

LIST OF ABBREVIATIONS

AMP, adenosine monophosphate; **AMPK**, AMP-activated protein kinase; **ATP**, adenosine triphosphate;
CFU, colony-forming unit(s); **CID**, collision-induced dissociation; **CLS**, chronological life span;**CR**, caloric restriction;
D, diauxic growth phase; **DDA**, data-dependent acquisition; **DIA**, data-independent acquisition; **DSK**, dual-specificity kinase;
HD, high density; **HPLC-MS**, high performance liquid chromatography coupled to mass spectrometry;
IMAC, immobilized metal affinity chromatography;
L, logarithmic growth phase; **LC-MS/MS**, liquid chromatography coupled to tandem mass spectrometry; **LD**, low density;
MOAC, metal oxide affinity chromatography; **MS**, mass spectrometry; **mTOR**, mechanistic/molecular/mammalian TOR;
non-CR, non-caloric restriction; **NQ**, non-quiescent;
PCD, programmed cell death; **PD**, post-diauxic growth phase; **Pho85**, phosphate metabolism, protein 85; **PKA**, protein kinase A; **PPP**, phosphoprotein phosphatase; **PPM**, metallo-dependent protein posphatase; **pSer**, phosphoserine; **P-site**, phosphosite; **pThr**, phosphothreonine; **PTM**, post-translational modification; **PTP**, protein-tyrosine phosphatase; **pTyr**, phosphotyrosine;
Q, quiescent;
RLS, replicative life span; **ROS**, reactive oxygen species; **RT**, room temperature;
Ser, serine; **Snf1**, sucrose non-fermenting, protein 1; **ST**, stationary growth phase; **STK**, serine/threonine kinase;
Thr, threonine; **TOR**, target of rapamycin; **TORC1 (2)**, target of rapamycin complex 1 (2); **Tyr**, tyrosine;
WT, wild-type strain;
YEPD, yeast extract (1%) with peptone (2%) with glucose (0.2% for CR and 2% for non-CR).

Organisms:
C. elegans*, Caenorhabditis elegans;* ***D. melanogaster****, Drosophila melanogaster;* ***S. cerevisiae****, Saccharomyces cerevisiae;* ***S. pombe****, Schizosaccharomyces pombe.*

Chemicals/Reagents:
ABC, ammonium bicarbonate; **ACN**, acetonitrile; **BSA**, bovine serum albumin; **DTT**, dithiothreitol; **EtOH**, ethanol; **FA**, formic acid; **IAA**, iodoacetamide; **TCA**, trichloroacetic acid; **TFA**, trifluoroacetic acid.

LIST OF FIGURES

LIST OF TABLES

CHAPTER I: INTRODUCTION

1: *Saccharomyces cerevisiae*

1.1: Model organism

Among the many advantages of using *Saccharomyces cerevisiae (S. cerevisiae)* is the availability of its mutant library created in 1998-2002 (Giaever and Nislow, 2014). My research takes advantage of all the features that make yeast an ideal model organism: 1) short chronological lifespan (which does not exceed several weeks for wild-type cells cultured in a nutrient-rich medium), 2) known ways to extend chronological lifespan (such as dietary caloric restriction, certain mutations, exogenous additives like lithocholic acid and some anti-aging plant extracts), 3) easy to study chronological lifespan, 4) availability of mutants (particularly the TOR1 deletion mutant), 5) evolutionarily conserved signalling pathways (invoking potential medical relevance), and 6) a multifaceted body of knowledge from the full genome sequence to cell-to-cell interaction of this unicellular eukaryote. Furthermore, *S. cerevisiae*, like the other yeast model organism *Schizosaccharomyces pombe*, can proliferate in a haploid state thereby making mutant studies much easier. In fact, the MAT**α** strain used in my experiment is haploid. Therefore, haploid gene-deletion mutants are absolute knockouts, and no sexual reproduction can occur in the absence of a Mat**a** yeast strain in the culture. Nonetheless, diploid forms are also of interest since most metazoan cells are diploid thus allowing yeast to be a model for recombination studies.

My thesis is based on chronologically long-lived cell population of quiescent yeast cells. There are two main factors that allowed me to work on chronologically long-lived cells: dietary caloric restriction (CR, versus non-caloric restriction, non-CR) and quiescent (Q, versus non-quiescent, NQ) cell populations of yeast. In the following chapters, I will address the importance of these factors.

1.2: *S. cerevisiae* aging

The two known modes of aging in *Saccharomyces cerevisiae* are replicative aging and chronological aging. These modes of aging are applicable to aging of cells derived from other eukaryotic organisms, which brings forth the relevance of yeast as a model organism for studying aging.

The replicative mode of aging is defined by the number of daughter cells (buds) a mother cell can produce before becoming a senescent (i.e. becoming incapable to divide). In yeast, it is relatively easy to quantify the replicative age of a given cell by using a microscope to count the number of bud scars (which mark the places of daughter cell separation) on the surface of the mother cell. The chronological mode of aging is arguably the type of aging the public thinks of when aging is mentioned. Chronological aging quantifies the length of time a given cell is able to survive under favourable (normal) conditions; similar to a multicellular organism living *la vida loca*. The nuance is that the chronological aging of a cell is monitored after the cell becomes mitotically inactive. These two modes of aging can be proxies for aging of different types of cells in multicellular organisms. The replicative lifespan (RLS) is alike aging in mitotically active cells of metazoans (such as cells in the self-renewing tissues of skin and liver). The chronological lifespan is alike aging of mitotically inactive cell populations (such as neurons, but unlike immune stem cells).

Due to its relevance in self-renewing tissues, replicative life span is extensively studied. In fact, RLS has been studied using genetic, lipidomic, metabolomic, and proteomic approaches. Many of the discoveries in yeast found their application in other eukaryotic model organisms, including human health and cancer research. Because both RLS and CLS are inevitably tied to major cellular events like regulation of cell cycle transitions, programmed cell death, and nutrient processing, the regulatory networks of these modes of aging partially (but not completely) overlap. Both RLS and CLS are under control of the same set of signaling pathways. Of interest are the Sch9 and protein kinase A (PKA) pathways, both of which are integrated into a network that includes the TOR pathway (Powers RW 3rd *et al*, 2006).

From individual experiments and cross-sectional studies emerge patterns of a bigger picture. Yeast is often at the core and root of such branching studies applicable to many fields. For example, *S. cerevisiae* contributed to the characterization and subsequent understanding of eukaryotic aging through such approaches as genetics, proteomics, lipidomics, and metabolomics. This allowed for formulations and updates of working models of normal aging in other organisms.

1.3: Hallmarks of aging

Several hallmarks of aging have been described in literature (López-Otín *et al*, 2013). These include primary, antagonistic, and integrative hallmarks (López-Otín *et al*, 2013). Primary hallmarks are causes of damage – and aging is the accumulation of damage (López-Otín *et al*, 2013). Antagonistic hallmarks arise as a response to the damage and initially, in small doses, have a protective/positive effect; yet, when such responses are overstimulated, they cause harm and thus promote aging (López-Otín *et al*, 2013). Integrative hallmarks arise when primary and antagonistic hallmarks damage the tissue beyond the repair mechanisms of a particular tissue (López-Otín *et al*, 2013). Primary hallmarks include genomic instability (affecting nuclear and mitochondrial DNA integrity, and nuclear lamina stability), telomere attrition (most relevant in mammals), epigenetic alterations (chromatin and DNA state and aberrant transcription and transcription products, with arguably leading roles of sirtuins genes), and loss of proteostasis (López-Otín *et al*, 2013). The latest is of particular interest to my phosphoproteomics research notably due to target of rapamycin (TOR) system involvement in longevity. Antagonistic hallmarks include deregulation of nutrient-sensing systems (where TOR often plays a role, as well as AMPK, sirtuins, and the insulin and IGF-1 signaling pathway in multicellular model organisms), mitochondrial dysfunction (with consideration of ROS and sirtuins genes), and cellular senescence (in this context argued as an initially protective process ridding the organism of damaged cells) (López-Otín *et al*, 2013). The integrative hallmarks are relevant to multicellular organisms and include stem cell exhaustion and alterations of intercellular communication (López-Otín *et al*, 2013). All the hallmarks are arguably observed in normal aging cells/organisms, accelerate aging if exaggerated, and increase healthspan/lifespan of normal aging cells if abolished (López-Otín *et al*, 2013).

1.4: Quiescence

In the context of yeast cells, quiescent cells are the cells arrested at G1, and surviving in G0. Several facets need to be taken in consideration. For one, there are certain triggers that will coax the yeast population to differentiate into quiescent (Q) and non-quiescent (NQ) subpopulations/populations (in this report called populations). Such triggers include exhaustion of dietary glucose; notably, caloric restriction (CR) without malnutrition. For two, the conditions under which the culture has grown previously have an effect on the timing of the exit from G1

(Mohammad and Titorenko, 2018). In fact, under non-CR conditions, cells enter quiescence at late G1 (failure to go through with checkpoint START A) (Mohammad and Titorenko, 2018). Under CR, cells enter quiescence at early G1 (Mohammad and Titorenko, 2018). For three, when the cells initially enter G0, they are not differentiated and are high density (in Percoll density gradient) (Leonov *et al*, 2017).

Previous research in our lab has described several characteristics of quiescent yeast cells (Leonov *et al*, 2017). The Q cells are characterized by increased reproductive competence, increased glycogen, trehalose, and cardiolipin concentrations, decreased triacylglycerol concentration, decreased reactive oxygen species (ROS) concentration and oxidative molecular damage, increased mitochondrial functionality, increased thermal and oxidative stress resistances, and decreased susceptibilities to apoptotic and liponecrotic regulated cell deaths (RCDs) (Leonov *et al*, 2017). Also, other properties have been described, such as: lower expression rates, translation from internal initiation sites, gene repression, inhibition of mRNA degradation, lower protein synthesis rate, chromosome condensation, and thicker cells walls (Gray *et al*, 2004, and references within). Such properties have been described previously in literature (Allen *et al*, 2006). Other important features of quiescent cell population are reproductive competence and ability to synchronously re-enter the mitotic life cycle (Leonov *et al*, 2017).

There are also physical properties that ensue from the physiological properties tying quiescence and caloric restriction. Quiescent cell population under CR are smaller than under non-CR while NQ cell population have similar sizes under both diets (Leonov *et al*, 2017). Additionally, Q cells are predominantly unbudded under both CR and non-CR conditions, in contrast with NQ population consisting of both budded and unbudded cells (Leonov *et al*, 2017). Both Q and NQ have a lesser proportion of budded cells under CR (Leonov *et al*, 2017).

The above-described properties of quiescent cells have been tied to the mechanisms/programs to delay of chronological aging. In fact, quiescence contributes to delay of chronological aging (Leonov *et al*, 2017). As such, it is relevant to describe the several stages tied to quiescence: entry into quiescence (exit from the G1 proliferative phase), maintenance of quiescence (metabolically active survival in G0), and entry into non-quiescence (committed from quiescence) (Leonov *et al*, 2017). These processes are dependent on several conditions such as the growth medium, as mentioned previously with the entry into quiescence being dependent on

the growth medium being CR or non-CR. In fact, the caloric content plays a big role in all three processes. The first, as previously mentioned, is the how early (under CR) or late (under non-CR) the population enters quiescence (Mohammad and Titorenko, 2018). The second is the prolonging of quiescent state maintenance under CR (Leonov *et al*, 2017). The third is the entry into NQ: the cells will commit to differentiation from Q to NQ (the terminal state leading to cell death) later under CR as opposed to under non-CR (Mohammad and Titorenko, 2018). From the above ensues that the quiescence state is not terminal. In fact, cells can exit quiescence and, thus, enter NQ state (Mohammad and Titorenko, 2018).

Historically, quiescent cells have been assumed to be the majority of the cells at stationary phase (ST) (Gray *et al*, 2004). In fact, here is a reminder about the relationship between the culture state and cell state grown in rich medium (such as YEPD). When the carbon source, such as glucose, is available the cells will proliferate quickly and thus the culture grows logarithmically (log phase, L). Upon significant drop in glucose availability, a diauxic shift (D) occurs, marking dramatic changes in the metabolic behavior of cells due to thorough rearrangement of its expression, proteome, metabolome, and lipidome. The culture then transitions into the post-diauxic phase (PD), in which cells proliferation is slowed down considerably compared to their log phase. At last, when the dietary glucose (carbon source) is depleted, the culture enters the stationary phase (ST), with many/most of its cells existing in a non-proliferative state termed quiescence (Gray *et al*, 2004). As such, quiescent cells form a population when glucose is depleted from the medium (at ST). Nevertheless, there are quiescent cells as early as during logarithmic stage (Leonov *et al*, 2017).

It is worth mentioning that entry into quiescence state seems to be inhibited by the protein kinase A (PKA) and by target of rapamycin (TOR) pathways under conditions of abundant/sufficient nutrients (including carbon content; in my experiments controlled by levels of glucose in growth medium). Therefore, upon diminished (but not depleted) nutrient levels, the nutrient-sensing TOR pathway is suppressed, causing the post-diauxic shift (PD). Then, upon complete glucose exhaustion, the TOR pathway is fully suppressed and therefore no longer suppresses the entry into quiescence. The PKA pathway responds in the same manner – in this context – to nutrient (glucose) depletion. Thus, upon glucose exhaustion (stationary phase), both TOR and PKA pathways are inhibited from inhibiting entry into quiescence. More details about the TOR and PKA pathways in the following sections. Also worth consideration are cells deficient in TOR.

These cells cannot suppress entry into quiescence via the TOR pathway regardless of the nutrient levels, but the PKA pathway can still inhibit entry into quiescence under high nutrient condition.

1.5: Dietary caloric restriction

The benefits of dietary caloric restriction without malnutrition have been noted in many organisms. In fact, humans have been adamant about intermittent fasting for centuries. With humans, however, it is a challenge to make sure the individual under fasting is not malnourished given their lifestyle and current health. In yeast, however, it is much easier to insure a caloric restriction regime since the organisms are unicellular, mostly homogeneous in behaviour in culture, and have well studied nutritional demands. While researchers sometimes focus on studying mutants to identify the shortening of the lifespan, it is easier to study the prolonging of lifespan. In fact, if a mutant causes a shortened lifespan (be it RLS or CLS), it may not be a direct agent but rather a general deregulating factor leading to random cell death (Kaeberlein and Kennedy, 2005). Since CR effects of both RLS and CLS have been noted, researchers naturally began investigating the mechanisms of action behind this intervention.

Notably, the success of caloric restriction in CLS extension is achieved through dampening of the TOR pathway (Power RW 3rd *et al*, 2006). In the work by Power III et al, the research group screened yeast mutants for extended CLS, and found that several mutants of reduced TOR pathway signalling, and inhibition of TOR signalling by exogenous manipulations (amino acids depletion or TOR-inhibiting drug administration) all lead to an increase in CLS (Power RW 3rd *et al*, 2006).

1.6: Target of Rapamycin (TOR)

The TOR (target of rapamycin) pathway is one of the highly conserved pathways across eukaryotes. The TOR pathway is of interest from two major aspects: scientific curiosity and human health. In fact, aberrations of the TOR pathway lead to severe cellular and organismal issues. This includes tuberous sclerosis (hyperactive mTORC1 due to defective upstream regulators TSC1/2 leads to tumours) (Kim *et al*, 2017). In fact, active mTORC1 – that is under high nutrient conditions – positively affects two major cellular processes (which are incidentally crucial for phosphoproteomics): ribosome biogenesis and protein synthesis (Humphrey et al, 2015). Therefore, massive upregulation can favour tumour growth by allowing the cell

accumulation of proteins while also denying programmed cell death pathways. Indeed, mTORC1 indirectly inhibits initiation of programmed cell death through apoptosis.

1.6.1. Rapamycin

The TOR1 and TOR2 genes were found as yeast mutants resistant to rapamycin (and henceforth called target of rapamycin) in 1991 (Heitman *et al*, 1991). In *S. cerevisiae*, only TOR1 (but not TOR2) mutants are fully rapamycin-resistant (Heitman *et al*, 1991). Later, TOR1 and TOR2 proteins were found to be paralogs from genome duplication. Treatment of cells with the antibiotic rapamycin (or rapamycin-like compounds) leads to cell growth defects through low protein and ribosomal synthesis, incompetent accumulation of nutrient-storage compounds (such as glycogen and glycerol) required for long-term survival, as well as spacio-temporal developmental issues in multicellular organism. Rapamycin indirectly inhibits translation initiation by directly inhibiting receptor at the cell surface therefore preventing TOR1 association with Raptor (KOG1) and LST8 into TORC1 protein complex. Rapamycin binds to FKBP12 (FK506-binding protein 12) forming FKBP12-rapamycin complex that inhibits TOR (Raught *et al*, 2001) (TOR1 but not TOR2 in yeast) activity. In a heterozygous cell, a heterozygous mutation of FKBP (one mutant allele, one WT allele) one WT copy of FKBP is sufficient to bind to rapamycin and irreversibly bind to TOR thereby inhibiting TOR. A heterozygous mutation in TOR that cannot bind FKBP-rapamycin complex is sufficient to avoid inhibition by rapamycin (Florian *et al*, 2007). TORC2, unlike TORC1, is not sensitive to rapamycin treatment (Wullschleger *et al*, 2006).

Notably, the TOR pathway refers to two core protein complexes, TORC1 and TORC2. Both TOR1 and TOR2 proteins are part of the protein complexes TORC1 and TORC2 – TOR1 participates in TORC1 only, while TORC2 participates in both complexes. When referring to the TOR pathway in the context of dietary calorie restriction it is of relevance to consider the TORC1 protein complex as it is nutrient-sensing, whereas TORC2 is cell cycle dependant.

TORC1 and TORC2 complexes in yeast have overlapping functions (Florian *et al*, 2007).

In *S. cerevisiae,* there are two highly similar TOR proteins (coded by TOR1 and TOR2 genes). These proteins may be referred to as mechanistic target of rapamycin (mTOR) because of the identified counterparts in metazoans. Only one copy of TOR protein has been identified in metazoans (Raught *et al*, 2001). In mammals, the TOR protein, mTOR, has shared identity to

both TOR1 and TOR2; mammalian TOR is also called FRAP, FRAP1, FRAP2, RAFT1, RAPT1 (UNIPROT/P42345). *Caenorhabditis elegans* worms have CeTOR (alias target of rapamycin homolog, lethal protein 363) (UNIPROT/Q95Q95). In drosophila, there is TOR with more shared identity with TOR2 than with TOR1. Please note that mTOR is also often referred to as mammalian TOR, in the context of mammals (often: humans). Therefore, referring to mTOR in the context of yeast does not imply that yeast have mammalian TOR yet implies that yeast mTOR (TOR1 and/or TOR2) acts identically to mTOR in mammals, worms, and flies. The mTOR is a kinase phosphorylating its targets such as SCH9 (yeast; S6 kinase-1 (S6K) in mammals and flies; RSK-1 in worms). Phosphorylated S6K can phosphorylate ribosomal S6 protein, eIF4B (thus allowing eIFB association with eIF4A) and PDCD4 (not found in yeast; inhibitor of eIF4A) thus leading to acceleration of translation (via mRNA leaders unwinding promoting ribosomal binding) (Weaver p549-551). The protein eIF4A is also regulated by Snf1 (sucrose non-fermenting protein 1); Snf1 is active upon glucose exhaustion, maintaining homeostasis and cell growth.

1.6.2. Upstream of TOR: AMPK

TOR being part of a nutrient-sensing signaling pathway has not only the ability to respond to intracellular nutrient/energy levels, but also to affect downstream proteins leading to changes in the cell functioning. Under high nutrient conditions (such as while yeast are grown in nutrient-rich medium and glucose is abundant), TOR can phosphorylate its targets (such as SCH9 in yeast). Conversely, under low nutrients, TOR is inactive. The inverse is true for AMPK (AMP-activated protein kinase) an upstream regulator of TOR. Under high nutrients (high ATP – low AMP – high energy), AMPK is inactive. Under low nutrient (high AMP – low energy), AMPK is activated and can inhibit TORC1 (via TOR). Tying this to dietary caloric restriction: under CR, TOR is inactive and is inhibited by active AMPK. Some interventions, such as treatment with metformin (in worms and mice) mimic the benefits of caloric restriction because metformin activates AMPK (López-Otín *et al*, 2013). In sum, high nutrient conditions allow TOR to promote anabolism and normal cell function, while low nutrient conditions inhibit TOR, and allow for catabolism and stress response (López-Otín et al 2013).

1.6.3. Downstream of TOR: Sch9

Another important protein tying nutrient-sensing and aging is SCH9 (a Ser/Thr protein kinase). Like other core signalling proteins, SCH9 has homology with other eukaryotes (SGK-1, AKT-2, and AKT-1 in *C. elegans*; S6K in mammals). The Sch9 protein is activated by phosphorylation by TORC1, and can then inhibit RIM15 which is an agent in cell cycle arrest favoring quiescence. Active SCH9 suppresses stress response genes transcription while promoting ribosomal biogenesis (Leonov *et al*, 2017) (a feature commonly attributed to TOR).

In addition to TORC1 (yeast), there are 3 more core proteins required for adequate response of the cell to nutrient depletion: PKA (protein kinase A), Snf 1 (sucrose non-fermenting, protein 1), and Pho85 (phosphate metabolism, protein 85) (Leonov *et al*, 2017). In tandem or in exclusivity, these proteins regulate such downstream effector proteins as: Rim15, Sch9 (as discussed above), Yak1, Mck1, Msn2/4 and Gis1, Hsf1, Gln3, Gsy2, Atg1-Atg13 complex, Sfp1, eIF2α, Crz1, Igo1 and Igo2 (paralogs), ad Mpk1 (Leonov *et al*, 2017). These cores – TORC1, PKA, Snf1, and Pho85 – are also required for cell cycle arrest (at G1), subsequent differentiation into Q/NQ subpopulations, and maintenance of the quiescent state (Leonov *et al*, 2017).

2: PhospoProteomics

2.1: Phosphorylation

The field of phosphoproteomics is the study of post-translational modification of phosphorylation of proteins. Such phosphorylation is most often carried out by a protein kinase, which adds a phosphate (PO_4) group to a polar group of an amino acid. Hence, the apolar/hydrophobic amino acid becomes polar/hydrophilic (Ardito *et* al, 2017). Posttranslational phosphorylation is a reversible modification. While the addition is mediated by protein kinases, the dephosphorylation is usually executed by protein phosphatases. The kinases can phosphorylate the hydroxyl (OH) group of an amino acid (such as serine, threonine, and tyrosine) acting as phosphoryltransferases, generally sourcing the phosphate group from the ultimate biological phosphate donor: adenosine triphosphate (ATP). The phosphatases remove the phosphate, but do not perform directly the reverse reaction, in terms of chemistry. The phosphatases hydrolyze at the phosphoric acid monoesther (Ardito *et* al, 2017) ($R\text{-}O\text{-}PO_3 + H_2O \rightarrow R\text{-}OH + PO_4$ where R is an amino acid) site restoring the OH group of the amino acid. In the rare event of phosphorylation of aspartate (such as in threonine biosynthesis pathway in yeast

(Yeast pathways, 2007)), the phosphate group addition occurs at the carboxylic acid. Another rare event is phosphorylation of histidine on its imidazole ring.

2.2: Kinases

There are several types of protein kinases (henceforth called kinases) and protein phosphatases (henceforth called phosphatases) generally classified by their substrates. For kinases, the classification is by the phosphorylated amino acid. Most known kinases are serine/threonine kinases (STKs) (Ardito *et* al, 2017). Serine is most prevalent phosphosite (Psite), with an estimate of about 86% Psites being on serine while threonine Psites are estimated at about 12% (Ardito *et* al, 2017). A lesser proportion are tyrosine kinases (TKs); tyrosine Psites constituting about 2% (Ardito *et* al, 2017). The smallest portion is serine/threonine/tyrosine kinases (dual-specificity kinases; DSKs) which can also phosphorylate STKs and TKs (Ardito *et* al, 2017). Protein kinases may have discrete or overlapping sets of substrates effectively allowing many kinases to phosphorylate several sites on a given protein (Humphrey *et al,* 2015).

2.3: Phosphatases

Phosphatases are also classified by their specificity. Unsurprisingly, the most important are phosphatases that can dephosphorylate the most abundant Psites (phosphoserine/pSer, phosphothreonine/pThr, and phosphotyrosine/pTyr). The two described families are phosphoprotein phosphatases (PPPs) and metallo-dependent protein phosphatases (PPMs) (Ardito *et* al, 2017). Notably, the metal dependency is mostly a regulatory method as the metal (often magnesium/Mg^{2+}) binds ATP to allow the above-described phosphate transfer. Another family of phosphatases are protein-tyrosine phosphatases (PTPs). These generally have higher selectivity for pTyr than do PPPs and PPMs, but are not exclusive to pTyr dephosphorylation, and even operate non-protein targets (Ardito *et* al, 2017).

2.4: Roles of phosphorylation

On the molecular level, protein phosphorylation is a critical modification playing several roles in the functioning of the cell, as reviewed by Ardito *et al* (Ardito *et* al, 2017). One of the functions of phosphorylation is to activate/deactivate a protein target (Ardito *et* al, 2017). The simplest model would be a protein that depends on only one Psite and is either turned on upon being

phosphorylated (inactivated upon dephosphorylation) or turned off upon phosphorylation (activated upon dephosphorylation). In reality, most proteins are likely under the control of several Psites and multiple kinases at once. A prominent reason for the change in the activity of the target is a change it its conformation (Humphrey *et al,* 2015). A second function of phosphorylation is to allow for protein-protein interactions which are generally temporary yet crucial in signal transduction (Humphrey *et al,* 2015; Ardito *et* al, 2017). A third function is inducing subcellular translocation of the target (Humphrey *et al,* 2015; Ardito *et* al, 2017). The forth utility is influencing other PTMs that rely of the phosphorylation state (Humphrey *et al,* 2015; Ardito *et* al, 2017). A fifth role plays out in the production/recycling of ATP (Ardito *et* al, 2017) – a crucial role for it is in the phosphate groups that ATP holds its power. Phosphorylation may also play roles in the turnover of the protein (Humphrey *et al,* 2015).

2.5: Approaches

To answer questions on phosphorylation, one can use *in vivo, in vitro* and/or *in silico* approaches. The lively *in vivo* approach is straightforward: isolate and study the phosphosites under given conditions. While the techniques, software, and machines to allow this are relatively new, the idea is not. In fact, phosphorylation events had been studied by radiolabeling for over half a century using ^{32}P. While this approach was valuable in detecting phosphorylation state, it did not yet inform the researchers about which amino acids were phosphorylated (coupling radiolabeled proteins to restriction enzymes did to some extent) until these samples were input to a mass spectrometer. With the advances of mass spectrometry, precise Psite mapping became possible, first using different labelling techniques and now label-free. Similarly, *in vitro* studies are a staple for proteomics (notably in protein-protein interactions). Rather than treating whole cell populations, a protein mixture can be incubated with protein kinase(s) of interest and analysis performed as *in vivo* be it radiolabeling or MS. The *in vitro* approach is not the better to use in the context of studying the active phosphoproteome of the cells, since kinases and phosphatases in a live environment do not necessarily operate (active/inactive, rates, competition, etc) as in an artificial environment. However, the *in vitro* studies are useful in finding potential phosphosites. Similarly, the experiment can be designed as a flow-through with either a fixed target (protein of interest) with all known kinases flown over or with fixed kinase with proteins flown over – both experiments seeking to establish potential protein interactions. A narrower biochemical approach

can be used to study the speed of reactions in a given pathway, for example, to determine which reactions take precedence under given conditions. While such kinetics studies add depth to given pathways, they are not contributing much to the overall understanding of the phosphoproteomes. A trend, however, emerged; kinase and phosphatases enzyme activity assays have shown that phosphatases generally execute their function faster than do kinases. This makes phosphatases a particular threat for proteomic samples.

The modern toolkit to study phosphorylation events also includes immune-targeting. With immunodetection, the costly issue is access to antibodies. While some antibodies may have a wider range of binding (for example to the common phosphosites pSer, pThr, and pTyr (Thermo Fisher Scientific)), most have much narrower specificity to benefit isolation of target proteins. The antibodies can be used in Western blots, immune-precipitation, immune-histochemistry, ELISA (enzyme-linked immunosorbent assay), flow cytometry, and microarrays (Thermo Fisher Scientific). While this approach facilitates studies of proteins of interest, it is arguably not the best to study entirety of the phosphoproteome.

Like many aspects of molecular biology today, the phosphoproteome is digitalized (as discussed below) and thus available for *in silico* studies. Both *in vivo* and *in vitro* studies contribute to the current knowledge of the phosphoproteomes and thus make computer-learning possible. Notably, many predictions about protein interactions (including kinase-target events) can be made using software that compares compatibility between enzyme binding site(s) and potential target. These softwares are made possible by the improvement of bioinformatics. Bioinformatics also greatly developed the data processing.

2.6: Phosphoproteomes

Studying post-translational phosphorylation events gives insight to the state of the protein detected as well as its upstream regulators (protein kinase(s) and/or protein phosphatase(s)). For most phosphorylation sites generated by MS, there is no known kinase responsible. Moreover, many (arguably, most) P-sites are described in large numbers (with high confidence). Computations also predict that a large portion of the kinome (for any organism) is unknown (Needham *et al*, 2019).

To represent the gigantic datasets of phosphoproteomics, there are several approaches. A sensible start is to consider uploading the obtained datasets online to contribute to the global

discovery of phosphosites. In fact, websites such as phoshopep.org, phosphosite.org, phospho.elm.eu.org and networkin.info aim to accumulate phosphosite data (from *S. cerevisiae, C. elegans, D. melanogaster,* bacterial, and mammals/human studies) and on other PTM. A lot of information is shared and cross-referenced among these websites, and a great portion is manually curated. So these databases are not yet fully automated (in my opinion it is largely because there is no agreement in the proteomics community on how to share findings and how much to share without losing ownership of discoveries) but nonetheless provide practical guidance. One of such useful applications is the prediction of phosphosites and associated kinases. For my experiment, for example, I can compare the predicted phosphosites versus the obtained phosphosites. A major difficulty, however, is that the MS methods (and the sample preparation, such as the phosphopeptide enrichment) are different enough to make comparisons too ambiguous in their conclusions. As such, methods of data acquisition must be considered when comparing datasets yet the acquisition method is not always obvious when working with the above-mentioned websites. Nonetheless, there are also trusted websites that classify and orchestrate massive databases in a generally accepted way. These giants include UniProt (UniProtKB/Swiss-Prot that is manually curated and is reviewed and UniProtKB/TrEMBL that is unreviewed, automatically curated data both at uniprot.org), ExPASy (at expasy.org), Protein Data Bank (PDB at rcsb.org), and the National Center for Biotechnology Information (at ncbi.nlm.nih.gov/protein). The above websites are all free to access within the scientific community. There are paid softwares that task in predicting phosphorylation sites – among other features – but these most commonly rely on one or more of the aforementioned databases giants.

Having accumulated the lists of phosphosites on respective proteins, there must be biologically significant conclusions (or new hypotheses) drawn. For such purposes, the data can be viewed in several ways. One method is to classify the proteins by the biological and/or molecular function. In such presentation, suggestions can be made about the general state of the source cells. I present such data. Another way is to focus on a subset of protein of interest. For example, to focus on proteins already known or suggested to be involved in a pathway/process of interest. Such studies can lead to more honed and narrowed one-protein studies involving the isolation of said protein under given conditions and subsequent *in vivo* assays to describe novel features. That is not a path I have chosen for my masters project, although I do look at several proteins of interest. As with general proteomics, expression patterns can also be quantified. In fact, keeping

the same methods, I can compare relative protein abundance across samples. Having the relative abundance of certain key proteins of known pathways of interest, I can suggest the activity state of the given pathway in different cell populations. A more dynamic approach is to visualize the phosphoproteome as a network of nodes and branches, such as using Cytoscape (free software download available at cytoscape.org), with annotations about the PTM state. A more advanced method has been developed in which many more factors are integrated including interactive protein description and animations called the Minardo plot (a stunning example available at https://minardo.org/snapshots/mitosis for the phosphoregulation of mitosis).

3: Mass Spectrometry

The crown of my experiment is the use of mass spectrometry to study the phosphosites. Mass spectrometry has seen a lot of improvement in sensitivity, precision, accuracy, and depth of data acquisition; phosphoproteomics has tremendously benefited from this advancement. Higher sensitivity of MS instrument allows for smaller sample sizes since lower abundance molecules can be detected. Sample preparations methods are also central to proper analysis by mass spectrometry. The improvement in procedures allowed for detection of very low abundance proteins (Humphrey et al, 2015). That is a notable advantage in processing scarce samples such as patient tissues.

3.1: Phosphopeptide enrichment

To study the phosphoproteomes, samples should be phosphoenriched. In fact, processing non-enriched samples (i.e. peptides forming the entire proteome) yields much lower detection of Psites than enriched samples (i.e. primarily peptides with a phosphorylation event). Effectively, samples with potentially low abundance of phosphopeptides give in better to analysis when concentrated. The method used to concentrate phosphopeptides is metal oxide affinity chromatography (MOAC) using titanium dioxide (TiO_2) magnetic beads. Other metal oxide beads suitable for MOAC include zirconium dioxide (ZrO_2) and magnetite (Fe_3O_4) (Riley and Coon, 2016). The limitation of such approach is in the TiO_2 beads as they have a high affinity for pSer, pThr, and pTyr. As such, this methods aids in the detection of the most common PTM phosphosites. It is up to some debate in the literature as to the gravity of omitting to focus on the proteins with the instable phosphor-histidine and phosphor-aspartate. The consensus is that

obtaining high-quality data on a large number of stable Psites is valuable and unstable Psites require a different sample preparation.

An alternative enrichment method is using immobilized metal affinity chromatography (IMAC). Similar to MOAC, IMAC has a bias towards pSer, pThr, and pTyr (Thermo Fisher Scientific). IMAC requires transition metals – commonly iron cation, Fe^{3+}, for Fe^{3+}-IMAC – to bind the phosphorylated peptide (Riley and Coon, 2016; Thermo Fisher Scientific). The metal is chelated (as in MOAC) to be immobilized (hence, the name IMAC) on magnetic beads (like in MOAC) or on silica-based resins (Riley and Coon, 2016). The difference between MOAC and IMAC is in the chelated metals used – metal oxides in MOAC and metal cations in IMAC – rather than immobility/mobility as the IMAC name might suggest. It is argued that to obtain the optimal coverage of the phosphoproteome, a combination of IMAC and MOAC techniques may be needed (Riley and Coon, 2016).

3.2: Chosen MS methods

My research is a bottom-up proteomics approach to studying the phosphoproteomes. Typically, bottom-up proteomics uses a protease (in my study: trypsin) followed by MS analysis. The top-down approach would avoid proteases. In fact, top-down approach is focused on identifying the structure of the protein(s), which would be annihilated by proteolytic digestion. Bottom-up studies, however, identify the proteome. Notably, bottom-up approach is also referred to as shotgun (HPLC-MS).

Trypsin is a protease with high specificity cleaving at the C-terminus of lysine and arginine (Riley and Coon, 2016). Since the produced peptides are also suitable for MS analysis, trypsin is the most used protease in proteomics (Riley and Coon, 2016).

The chosen approach to compare samples was label-free. As the name suggests, there is no labeling introduced to my samples (radioactive, fluorescent, or otherwise). This meant that for analysis, each sample was run separately since there is no distinguishing feature (alias label) to indicate the origin or the sample.

Another feature of the protocol is liquid chromatography followed by tandem mass spectrometry (LC-MS/MS). Liquid chromatography ensures gradual release of samples (used reverse-phase HPLC).

There are two main ways to obtain data from mass spectrometric fragmentation: data-dependent acquisition mass spectrometry (DDA-MS) and data-independent acquisition MS (DIA-MS). As their names suggest, the difference lies in how the machine selects precursor ions for further fragmentation. In DDA, the machine relies on the freshly-generated spectra, in real time, before continuing. In DIA, the fragmentation is predefined by the researcher at a fixed m/z ratio. In the context of studying PTM, both DDA and DIA could be advantageous because the m/z of the functional group (example: phosphate group for phosphoproteomics) is know and can be incorporated into the workflows. The chosen mass spectrometry approach relied on data-dependant acquisition. This means that each fragmentation event was chosen based on the previous spectrum (previous fragmentation event result). Effectively, the sample peptide is ionized at the source (nano-electro-spray) generating the precursor ions. Their detection is mass spectrum 1 (MS1). The nine most abundant multiply-charged ions among each MS1 are chosen for collision-induced dissociation (CID) with dynamic exclusion. The generated ions are detected, generating MS2. If the fragmentation of the precursor ion caused the neutral loss of a phosphate group, another round of CID (with multistage activation) is induced. The resulting detected ions generate MS3. Another key word is neutral loss. This is pivotal in acquiring MS3 in DDA-MS phosphoproteomics: the spectra are continuously monitored for the fixed loss of phosphate group.

4: Purpose and objectives

The purpose of my work was to compare the phosphoproteomes of chronologically aging yeast *Saccharomyces cerevisiae*, using quantitative mass spectrometry. The purpose was met through a series of experiments. Yeast cultures were grown and studied under dietary caloric restriction (CR) (versus not restricted (non-CR)) in the context of quiescence (Q) (versus non-quiescence (NQ)) comparing wild-type (WT) and tor1 deletion mutant. Wild-type phosphoproteomes have been done in duplicate, while mutant phosphoproteome duplicate is to be carried out in the future by members of the lab. For WT, all four possible populations have been studied: CR-Q, CR-NQ, non-CR-Q, and non-CR-NQ. For the mutant, non-CR-NQ were nonexistent (please see chapter IV for details). For studying chronological aging, the yeast populations were harvested at different stages of culture growth (for five time points for each population).

By studying the phosphoproteome of each population, I gathered data about the phosphorylation state of proteins, discovered novel phosphorylation sites, confirmed known phosphorylation sites, and summarized kinases involved in the phosphorylation of above-mentioned phosphoproteins. By studying the phosphoproteomes of WT *S. cerevisiae*, I inferred how caloric restriction delays chronological aging. By comparing WT with TOR1-deficient mutant, I made inferences about the importance of TOR1 (notable as part of TOR1 protein complex, TORC1; a pro-aging kinase) in entrance into quiescence, maintenance of quiescence, and exit from quiescence under CR and non-CR conditions. I explored how TORC1 inactivity contributed to delaying chronological aging of Q and NQ populations.

CHAPTER II: MATERIALS AND METHODS

1.0: Note about water used

All water coming in contact with proteomics samples and equipment (that contacted samples) was fresh MilliQ pure water only. Tap and distilled water were only used for washing and rinsing the dishes, and relevant equipment was rinsed with fresh MilliQ water. Proteomic samples are those that would eventually come in contact with the mass spectrometer (i.e. not including culture samples taken for counting and plating; sterile water was used in those instances).

1.1: Yeast strains and growth conditions

Wild-type (WT) *Saccharomyces cerevisiae*. Culture grown in YEP (1% yeast extract, 2% peptone) liquid medium, with either 0.2% glucose, or 2% glucose. Medium volume / flask volume (Erlenmeyer flask) is 1:5. Culturing at 200 rpm constant rotational shaking, at 30°C.
Identical growth conditions for *tor1* deletion mutant *Saccharomyces cerevisiae*.

Table 1. *Saccharomyces cerevisiae* strains used

Strain name	Strain ID	Genotype	Source
Wild-type (WT)	BY4742	*MATα his3-Δ1 leu2-Δ0 lys2-Δ0 ura3-Δ0*	Thermo Fisher Scientific
Tor1 deletion mutant	BY4742 *tor1Δ*	*MATα his3-Δ1 leu2-Δ0 lys2-Δ0 tor1Δ ura3-Δ0*	Thermo Fisher Scientific

2: Separation of quiescent and non-quiescent cell populations by Percoll density gradient centrifugation

Mixing by pipetting 2 mL 1.5 M NaCl with 16 mL Percoll beads solution, in a 50 mL conical centrifuge Falcon tube. 4 mL of the Percoll-NaCl solution was transferred into 4 pollyallomer tubes for MLS-50 rotor [Beckman Coulter, Inc]; 4mL of Percoll-NaCl forms the density gradient. The 4 tubes were centrifuged at 25,000 × g (16,000 rpm) for 15 minutes at 4°C in MLS-50 rotor in Optima MAX ultracentrifuge [Beckman Coulter, Inc]. Sample of yeast cells was diluted to determine total cell count per mL of culture, using a hemocytometer [Fisher

scientific]. 1×10^9 cells were pelleted by centrifugation in conical centrifugation Falcon tubes at 3,400 rpm at room temperature in IEC Centra CL2 tabletop clinical centrifuge. Pelleted cells were gently resuspended in 500 µL of 50 mM Tris/HCl buffer (pH 7.5). The resuspended cells were overlaid on the prepared Percoll-NaCl gradient, and centrifuged at 5,000 rpm for 30 minutes at 25°C in an Optima MAX ultracentrifuge. The upper (low density) and lower (higher density) fractions of cell population were collected with a pipette, in separate 15 mL Falcon tubes, combining all similar fractions (low with low, high with high) from the same sample. Cells were washed twice with 50 mM Tris/HCl buffer (pH 7.5), and subsequently resuspended in the same buffer for storage (-80°C).

3: Protein preparation for digestion

3.1: Glass bead lysate

Cell sample was lysed using glass beads as follows. Cells were pelleted by centrifugation at 3,000 rpm for 60 seconds at room temperature in the Centra CL2 tabletop clinical centrifuge. The pellet was then gently resuspended in 500 uL of 2% CHAPS in 25 mM Tris/HCl buffer (pH 8.5) at RT. Resuspended cells were pelleted by centrifuging at 16,000 rcf for 15 seconds at RT, and the supernatant removed (1^{st} wash). A second wash was done in the same manner. The resulting pellet was resuspend in 1 mL of ice-cold 2% CHAPS in 25 mM Tris/HCl buffer (pH 8.5). Glass beads [SIGMA-ALDRICH] (about 250 uL; depending on cell volume initially used) were added to the sample. Samples were then vigorously shaken using a disrupter (courtesy of Brett lab) at 4°C.

Glass beads and cell debris were then pelleted by centrifugation at 16,000 rcf for 5 minutes at 4°C.

Immediately after centrifugation, supernatant of the glass bed lysate was transferred into a pre-chilled Eppendorf tube.

To measure protein concentration, Bradford assay followed before proceeding to protein precipitation.

3.2: Bradford protein assay

A standard curve was prepared using bovine serum albumin (BSA) in water. Bradford Reagent (BR) was diluted to 1X in water. Samples were added to 1 mL of Bradford Reagent, mixed by

vortexing (in an Eppendorf tube), and incubated for 10 minutes at room temperature. 30 seconds before the 10 minutes incubation end, the sample was pipetted into a clear, plastic cuvette, and inserted into the spectrophotometer*. Absorbance at 595 nm was read (blank = 1X BR).

**Technical note about spectrophotometers*: Due to the early demise of our grand spectrophotometer, Beckman Coulter spectrophotometer DU 800, I have temporarily used the Nanodrop 2000C [courtesy of Brett lab], until out new, beloved spectrophotometer arrived: BioMate 160 by Thermo Scientific. Therefore, not all experiments – while all samples within a given experiment – were read using the same spectrophotometer.

3.3: Protein precipitation

For phosphoproteomics, 200 µg of proteins was taken for each sample. To the required sample volume (for 200 µg of proteins), TCA (dissolved in water prior to addition) was added to a final concentration of TCA as 10%. Sample with TCA was vortexed and incubated on ice for 30 minutes, for precipitation. The cold sample was then centrifuged at 16, 000 x g for 10 minutes at 4°C. The supernatant was discarded. The compact pellet was washed with 80% ice-cold acetone by adding 1.4 mL of 80% acetone, incubating on ice for 15 minutes, and centrifuging at 16, 000 x g for 10 minutes at 4°C. Acetone discarded. This wash was done twice. To completely evaporate the acetone, the samples were put in SpeedVac for about 5 minutes. Dry pellets ready for SDS-PAGE.

3.4: SDS-PAGE

To the dry pellet protein samples, SDS-PAGE sample buffer* is added: 193.4 µL of sample buffer with 6.6 µL of 2M Tris, for a protein concentration of 1 µg/µL. The pellet is resuspended in the denaturing sample buffer, and incubated overnight at RT. Samples were loaded on SDS-polyacrylamide gels (please see specifications below). Samples were run at 200V (constant) no more than 15 minutes: allowing all proteins to enter the running gel, while avoiding thorough separation (please see protein extraction). The gels were fixed with fixing solution (40% ethanol with 10% acetic acid), for 15 minutes on shaker at 55 rpm in clear plastic dishes with lids). After thorough rinsing with water, gels were stained with QC Colloidal Coomassie Blue for 1 hour on shaker at 55 rpm. Then, gels were destained with water for 4 15 minute intervals changing water after each 15 minutes on shaker at 55 rpm. Destained gels are ready for protein extraction.

*The SDS-PAGE sample buffer is 2 % SDS, 10 % Glycerol, 5 % β-mercaptoethanol, 0.005% bromophenol blue in 62.5 mM Tris/HCl (pH 6.8).

Running gel: 12.5% acrylamide/bis-acrylamide with 1% SDS in 0.375 M Tris/HCl (pH8.8).

Stacking gel 4% acrylamide/bis-acrylamide with 1% SDSin 0.125M Tris/HCl (pH 6.8) .

Electrode buffer: 0.1% SDS, 0.3 %, 1.44% glycine (final pH 8.3; no adjustment required).

4: Protein digestion and peptide extraction

Protocol courtesy of CBAMS – rewritten for thesis.

Protein samples in SDS-polyacrylamide gels were excised from gels into pieces of approximately 1x1x0.5 mm and placed into 1.5 mL Eppendorf tubes. Samples were reduced using 50 mM NH_4HCO_3 (Ammonium bicarbonate = ABC) with 10mM DL-Dithiothreitol (DTT) for 30 minutes. Solution discarded. Samples were then alkylated using 50 mM iodoacetamide in 50 mM ABC, away from light. Solution was discarded. Samples were then subjected to a series of washes with increasing acetonitrile (ACN) concentrations – all at RT. 1st wash using 50 mM ABC for 15 minutes. 2nd wash using 25 mM ABC with 5% ACN for 15 minutes. 3rd and 4th washes using 25mM ABC with 50% ACN for 30 minutes each. 5th wash using 100% ACN for 10 minutes. To completely remove ACN, gel pieces were dried in SpeedVac for 8 minutes (at 43°C).

The dried gel pieces were rehydrated with a 0.01 μg/μL trypsin in 25mM ABC solution (with a 1:20 trypsin to proteins ratio). Digestion was incubated overnight at 30°C.

The peptides (i.e. the digested sample proteins in gel pieces) were extracted using extraction solution (volume = 4 volumes of trypsin solution used): 60% ACN with 0.5% formic acid. To extract, the extraction solution is added to sample, vortexed, incubated for 15 minutes at room temperature and collected. There were3 extractions (collecting each round into the same 1.5 mL Eppendorf tube). Peptide samples were dried in SpeedVac for several hours.

Dry peptides are ready for phosphopeptide enrichment.

5: Phosphopeptides enrichment by TiO_2

Protocol courtesy of GE Healthcare Life Sciences (beads manufacturer; instructions 28-9537-65 AB) – rewritten for thesis.

Sample peptides are resuspended in a total volume of 250 µL of binding buffer (1M glycolic acid in 80% acetonitrile with 5% trifluoroacetic acid). Titanium dioxide (TiO_2) magnetic beads slurry (50 µL handled with cut pipette tips) was equilibrated by removing storage solution and washing with binding buffer (no incubation). Sample was then applied to beads, resuspended, and incubated with 360 rotation for 30 minutes. The buffer was removed. The beads were washed once using 500 µL of binding buffer, and then washed twice using 500 µL of wash buffer (80% ACN with 1% TFA). Sample was then eluted from the beads using elution buffer (5% ammonium hydroxide, pH12): adding 50 µL of elution buffer, incubating for 5 minutes, and collecting the eluate. Elutes for a total of 100 uµ (i.e. twice), combining the eluates.

Notes: When working with the magnetic beads, using the MagRack 6, applied solutions without magnet and removed solutions (with pipette) with magnet; resuspending solutions by manual inversion. Incubating sample with beads using a 360 rotation rack at RT.

6: Mass spectrometry

To prepare sample peptides for mass spectrometry, samples were dried in SpeedVac. The dry peptide pellets were reconstituted in 2% acetonitrile with 1% formic acid, to inject 200 ng in 5 µL (injection volume). The method used is reverse-phase high performance liquid chromatography coupled to tandem mass spectrometry (RP-HPLC-MS/MS) using EASY-nLC™ II coupled to LTQ Orbitrap Velos (nanospray ion source; MS1 resolution of 60 000). Column used is 10 cm by 100 µm C18 packed in-house. For this label-free identification of phosphopeptides, used neutral-loss induced MS3, with multistage activation. The total run time was 92 minutes, with 90 minutes gradient (from 3% acetonitrile with 0.1% formic acid to 97% acetonitrile with 0.1% formic acid) with a constant sample elution of 400 nL per minute.

7. Software

Thermo Proteome Discoverer 2.2.0.388 and SEQUEST were used to search *Saccharomyces cerevisiae* databases (SwissProt TaxID=559292_and_subtaxonomies, v2017-10-25; TrEMBL

TaxID=559292, v2017-10-25), using custom workflows. Reported peptides and proteins have a set false discovery rate < 1%.

Proteome Discoverer 2.2.0.388 (PD2.2) was also used to generate several figures. Microsoft Office was used to process the data exported (or extrapolated) from PD2.2 for data presentation purposes. Helper computer applications (such as Microsoft Windows Paint) were also used to present data. Microsoft Office Word was used in writing of this thesis – converted to PDF/A using Abode Acrobat.

CHAPTER III: PHOSPHOPROTEOMES OF CHRONOLOGICALLY AGING WILD-TYPE YEAST

Note: High density cells (HD; in Percoll gradient) are mainly quiescent (Q) while low density cells (LD; in Percoll gradient) are mainly non-quiescent (NQ) (Leonov *et al.* 2017). As such, I used HD/LD in annotation of data (to avoid bias in case of reassessment of data). Nonetheless, I use HD/Q and LD/NQ interchangeably in chapters III and IV).

1. Hypothesis

Considering that reversible protein phosphorylation regulates many (if not all) biological processes, it is plausible that this type of post-translational protein modification is used to regulate the biological processes required to maintain the state of quiescence and the responses of quiescent and non-quiescent cells to caloric restriction. Therefore, the phosphoproteomes of WT yeast were expected to be significantly different between CR-HD and CR-LD, non-CR-HD and non-CR-LD, as well as between CR-HD and non-CR-HD, and CR-LD and non-CR-LD; assuming that HD are primarily quiescent and that LD are mainly non-quiescent.

2. Results and Discussion

I found hundreds of phosphorylated proteins in samples recovered at each of the five days of collection (days 0, 1, 2, 5, and 7). The tables below (Tables 2.1 – 2.5) outline the number of phosphoproteins and peptide spectrum matches (PSMs) in chronological order where day 0 represents the first day after mid-exponential growth. Since the WT data was done in duplicate, data for both experiments (experiments 1 and 2 in Tables 2.1-2.5) is provided. Please see supplemental figures for relative sample abundances across these experiments; all sample abundances were similar (Figures S6A-B for experiment 1, and Figures S7A-B for experiment 2). The peptide spectrum matches are the number of detected peptides contributing to identification of proteins. The number of PSMs, however, is not the number of peptides identified; some peptides, for example, may contribute to the identification of several proteins (such as peptides that are common among a protein family). The PSMs were filtered to only very high confidence peptides (meaning that less than 1 % of the identified peptides from spectra are due to false discovery). Some peptides may be identified multiple times, if they are present in multiples in the sample. Less abundant peptides are nevertheless captured by the mass

spectrometer. When such low abundance fragments do not meet the stringent qualification, they are not used in assignment to identify proteins. This, therefore, leads to missed identification of very low abundance proteins. In the context of label-free experiment, this can be remedied to some extend by making large studies that combine all relevant samples plus a pooled sample for the analysis. One of the benefits is identifying more proteins. Since the system is given more spectra to analyze; by aligning peptide retention times, for example, the software (I used Thermo Proteome Discoverer 2.2.0.388 and SEQUEST) can increase the confidence of assigning spectra to peptide and therefore have more peptides to match to proteins thus possibly leading to more proteins detected.

The repeat of the experiment of studying the effects of caloric restriction on quiescent and non-quiescent WT yeast cells yielded less phosphoproteins. I believe that the main contributing factor was using a different batch of titanium dioxide beads. It is inevitable to use different batches, due to the shelf life of the beads. I have no claims to the manufacturer, however. I also used a different batch of trypsin for each experiment. This did not have a significant effect, happily, as can be seen from the low missed cleavages by trypsin (i.e. high zero missed cleavages): 45.48% no missed cleavage, 37.14% 1 missed cleavage, and 17.37% 2 missed cleavages in experiment 1 (with higher phosphoprotein count post analysis) and 50.99% no missed cleavage, 36.14% 1 missed cleavage, and 12.87% 2 missed cleavages in experiment 2 (with lower phosphoprotein count) (please see supplemental figure S9 for experiment 1, and S10 for experiment 2 missed cleavage percentages). The cleavage sites are predicted by the software and compared to sample.

Table 2.1. Phosphorylated proteins found in WT *Saccharomyces cerevisiae* – day 0

Diet	Density	Experiment	Number of PSMs	Number of phosphoproteins
CR	**LD**	**1**	7621	647
		2	2819	115
	HD	**1**	7759	695
		2	4197	373
non-CR	**LD**	**1**	7772	668
		2	4788	439
	HD	**1**	9170	802
		2	5136	439

Table 2.2. Phosphorylated proteins found in WT *Saccharomyces cerevisiae* – day 1

Diet	Density	Experiment	Number of PSMs	Number of phosphoproteins
CR	**LD**	**1**	6963	611
		2	3491	295
	HD	**1**	6319	524
		2	6970	502
non-CR	**LD**	**1**	7448	662
		2	5183	409
	HD	**1**	9200	788
		2	2991	308

Table 2.3. Phosphorylated proteins found in WT *Saccharomyces cerevisiae* – day 2

Diet	Density	Experiment	Number of PSMs	Number of phosphoproteins
CR	**LD**	**1**	7559	644
		2	2286	245
	HD	**1**	8126	701
		2	5602	505
non-CR	**LD**	**1**	6029	553
		2	2477	291
	HD	**1**	7045	589
		2	2748	297

Table 2.4. Phosphorylated proteins found in WT *Saccharomyces cerevisiae* – day 5

Diet	Density	Experiment	Number of PSMs	Number of phosphoproteins
CR	**LD**	**1**	6688	530
		2	2055	230
	HD	**1**	8899	528
		2	3621	349
non-CR	**LD**	**1**	5626	392
		2	5536	536
	HD	**1**	9872	756
		2	260	69

Table 2.5. Phosphorylated proteins found in WT *Saccharomyces cerevisiae* – day 7

Diet	Density	Experiment	Number of PSMs	Number of phosphoproteins
CR	**LD**	**1**	7943	658
		2	3680	360
	HD	**1**	8913	329
		2	4836	410
non-CR	**LD**	**1**	6412	482
		2	8158	449
	HD	**1**	9873	761
		2	4665	226

Following the general assessment of total phosphorylated proteins identified, principal component analysis (PCA) was done on the samples to see if diet and/or density had the expected effect of qualifying the samples as significantly different. The PCA using phosphoproteins is seen in Figure 1 (The data shown is from experiment one as seen in Tables 2.1-2.5). The first principal component (PC) accounts for 21.5% of the variability in the data, and the second PC for 17.5%. The principal components were drawn, by the software, from spectra. A pool sample was used to better the quantization; note that the pool sample is not necessarily a pool of the samples for the given experiment. Rather, the pool is a mixture of different phosphopeptide samples from another experiment – this explains why the pool sample is not necessarily at the center of the PCA plot. Figure 1A highlights samples based on their diet only. There is indeed a difference between the samples based on the diet alone. CR are samples initially grown on 0.2% glucose in YEP medium, while non-CR are cultures grown initially on 2% glucose in YEP medium (please see chapter II). Figure 1B presents the same PCA but with only the density being made evident. It may seem that the samples have no clear trend, but that is explained by Figure 1C. Indeed, Figure 1C shows both diet and density of the samples. The pattern is: samples are more similar based on their diet (across densities) than by their densities (across diets). CR-HD are more similar to CR-LD than to non-CR-HD: quiescent cells from different diets have significantly different phosphoproteomes. Comparatively, CR-LD are more similar to CR-HD than to non-CR-LD: non-quiescent cells from different are also dramatically different from each other. In conclusion, quiescent (HD) cells are more different from each other (CR-HD vs. non-CR-HD) than are non-quiescent (LD) cells across diets. Figure 1D identifies all the samples. In Figure 1D, closer to the center of the plot, two overlapping samples are seen:

non-CR D5 LD and CR D7 LD – where D stands for day. Also close to them are populations D7 non-CR LD and arguably D5 CR LD. These cultures come from different diets of chronological old WT cells. Their common feature is the low density. So, these chronologically old, non-quiescent cells have similar phosphoproteomes. That is most likely because these non-quiescent cells are converging on senescence and death. Their quiescent counterparts (for both CR and non-CR, days 5 and 7) are far removed from them: day 5 are in upper left quadrant while day 7 are in the upper right quadrant. While the samples of the same diet are close to each other, the samples of the same age of different diets are far removed. This indicates that these WT quiescent populations age in similar ways for a given diet (CR or non-CR).

Figure 1. Principal component analysis of phosphorylated proteins found in WT *S. cerevisiae* under CR/non-CR with different population densities, at different chronological ages

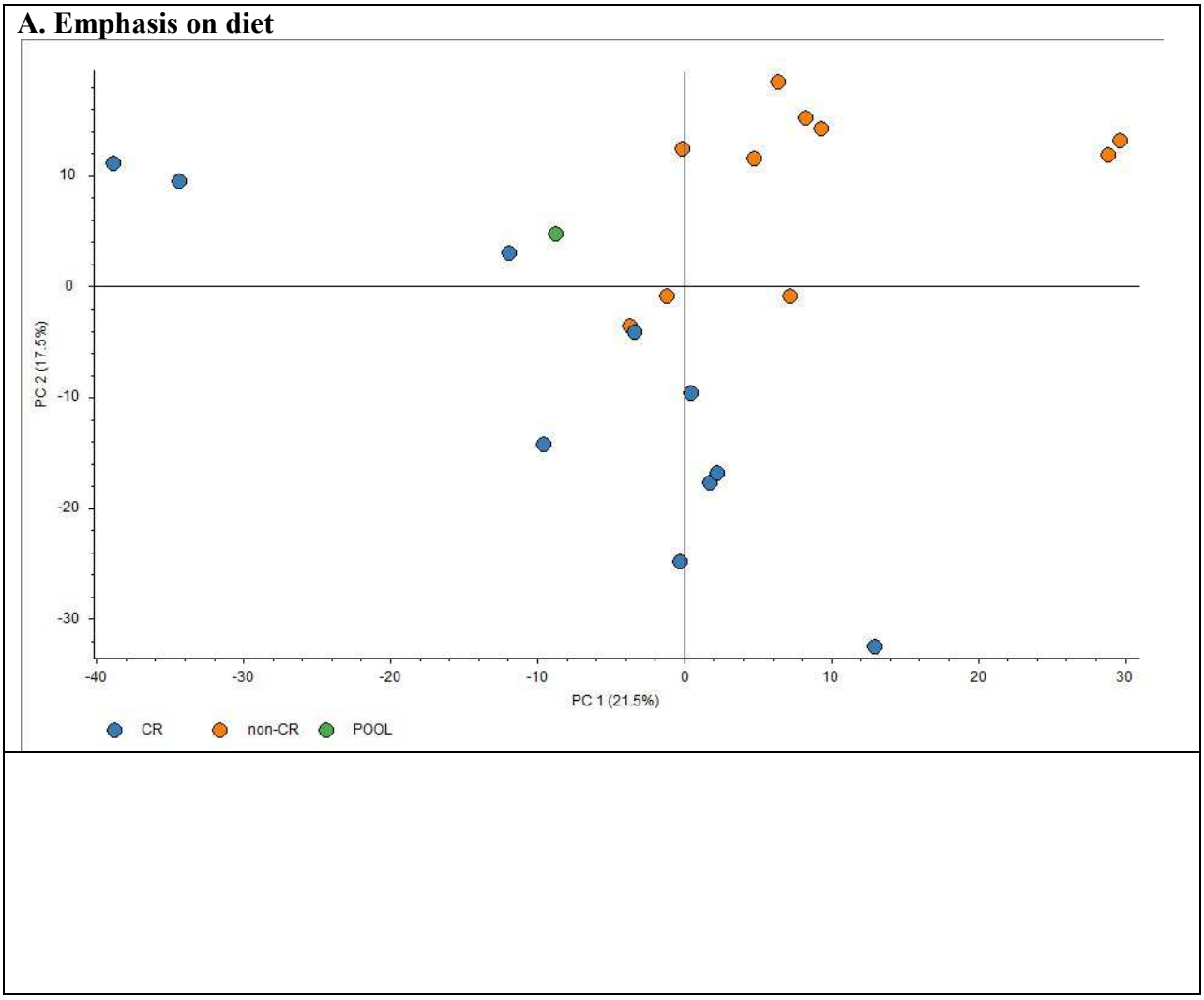

B. Emphasis on density

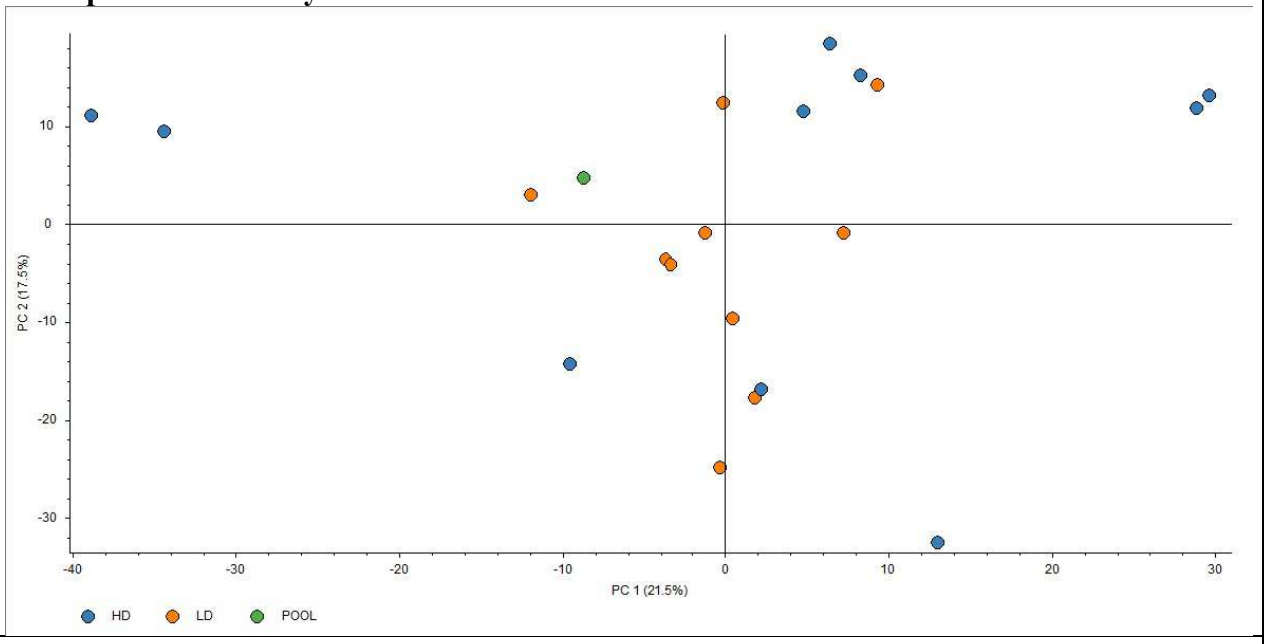

C. Emphasis on diet and density

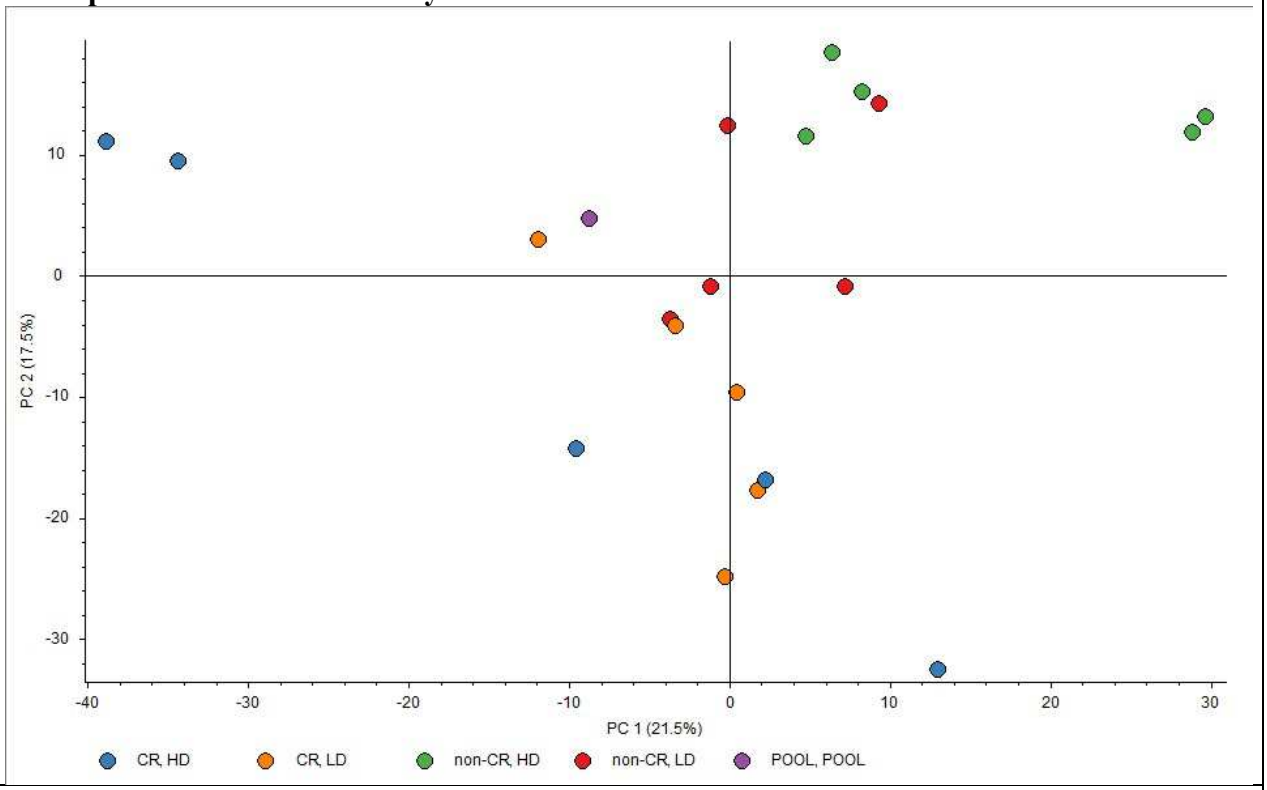

D. All samples identification

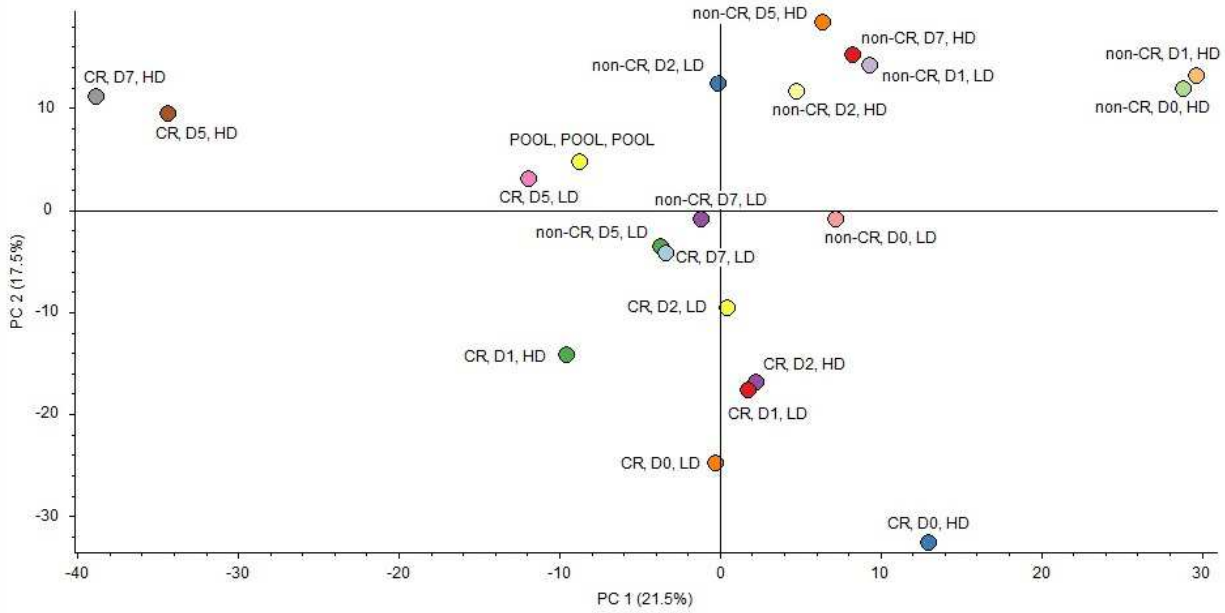

Given the trends from the PCA across time, I looked at each time point separately: comparing different populations of the same chronological age. The difference between the phosphoproteomes is quantified by the number of unique phosphoproteins – proteins that are found in one sample but not in its comparable counterpart and vice versa. In fact, this was observed, as seen in Figures 1.1-1.5 of such unique phosphoproteins in chronological age of yeast. (Please note, only one repeat is shown in Figures 1.1-1.5; this is data from experiment 1.) Figures 1.1-1.5 are in chronological age of samples (Figure 1.1 – day 0, Figure 1.2 – day 1, Figure 1.3 – day 2, Figure 1.4 – day 5, Figure 1.5 – day 7). Within each of these figures, I show the number of unique and shared phosphoproteins. Figures A compare CR-HD to CR-LD (CR diet, different densities), Figures B compare non-CR-HD to non-CR-LD (non-CR diet, different densities), Figures C compare CR-HD to non-CR-HD (different diets, high density), and Figures D compare CR-LD to non-CR-LD (different diets, low density). There is generally about a thousand (lowest 807 in Figure 1.4D, and 1091 highest in 1.2B) shared phosphorylated proteins. This is expected and generally represents housekeeping proteins that are required in the phosphorylated state. A caveat of this quantization is that some of the shared proteins may have a different phosphorylation state – different phosphosites – detected. Among the unique phosphoproteins, however, there is no question: they are either found or not found in qualifying amounts. There are generally a few dozen (lowest: 13 seen in Figure 1.4B) to over a hundred

(highest: 255 in 1.5C) of such proteins. These phosphoproteins agree that the phosphoproteomes of each sample is its unique signature given the diet, density, and age.

Figure 1.1. Number of phosphoproteins unique to sample in WT *S. cerevisiae* – day 0

A.

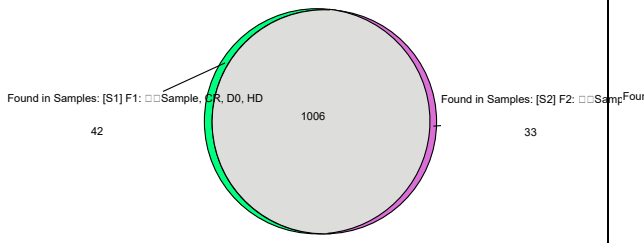

Colour	Exclusive	Total	Found in sample
	42	1048	CR, D0, HD
	33	1039	CR, D0, LD
	1006	1006	CR, D0, HD and CR, D0, LD
Sum	1081		

B.

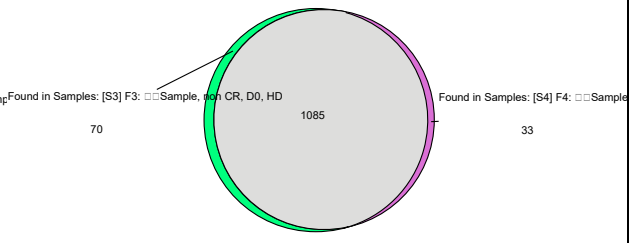

Colour	Exclusive	Total	Found in sample
	70	1155	non-CR, D0, HD
	33	1118	non-CR, D0, LD
	1085	1085	non-CR, D0, HD and non-CR, D0, LD
Sum	1188		

C.

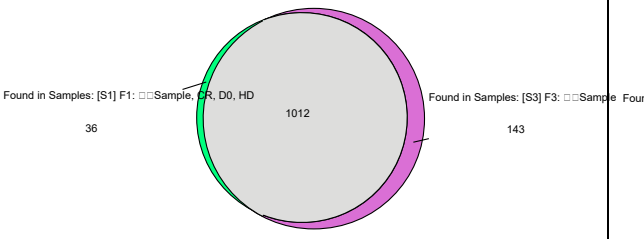

Colour	Exclusive	Total	Found in sample
	36	1048	CR, D0, HD
	143	1155	non-CR, D0, HD
	1012	1012	CR, D0, HD and non-CR, D0, HD
Sum	1191		

D.

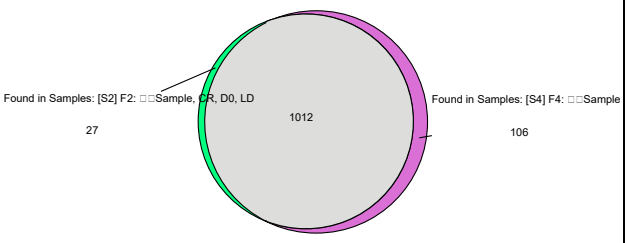

Colour	Exclusive	Total	Found in sample
	27	1039	CR, D0, LD
	106	1118	non-CR, D0, LD
	1012	1012	CR, D0, LD and non-CR, D0, LD
Sum	1145		

Figure 1.2. Number of phosphoproteins unique to sample in WT *S. cerevisiae* – day 1

A.

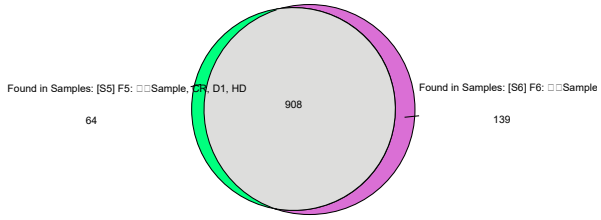

Colour	Exclusive	Total	Found in sample
	64	972	CR, D1, HD
	139	1047	CR, D1, LD
	908	908	CR, D1, HD and CR, D1, LD
Sum	1111		

B.

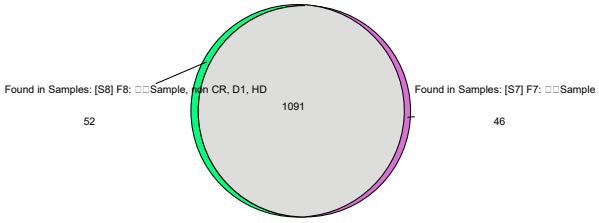

Colour	Exclusive	Total	Found in sample
	52	1143	non-CR, D1, HD
	46	1137	non-CR, D1, LD
	1091	1091	non-CR, D1, HD and non-CR, D1, LD
Sum	1189		

C.

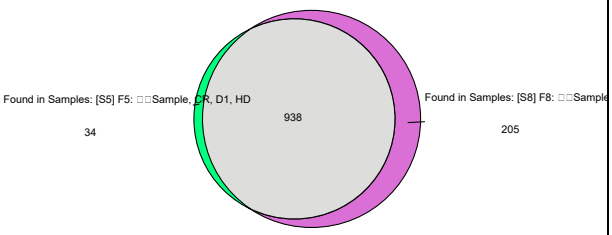

Colour	Exclusive	Total	Found in sample
	34	972	CR, D1, HD
	205	1143	non-CR, D1, HD
	938	938	CR, D1, HD and non-CR, D1, HD
Sum	1177		

D.

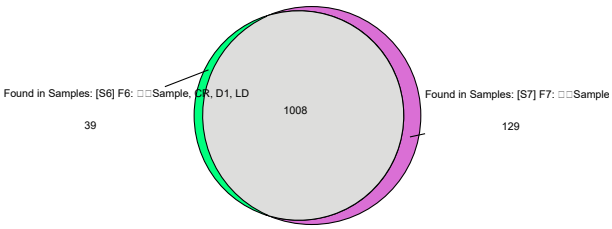

Colour	Exclusive	Total	Found in sample
	39	1047	CR, D1, LD
	129	1137	non-CR, D1, LD
	1008	1008	CR, D1, LD and non-CR, D1, LD
Sum	1176		

Figure 1.3. Number of phosphoproteins unique to sample in WT *S. cerevisiae* – day 2

A.

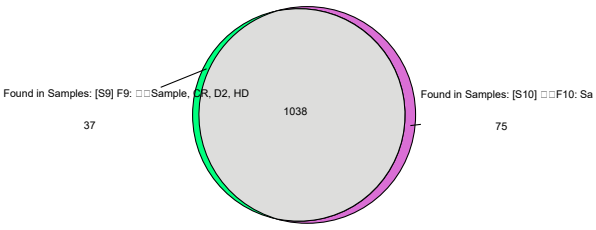

Colour	Exclusive	Total	Found in sample
	37	1075	CR, D2, HD
	75	1113	CR, D2, LD
	1038	1038	CR, D2, HD and CR, D2, LD
Sum	1150		

B.

Colour	Exclusive	Total	Found in sample
	40	1026	non-CR, D2, HD
	116	1102	non-CR, D2, LD
	986	986	non-CR, D2, HD and non-CR, D2, LD
Sum	1142		

C.

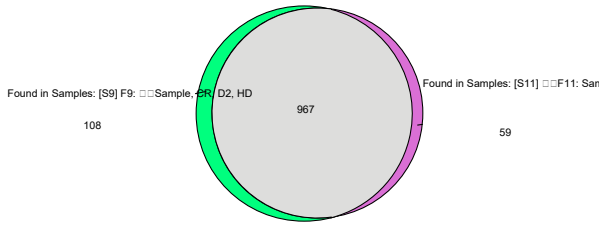

Colour	Exclusive	Total	Found in sample
	108	1075	CR, D2, HD
	59	1026	non-CR, D2, HD
	967	967	CR, D2, HD and non-CR, D2, HD
Sum	1134		

D.

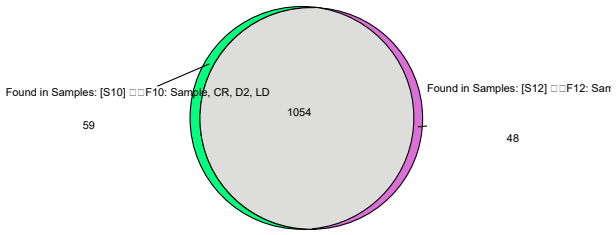

Colour	Exclusive	Total	Found in sample
	59	1113	CR, D2, LD
	48	1102	non-CR, D2, LD
	1054	1054	CR, D2, LD and non-CR, D2, LD
Sum	1161		

Figure 1.4. Number of phosphoproteins unique to sample in WT *S. cerevisiae* – day 5

A.

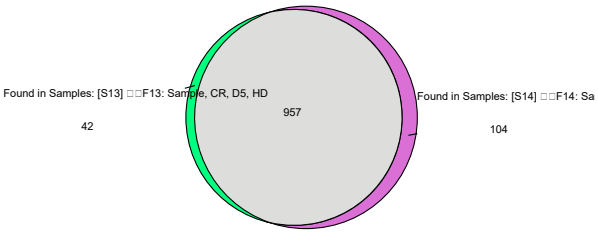

Colour	Exclusive	Total	Found in sample
	42	999	CR, D5, HD
	104	1061	CR, D5, LD
	957	957	CR, D5, HD and CR, D5, LD
Sum	1103		

B.

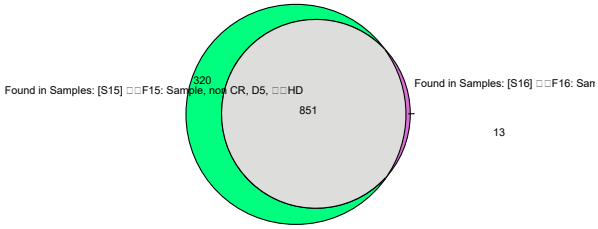

Colour	Exclusive	Total	Found in sample
	320	1171	non-CR, D5, HD
	13	864	non-CR, D5, LD
	851	851	non-CR, D5, HD and non-CR, D5, LD
Sum	1184		

C.

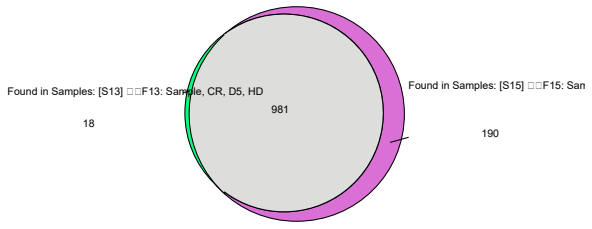

Colour	Exclusive	Total	Found in sample
	18	999	CR, D5, HD
	190	1171	non-CR, D5, HD
	981	981	CR, D5, HD and non-CR, D5, HD
Sum	1189		

D.

Colour	Exclusive	Total	Found in sample
	254	1061	CR, D5, LD
	57	864	non-CR, D5, LD
	807	807	CR, D5, LD and non-CR, D5, LD
Sum	1118		

Figure 1.5. Number of phosphoproteins unique to sample in WT *S. cerevisiae* – day 7

A.

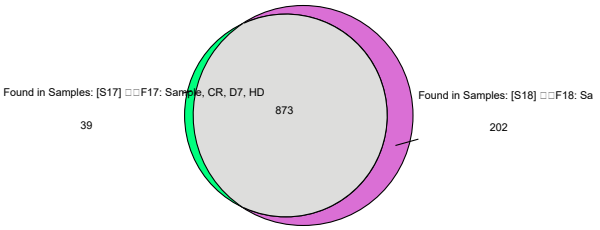

Colour	Exclusive	Total	Found in sample
	39	912	CR, D7, HD
	202	1075	CR, D7, LD
	873	873	CR, D7, HD and CR, D7, LD
Sum	1114		

B.

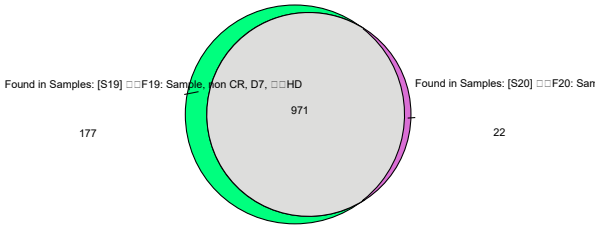

Colour	Exclusive	Total	Found in sample
	177	1148	non-CR, D7, HD
	22	993	non-CR, D7, LD
	971	971	non-CR, D7, HD and non-CR, D7, LD
Sum	1170		

C.

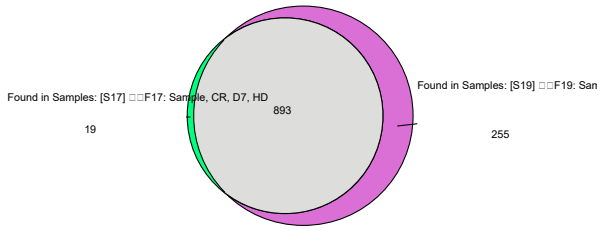

Colour	Exclusive	Total	Found in sample
	19	912	CR, D7, HD
	255	1148	non-CR, D7, HD
	893	893	CR, D7, HD and non-CR, D7, HD
Sum	1167		

D

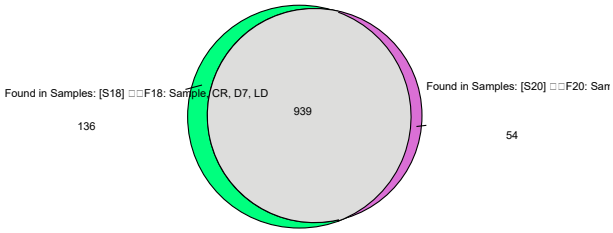

Colour	Exclusive	Total	Found in sample
	136	1075	CR, D7, LD
	54	993	non-CR, D7, LD
	939	939	CR, D7, LD and non-CR, D7, LD
Sum	1129		

Among all the phosphorylated proteins (not exclusively the unique proteins discussed above), most of the found phosphoproteins localized to cytoplasm/cytosol, nucleus, and membranes (as can be seen from supplemental Figures S1-S5). The localization assignment was seen through the Proteome Discoverer and SEQUEST software, which relies on UniProt as the source database (please see methods), since that is the database I used in my workflows. It is possible to use other databases, but UniProt has the most numerous, reliable proteomics data for *Saccharomyces cerevisiae*. The nuance with the assignment of protein localization is two-folded. For one, the database provides all the possible subcellular localizations of the protein in all possible states of the cell and of the protein. So it is not necessarily the phosphorylated form of the protein that is found at these localizations. For example, a hypothetical protein with a phosphorylated serine was identified, and for this protein there are two localizations defined by

the database: one in a non-phosphorylated state in the nucleus, and another in the cytoplasm when tyrosine (not identified in study) is phosphorylated. So, I count this protein as contributing to both the nuclear and cytoplasmic proteins identified, while its true localization at the time of collection is speculative. Moreover, many of the found phosphosites in the experiment are novel (not described in literature before, at least not in the major databases of UniProt and BioGrid; lists not shown in this thesis). For two, a single protein may have more than one subcellular localization assigned to it. In fact, proteins – be they phosphorylated or not – are known to be able to translocate (by different mechanisms). Therefore, the quantization of subcellular localization among the phosphorylated proteins identified is a trend more than concrete values, since it is not known where the protein was at the time of collection. Elaborate experiments on protein localizations (such as visualization under the microscope by using fluorescent tags on proteins of interest) would be required to assign protein localization with certitude. Nevertheless, I considered the trends of such localization. The majority of the phosphorylated proteins was found in cytoplasm/cytosol. This is expected of phosphorylated proteins that may be involved in signaling pathways. In fact, protein phosphorylation is one of the post-translational modifications that allows for protein subcellular relocalization. Moreover, phosphorylation also has a role in signaling that alters expression such as by the phosphorylation of transcription factors. Thus, detecting many proteins that may be localized in the nucleus is also plausible. Detecting numerous proteins that may localize to membranes indicates that many proteins may be tethered to a membrane (any membrane). Somewhat lesser, but still weighty part of the phosphoproteomes may also localize to the mitochondria. Since the mitochondria are signaling hubs, such localization is plausible.
Additionally, novel phosphorylation sites have been identified (not shown in this thesis).

Overall, the hypothesis was correct in that the yeast populations of different quiescent state under the same diets are different from each other, and that populations under different diets (but the same state of quiescence) are also different from each other. Furthermore, diet and density (indicative of the quiescence/not of the cells) were consistent trends for the WT cultures. Additionally, localization of phosphoproteins of interest suggested that phosphorylation identified might be from cell signaling pathways. Finally, the approach of looking at the

phosphoproteomes of WT yeast under calorie restriction (or no restriction) in the context of quiescent/not cells is an exploration study that has not yet been done (to best of my knowledge).

CHAPTER IV: PHOSPHOPROTEOMES OF CHRONOLOGICALLY AGING TOR1 MUTANT YEAST

1. Hypothesis

Considering that TOR1 is one of the major protein kinases known to phosphorylate many proteins implicated in various cellular processes, it is plausible that this nutrient-sensing protein kinase is involved in the phosphorylation of many proteins essential for the response of quiescent and non-quiescent yeast cells to caloric restriction. Thus, it was expected that the phosphorylation patterns of quiescent and/or non-quiescent cells carrying the *tor1* mutation differ based on the culture diet and/or state of quiescence. It was also expected to find novel phosphorylation sites from the cultures lacking TOR1.

2. Results and Discussion

I identified hundreds of proteins in *tor1* deletion mutant yeast populations, initially grown under caloric restriction or not calorically restricted conditions (Tables 3.1 shows the number of identified phosphoproteins, in chronological order). The TOR1 protein, as part of the TORC1 complex, responds to nutrient levels. Under high nutrient (such as initially abundant glucose in YEP medium; non-CR), TORC1 can promote anabolic pathways such as ribosomal synthesis. Restricting TORC1 activity leads to chronological lifespan increase (please see introduction), such as when growing in glucose-poor conditions (CR) or cell not having TOR1 protein. Therefore, the phosphoproteomes of cells grown under conditions that inhibit TORC1 (TOR1 being at the core) activity are expected to be similar to phosphoproteomes of cells with *tor1* gene deletion. Moreover, WT-CR (HD and LD) are expected to be similar to *tor1* mutant under CR (HD and LD). Under non-CR, the WT (with TOR1 functioning normally) and the *tor1* mutant phosphoproteomes are expected to be significantly different, because of the protein kinase activity of TORC1.

Furthermore, there were very low to no LD cells in non-CR. (Reminder: high density (HD) population is mainly quiescent (Q) cells, while low density (LD) population is mainly non-quiescent (NQ) cells.) This indicates that yeast lacking TOR1 and initially grown under high calorie condition mostly differentiate into quiescent (HD) cells. For all samples, hundreds of phosphorylated proteins were identified, as seen in Table 3.1 below.

Table 3.1. Phosphorylated proteins found in *tor1* deletion *Saccharomyces cerevisiae*

Day	Diet	band	Number of peptide spectrum matches	Number of phosphoproteins
0	CR	LD	1961	209
		HD	2165	277
	non-CR	HD	4291	478
1	CR	LD	4394	406
		HD	6914	580
	non-CR	HD	3735	440
2	CR	LD	4144	445
		HD	5086	494
	non-CR	HD	8072	731
5	CR	LD	4158	400
		HD	4774	502
	non-CR	HD	4675	495
7	CR	LD	4015	378
		HD	4916	385
	non-CR	HD	4911	505

The protein-level principal component analysis (PCA) was done to assess the differences between the phosphoproteomes of the *tor1* mutants and can be seen in Figure 2. Figure 2A highlights the differences in the samples based on their diet (CR – initially grown on 0.2% glucose in YEP, and non-CR – initially grown on 2% glucose in YEP). There is a significant difference, as the non-CR samples are consistently distinguishable from CR samples on both the first (which accounts for a total of 25.5% of variability in the data) and second (which accounts for a total of 17.5%) principal components. In Figure 2B, with the density as the label, the pattern is not as clear. This is clarified by 2C whence both diet and density are labeled. The non-CR-HD (no LD under this diet – please see above) are different from the CR-HD and CR-LD samples, while CR-HD and CR-LD are comparatively more similar to each other. Figure 2D shows all the labels of samples. A pattern is seen for the CR samples: for the same age, the samples are more distinguished based on PC1 than on PC2. These patterns can be seen more clearly in Figure 2E with only the CR samples shown. For days 2 and 7 the CR samples (see line 3 and 5 respectively in figure 2E) exhibit pattern with CR-LD having a lower PC1 value than

CR-HD, while all other sample have HD with a lower PC1 value than LD. Among the CR samples, there is clear distinction between HD and LD populations. The least variation is in the oldest populations, at day 7, with about 11.5% on PC1 and 0.5% on PC2 (line 5 in Figure 2E). The variation is consistently larger in younger populations. To the first decimal, the approximate distance between the points in the given PC1 (29.5%) and PC2 (19.4%) plot are 11.5% at day 7 (line 5), 27% at day 5 (line 4), 33% at day 2 (line 3), 40.7% at day 1 (line 2), and 31.8% at day 0 (line 1). Only day 0, the youngest population, stands out. This is most likely because at day 0 the culture is not yet at the diauxic stage (like day 1 would be; day 5 would be post-diauxic, and day 7 stationary). Many early commitment proteins are therefore expected to be expressed and phosphorylated – the very proteins that may help in the entry into quiescence, for example. At later age, the programs of quiescence maintenance are in effect. So, the phosphoproteomes are still significantly different (for the given age and culture, at different densities), but are less different from each other as they age together.

Figure 2. Principal component analysis of phosphorylated proteins found in *tor1* deletion mutant *S. cerevisiae* under CR/non-CR with different population densities, at different chronological ages

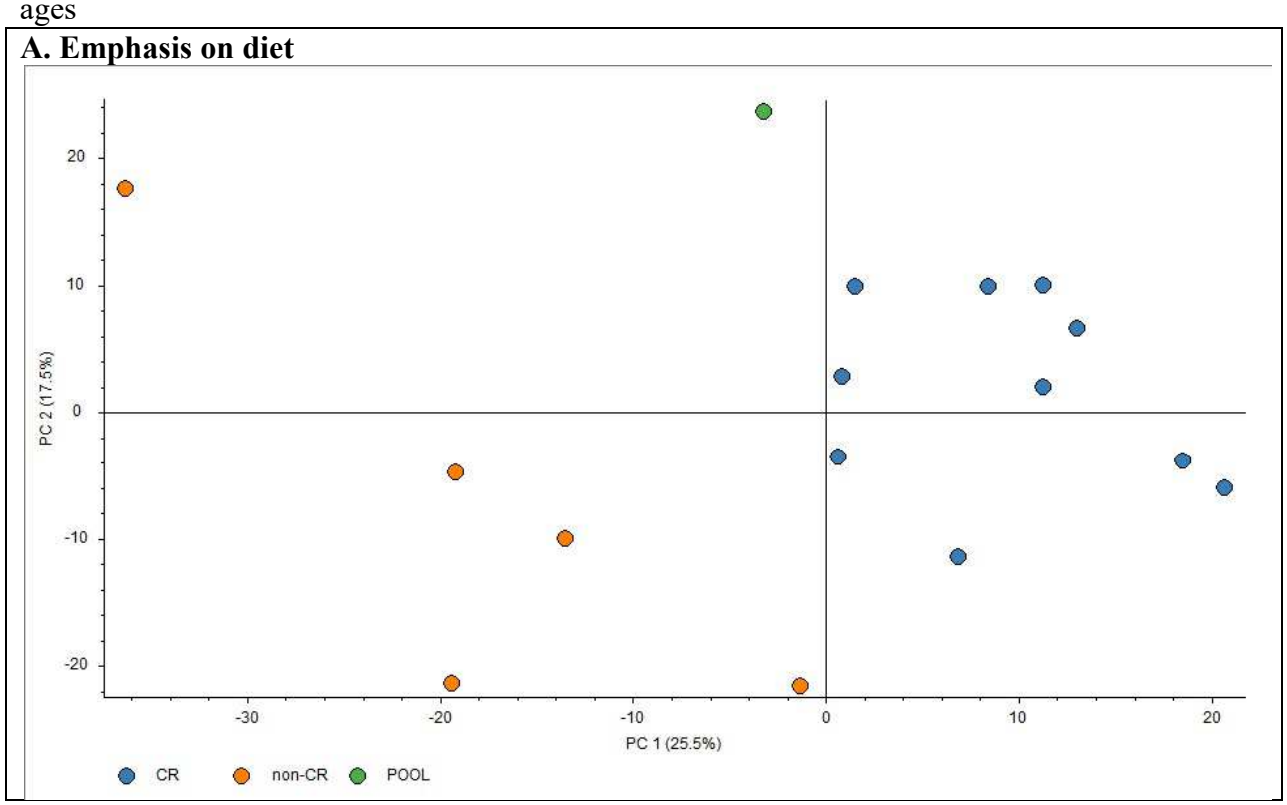

B. Emphasis on density

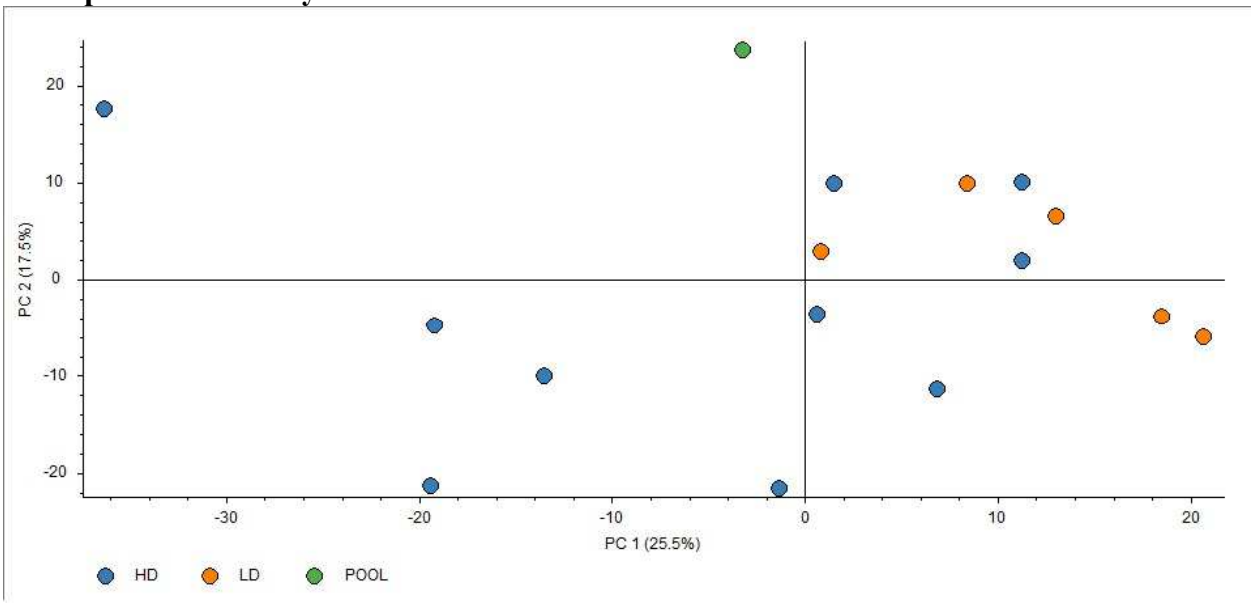

C. Emphasis on diet and density

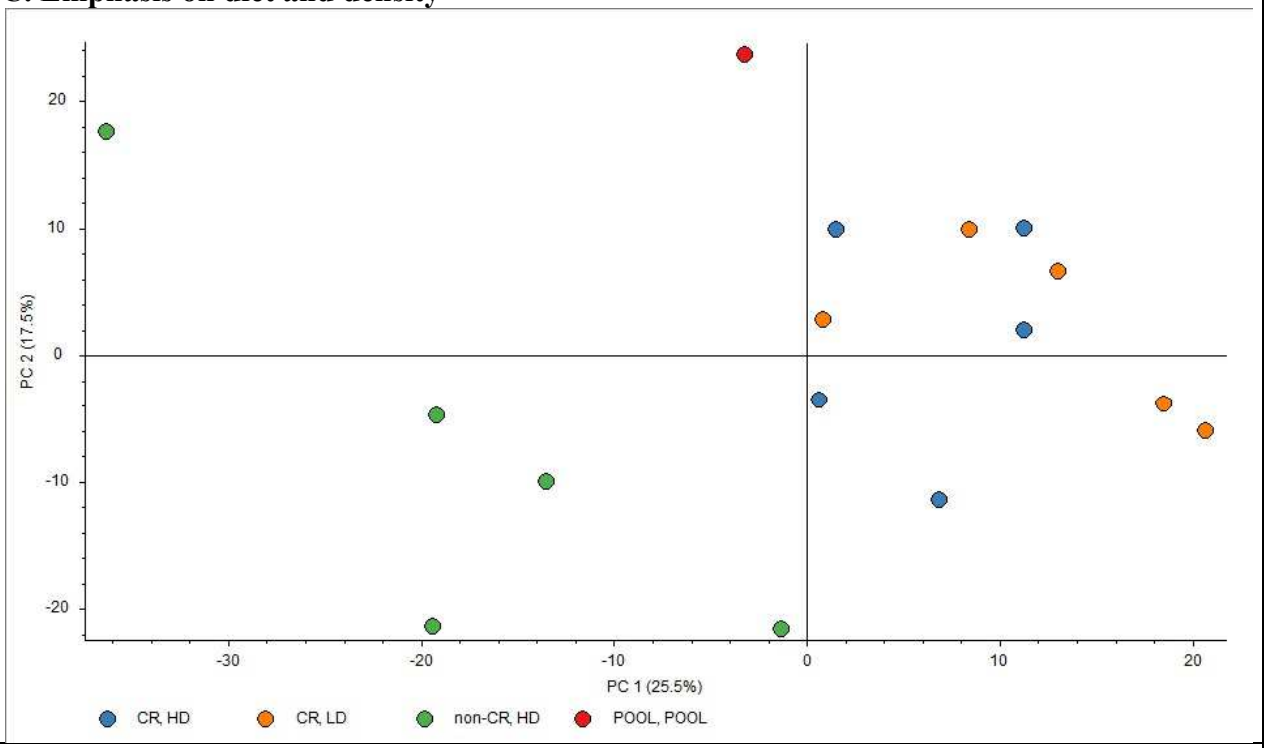

D. All samples identification

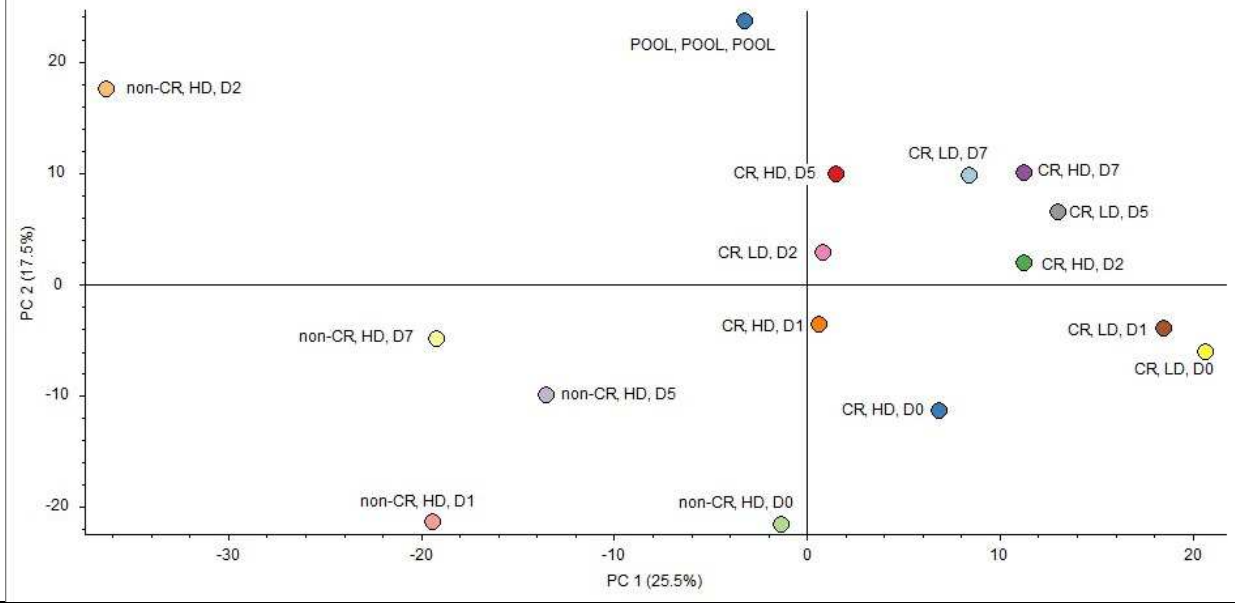

E. Only CR samples

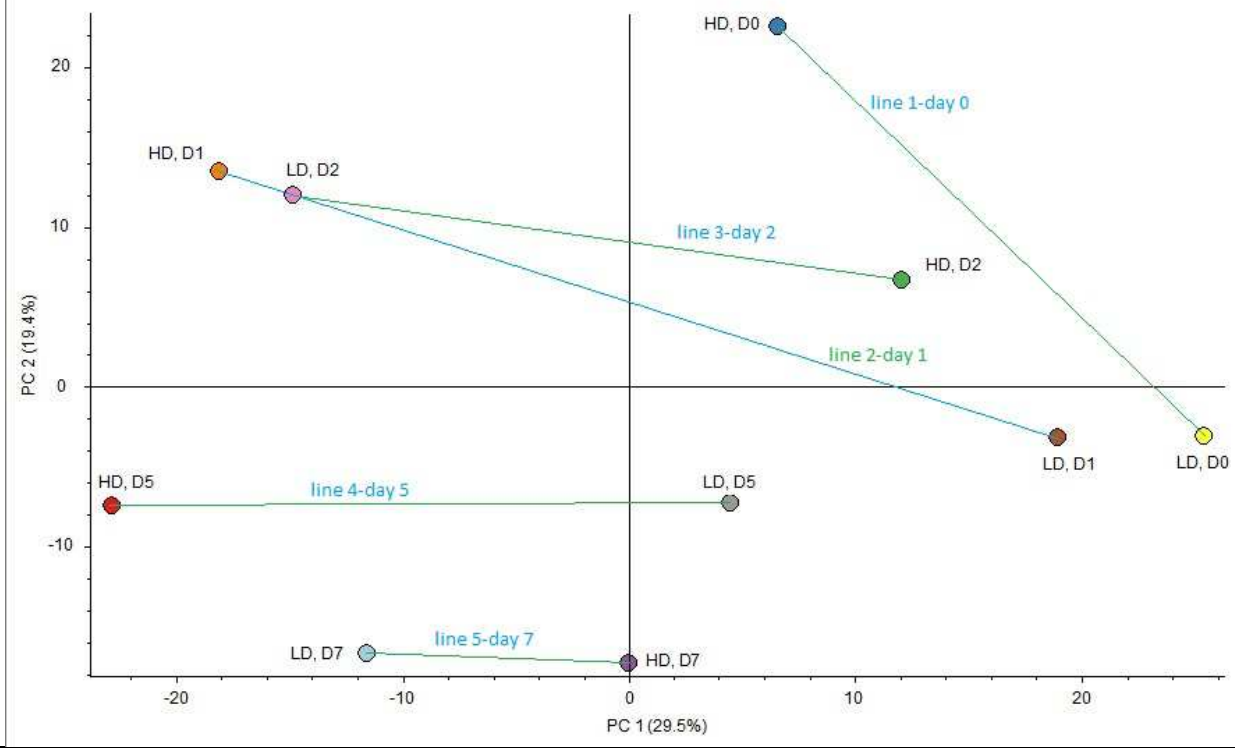

Among the identified phosphoproteins, I not only looked at the patterns (please see above), but also at the phosphorylation sites for unique phosphoproteins. The list of some of the phosphosites can be found in supplemental Tables S1-S10. When setting up the studies of samples within an experiment (such at all *tor1* gene deletion mutants), I processed the samples together with the addition of the pooled sample. As discussed in the previous chapter, I used a pool sample which allows for higher identification of peptides and therefore possible higher number of proteins. However, in the current set up of the software, I cannot assign the phosphosite (Psite) to the respective sample in was found in. In other words, I tradeoff the Psite source for identify more proteins by making a large study. Therefore, by looking at individual studies (i.e. the spectra of a single sample against the database) I regain the Psite assignment. In the supplemental Table S1-S10, I provide the Psites found by making a study along with Psites identified from individual studies. Evidently, I do not find all of the phosphorylated proteins in the individual studies, and so some information is lacking (as seen in Table S10). Moreover, the number of phosphorylated proteins that are unique to a sample in contrast to its comparable sample (see Figures 2.1-2.5) does not match the number of phosphorylated proteins in the Tables S1-S10 (which is why these tables are provided as supplemental material and not as the core of my thesis). The main reason that these quantities do not add up is due to the stringency of selecting the present/not proteins. From the large study, the software analyses and includes samples that have peaks that are not intense (i.e. low relative abundance of peptide fragment). While making the lists in Tables S1-S10, I manually selected only proteins that are found in high amounts in one sample and not found in the other sample. To clarify: I did not include samples that have a peak found (but are not high abundance) when selecting unique phosphoproteins. For example, a theoretical protein X may have a peak found in sample 1, but no peak found in sample 2: the Venn diagram would include such protein X as unique to sample 1 (not present in sample 2). Manually, however, I do not include such a protein X, because it is not in high abundance in sample 1.

As anticipated by the hypothesis, the populations (Q-CR, NQ-CR, and Q-non-CR) are different from each other. This can be seen by the number of unique phosphoproteins for the given sample pair comparison (as seen in Figures 2.1-2.5 in chronological order of the yeast culture). The relative abundance of all samples was uniform at the peptide level (Figure S8A), and at the protein level (Figure S8B).

Figure 2.1. Number of phosphoproteins unique to sample in *tor1* deletion *S. cerevisiae* – day 0

A.

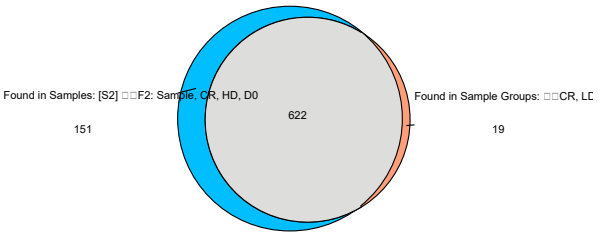

Colour	Exclusive	Total	Found in sample
	151	773	CR, HD, D0
	19	641	CR, LD, D0
	622	622	CR, HD, D0 and CR, LD, D0
Sum	792		

B.

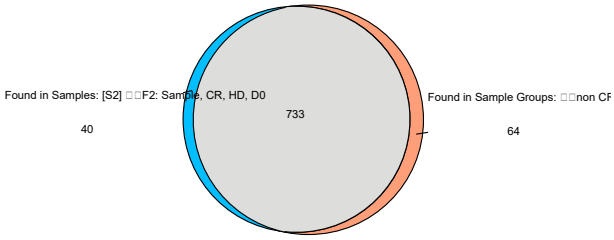

Colour	Exclusive	Total	Found in sample
	40	773	CR, HD, D0
	64	797	non-CR, HD, D0
	733	733	CR, HD, D0 and non-CR, HD, D0
Sum	837		

Figure 2.2. Number of phosphoproteins unique to sample in *tor1* deletion *S. cerevisiae* – day 1

A.

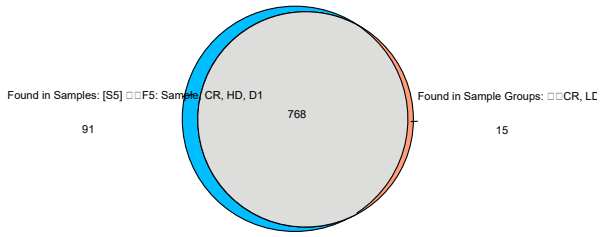

Colour	Exclusive	Total	Found in sample
	91	859	CR, HD, D1
	15	783	CR, LD, D1
	768	768	CR, HD, D1 and CR, LD, D1
Sum	874		

B.

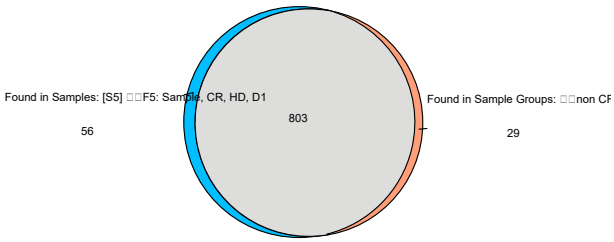

Colour	Exclusive	Total	Found in sample
	56	859	CR, HD, D1
	29	832	non-CR, HD, D1
	803	803	CR, HD, D1 and non-CR, HD, D1
Sum	888		

Figure 2.3. Number of phosphoproteins unique to sample in *tor1* deletion *S. cerevisiae* – day 2

A.

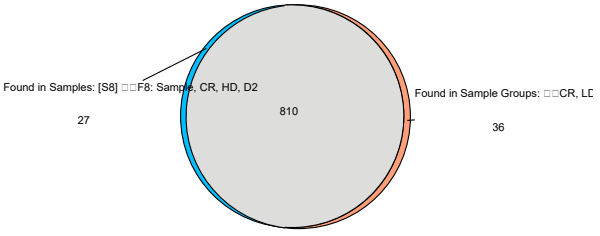

B.

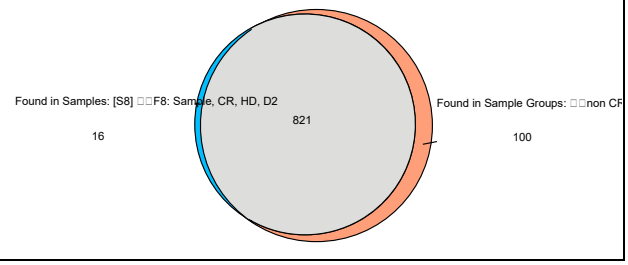

Colour	Exclusive	Total	Found in sample
	27	837	CR, HD, D2
	36	846	CR, LD, D2
	810	810	CR, HD, D2 and CR, LD, D2
Sum	873		

Colour	Exclusive	Total	Found in sample
	16	837	CR, HD, D2
	100	921	non-CR, HD, D2
	821	821	CR, HD, D2 and: non-CR, HD, D2
Sum	937		

Figure 2.4. Number of phosphoproteins unique to sample in *tor1* deletion *S. cerevisiae* – day 5

A.

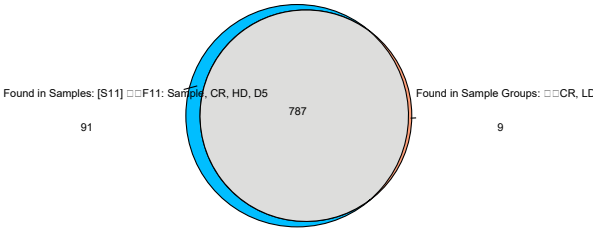

Colour	Exclusive	Total	Found in sample
	91	878	CR, HD, D5
	9	796	CR, LD, D5
	787	787	CR, HD, D5 and CR, LD, D5
Sum	887		

B.

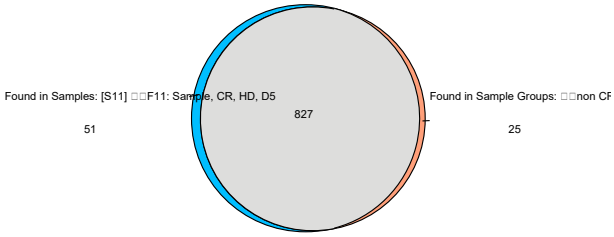

Colour	Exclusive	Total	Found in sample
	51	878	CR, HD, D5
	25	852	non-CR, HD, D5
	827	827	CR, HD, D5 and non-CR, HD, D5
Sum	903		

Figure 2.5. Number of phosphoproteins unique to sample in *tor1* deletion *S. cerevisiae* – day 7

A.

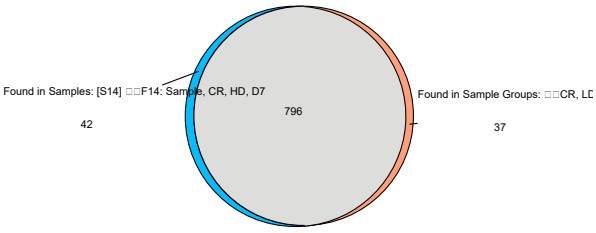

Colour	Exclusive	Total	Found in sample
	42	838	CR, HD, D7
	37	833	CR, LD, D7
	796	796	CR, HD, D7 and CR, LD, D7
Sum	875		

B.

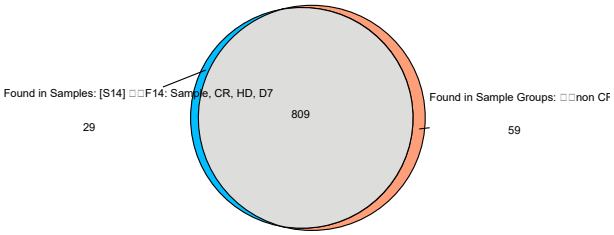

Colour	Exclusive	Total	Found in sample
	29	838	CR, HD, D7
	59	868	non-CR, HD, D7
	809	809	CR, HD, D7 and non-CR, HD, D7
Sum	897		

The hypothesis regarding discovery of novel phosphosites in this mutant model was confirmed by looking at the phosphorylation of unique proteins. There are novel Psites in the shared (not unique) phosphoproteins also (not shown in this thesis). Tables S1 and S2, for day 0, include a protein kinase search of the online databases Uniprot (at www.uniprot.org) and BioGrid (at www.thebiogrid.org); this search was done manually, by looking at all the PTM described for the

given protein. For this young cell population, among its unique phosphoproteins can be seen SCH9 (P11792) that has known residues under the control of TOR1 kinase activity. The sample SCH9 was exclusively found in is day 0 – CR – HD: chronologically young quiescent cells initially grown under calorie restriction condition. Since the cells lack TOR1, I expect these phosphosites to not be phosphorylated, unless there is another protein kinase known (or suggested) to overlap in phosphorylation. The residues of SCH9 known to be phosphorylated by TOR1 are S711, T723, S726, T737, S758, and S765 (in red in Table S1). As expected, none of these residues were found phosphorylated. The Psites found in this mutant are S288, S289, and S290. All three of these phosphosites have been previously described in literature; yet, have no putative protein kinase responsible for these phosphorylation events.

As mentioned before, many of the found phosphosites are novel. It is possible that they have been found previously be researchers. However, since there is no data available on the major databases (including UniProt, which has both manually curated and unverified, automatically assigned information), it can be said that these phosphosites are novel. An example of such Psites is found on uncharacterized membrane protein YDL218W (Q07629) with no known phosphosites. I found 15 novel phosphosites: T219, S220, S266, S272 Y279, S280, T281, S284, S288, Y289, T294, S299, S303, S305, T306 among which S272, S288, S303, S305, and T306 are from sample of HD cells initially grown under CR and harvested at day 0 (these Psites may be found in other samples as well) (Table S1). I also found novel phosphosites for previously described proteins such as for the nucleoside diphosphate kinase (YNK1; P36010) which has a single known phosphosite at T95. I found phosphorylated residues T95 (known), T104, S121, and S123 (Table S1). This protein has no described putative protein kinase responsible.

In conclusion, by studying *tor1* gene deletion mutant, I found that, as expected, the samples different greatly based on their diet (initially under calorie restriction or not) and based on their state of quiescence (for cultures initially grown under caloric restriction). I found that the absence of TOR1 allowed cells initially grown under not calorically restricted conditions to be mainly quiescent (high density). I also found many novel phosphorylation sites among the proteins.

REFERENCES

Allen C, Büttner S, Aragon AD, Thomas JA, Meirelles O, Jaetao JE, Benn D, Ruby SW, Veenhuis M, Madeo F, Werner-Washburne M. Isolation of quiescent and nonquiescent cells from yeast stationary-phase cultures. J Cell Biol. 2006 Jul 3;174(1):89-100.

Ardito F, Giuliani M, Perrone D, Troiano G, Lo Muzio L. The crucial role of protein phosphorylation in cell signaling and its use as targeted therapy (Review). Int J Mol Med. 2017 Aug;40(2):271-280. doi: 10.3892/ijmm.2017.3036. Epub 2017 Jun 22. Review.

Florian S, Hümmer S, Catarinella M, Mayer TU. Chemical genetics: reshaping biology through chemistry. HFSP J. 2007 Jul;1(2):104-14. doi: 10.2976/1.2752600. Epub 2007 Jul 12.

Giaever G, Nislow C. The yeast deletion collection: a decade of functional genomics. Genetics. 2014 Jun;197(2):451-65. doi: 10.1534/genetics.114.161620. Epub 2014 Jun 17. Review.

Gray JV, Petsko GA, Johnston GC, Ringe D, Singer RA, Werner-Washburne M. "Sleeping beauty": quiescence in Saccharomyces cerevisiae. Microbiol Mol Biol. Rev. 2004 Jun;68(2):187-206. Review.

Heitman J, Movva NR, Hall MN. Targets for cell cycle arrest by the immunosuppressant rapamycin in yeast. Science. 1991 Aug 23;253(5022):905-9. Retrieved from http://www.jstor.org.lib-ezproxy.concordia.ca/stable/2878946

Humphrey SJ, James DE, Mann M. Protein Phosphorylation: A Major Switch Mechanism for Metabolic Regulation. Trends Endocrinol Metab. 2015 Dec;26(12):676-687. doi: 10.1016/j.tem.2015.09.013. Epub 2015 Oct 20. Review.

Kaeberlein M, Kennedy BK. Large-scale identification in yeast of conserved ageing genes. Mech Ageing Dev. 2005 Jan;126(1):17-21. Review.

Kim LC, Cook RS, Chen J. mTORC1 and mTORC2 in cancer and the tumor microenvironment. Oncogene. 2017 Apr 20;36(16):2191-2201. doi:10.1038/onc.2016.363. Epub 2016 Oct 17. Review.

Leonov A, Feldman R, Piano A, Arlia-Ciommo A, Lutchman V, Ahmadi M, Elsaser S, Fakim H, Heshmati-Moghaddam M, Hussain A, Orfali S, Rajen H, Roofigari-Esfahani N, Rosanelli L, Titorenko VI. Caloric restriction extends yeast chronological lifespan via a mechanism linking cellular aging to cell cycle regulation, maintenance of a quiescent state, entry into a non-quiescent state and survival in the non-quiescent state. Oncotarget. 2017 Sep 1;8(41):69328-69350. doi: 10.18632/oncotarget.20614. eCollection 2017 Sep 19.

López-Otín C, Blasco MA, Partridge L, Serrano M, Kroemer G. The hallmarks of aging. Cell. 2013 Jun 6;153(6):1194-217. doi: 10.1016/j.cell.2013.05.039. Review.

Mohammad K, Dakik P, Medkour Y, **Mitrofanova D**, Titorenko VI. Quiescence Entry, Maintenance, and Exit in Adult Stem Cells. Int J Mol Sci. 2019 May 1;20(9). pii: E2158. doi: 10.3390/ijms20092158. Review.

Mohammad K, Titorenko VI. Yeast chronological aging is linked to cell cycle regulation. Cell Cycle. 2018; 17(9):1035-1036. doi: 10.1080/15384101.2018.1478670.

Needham EJ, Parker BL, Burykin T, James DE, Humphrey SJ. Illuminating the dark phosphoproteome. Sci Signal. 2019 Jan 22;12(565). pii: eaau8645. doi: 10.1126/scisignal.aau8645. Review.

Powers RW 3rd, Kaeberlein M, Caldwell SD, Kennedy BK, Fields S. Extension of chronological life span in yeast by decreased TOR pathway signaling. Genes Dev. 2006 Jan 15;20(2):174-84.

Raught B, Gingras AC, Sonenberg N. The target of rapamycin (TOR) proteins. Proc Natl Acad Sci U S A. 2001 Jun 19;98(13):7037-44. Review.

Riley NM, Coon JJ. Phosphoproteomics in the Age of Rapid and Deep Proteome Profiling. Anal Chem. 2016 Jan 5;88(1):74-94. doi: 10.1021/acs.analchem.5b04123. Epub 2015 Nov 19. Review.

Thermo Fisher Scientific. Phosphorylation. Retrieved from https://www.thermofisher.com/ca/en/home/life-science/protein-biology/protein-biology-learning-center/protein-biology-resource-library/pierce-protein-methods/phosphorylation.html

UniProt Consortium European Bioinformatics Institute Protein Information Resource SIB Swiss Institute of Bioinformatics. (2019). Serine/threonine-protein kinase mTOR. Retrieved from https://www.uniprot.org/uniprot/P42345

UniProt Consortium European Bioinformatics Institute Protein Information Resource SIB Swiss Institute of Bioinformatics. (2019). Target of rapamycin homolog. Retrieved from https://www.uniprot.org/uniprot/Q95Q95

Weaver, R. F. (2012). *Molecular biology* (5th ed.). Chapter 17.3. Control of initiation. p549-551. New York: McGraw-Hill.

Wullschleger S, Loewith R, Hall MN. TOR signaling in growth and metabolism. Cell. 2006 Feb 10;124(3):471-84. Review.

Yeast pathways – SGD - Saccharomyces cerevisiae Pathway: superpathway of threonine biosynthesis. https://pathway.yeastgenome.org/YEAST/NEW-IMAGE?type=PATHWAY&object=PWY3O-7 Created 09-Aug-2007 by Krieger C , SGD

Figure S1. Cellular localization of phosphoproteins found in WT *Saccharomyces cerevisiae* – day 0

A. Phosphoproteins per sample

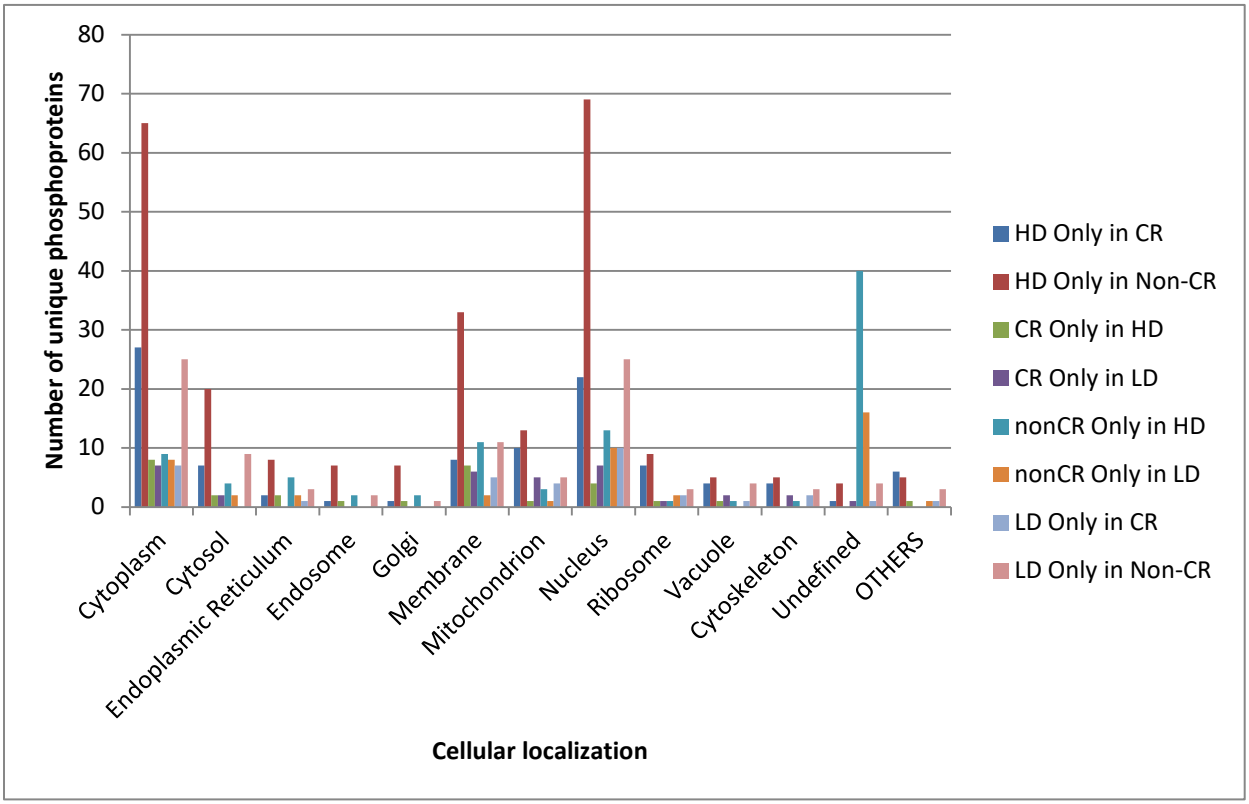

B. Phosphoproteins groups

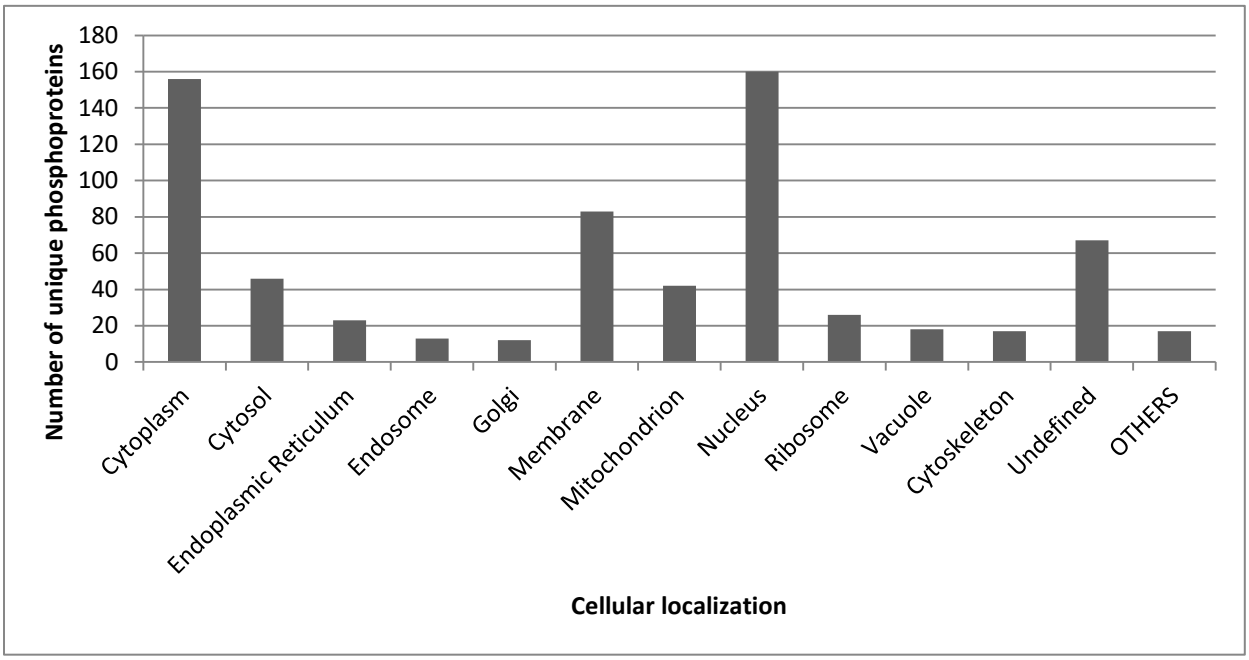

Figure S2. Cellular localization of phosphoproteins found in WT *Saccharomyces cerevisiae* – day 1

A. Phosphoproteins per sample

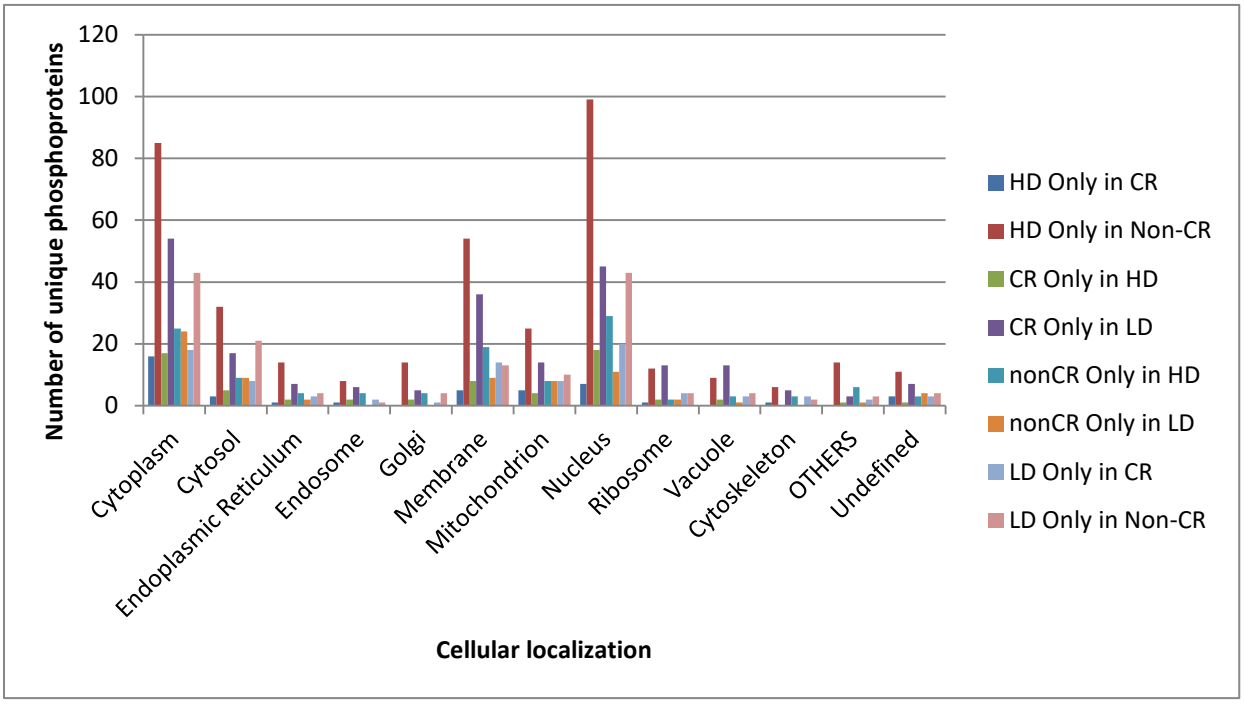

B. Phosphoproteins groups

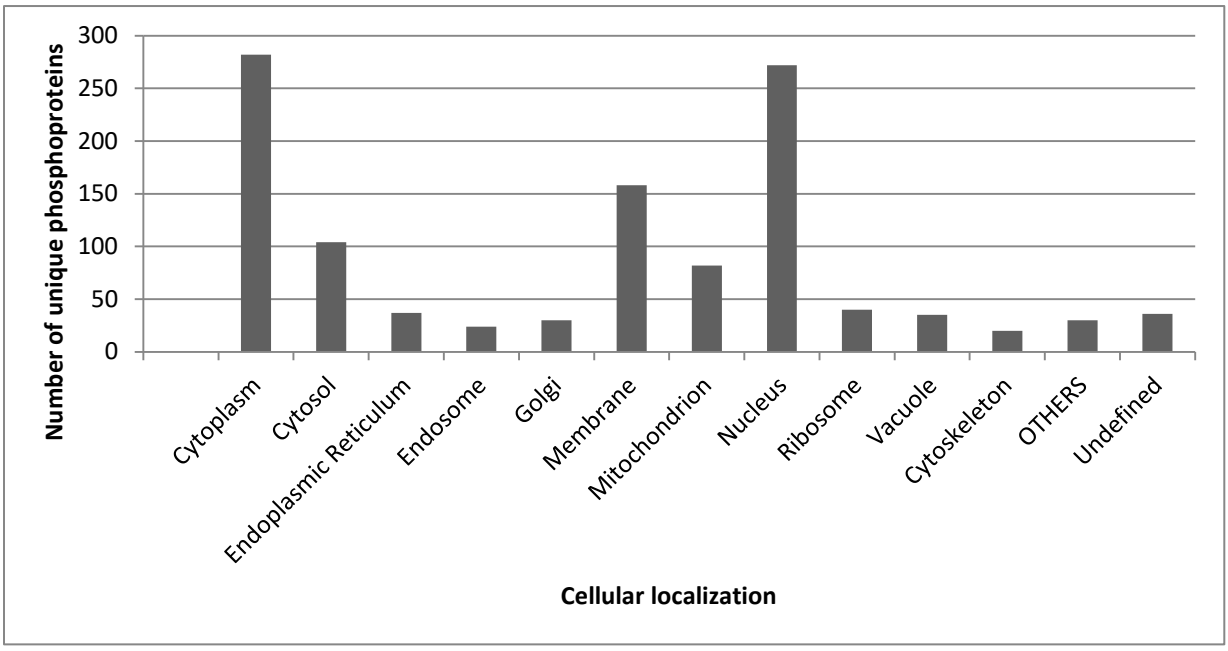

Figure S3. Cellular localization of phosphoproteins found in WT *Saccharomyces cerevisiae* – day 2

A. Phosphoproteins per sample

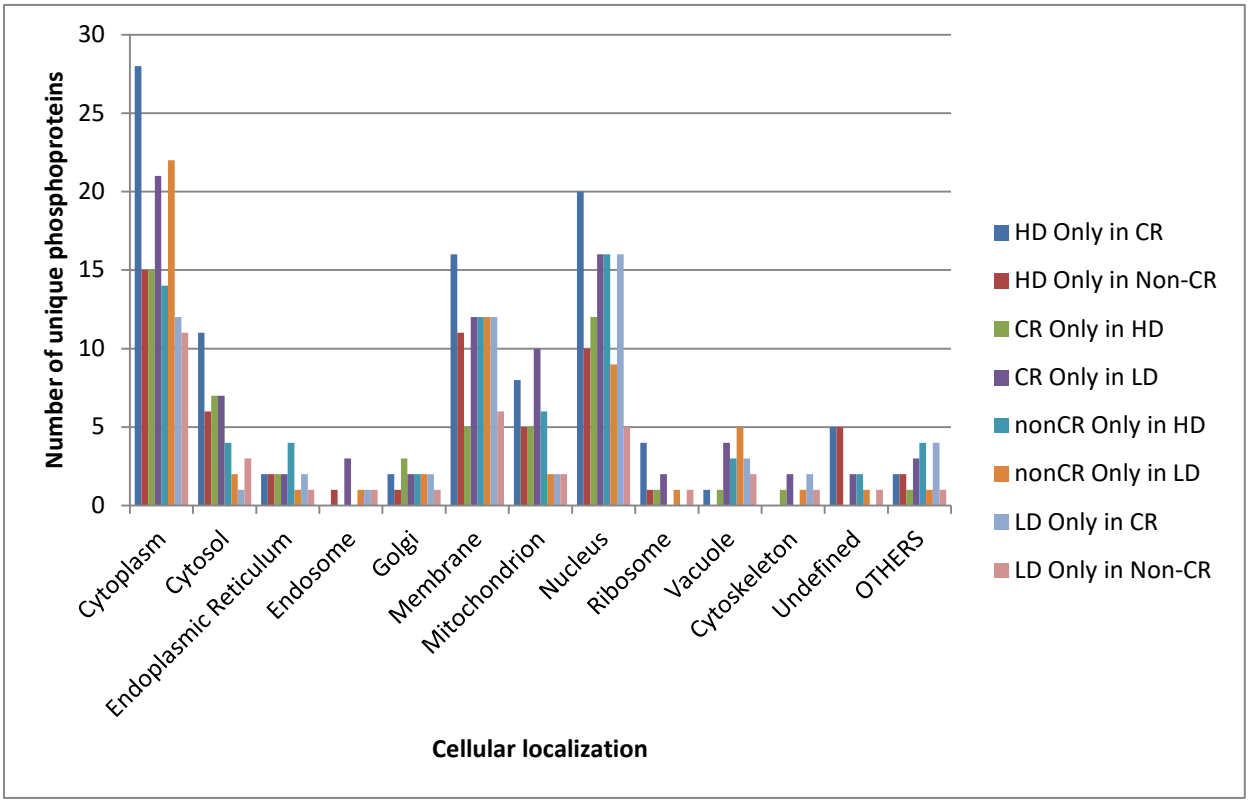

B. Phosphoproteins groups

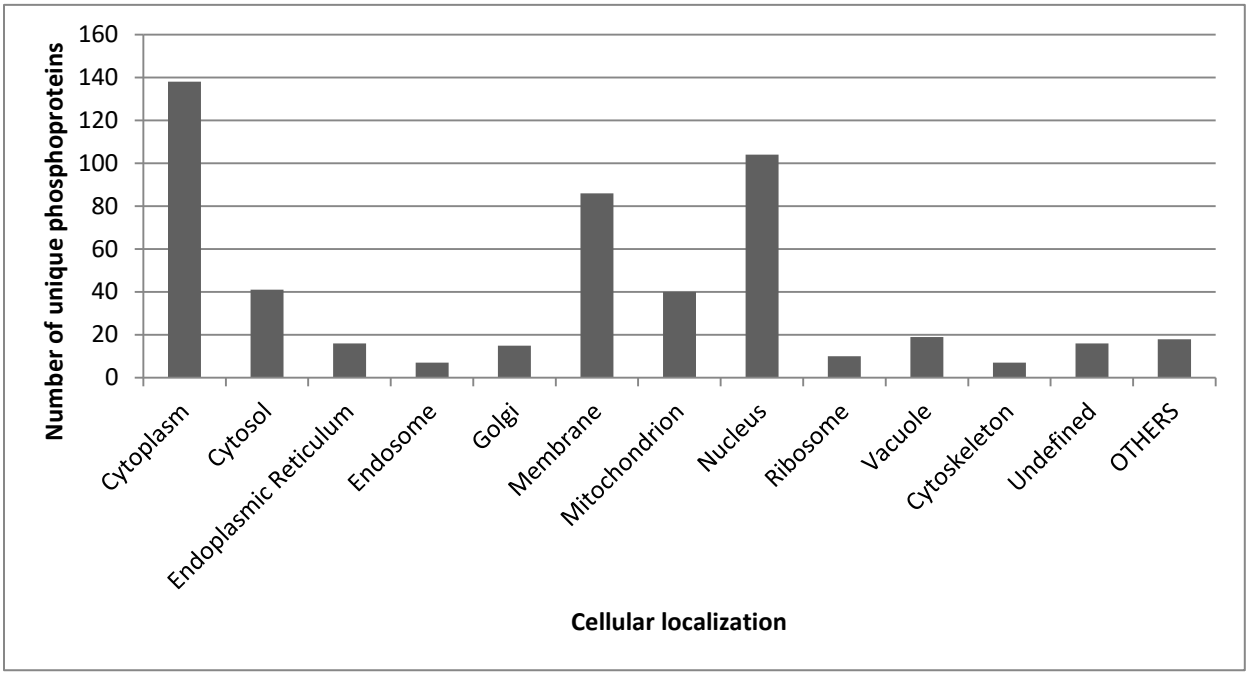

Figure S4. Cellular localization of phosphoproteins found in WT *Saccharomyces cerevisiae* – day 5

A. Phosphoproteins per sample

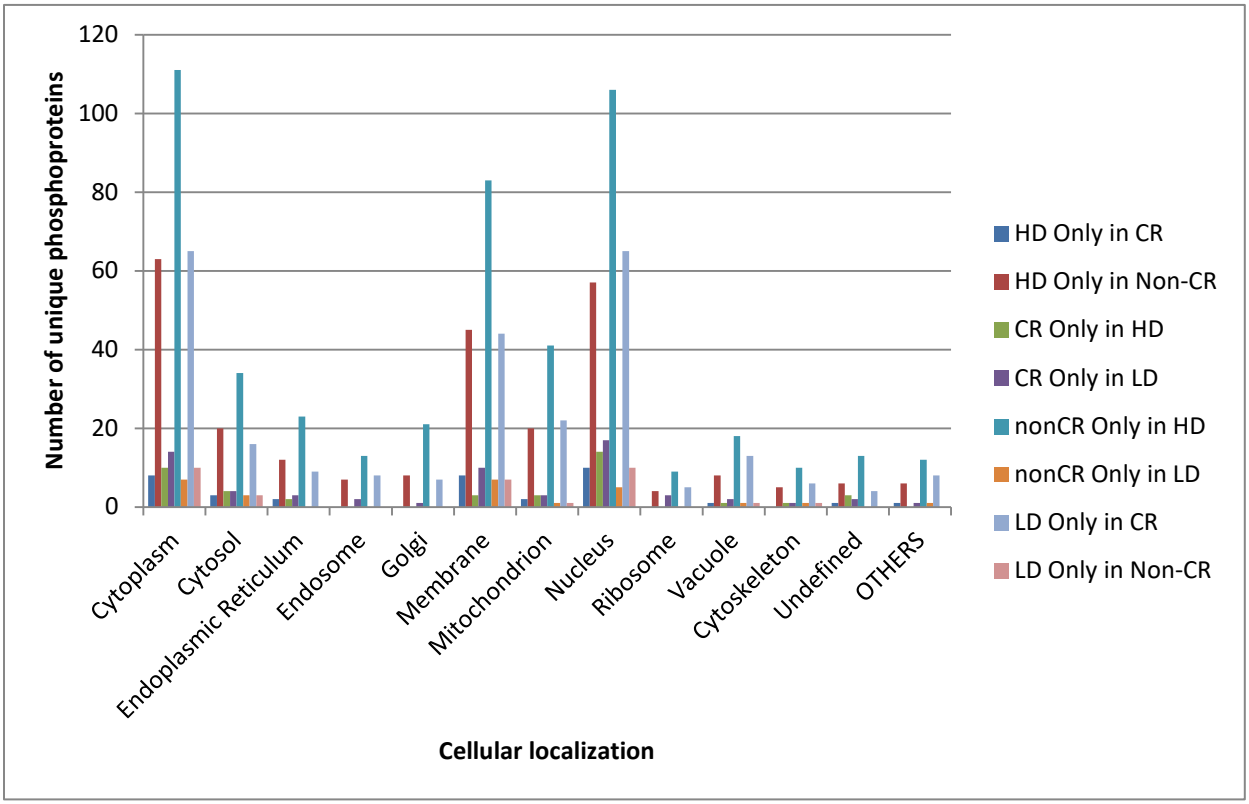

B. Phosphoproteins groups

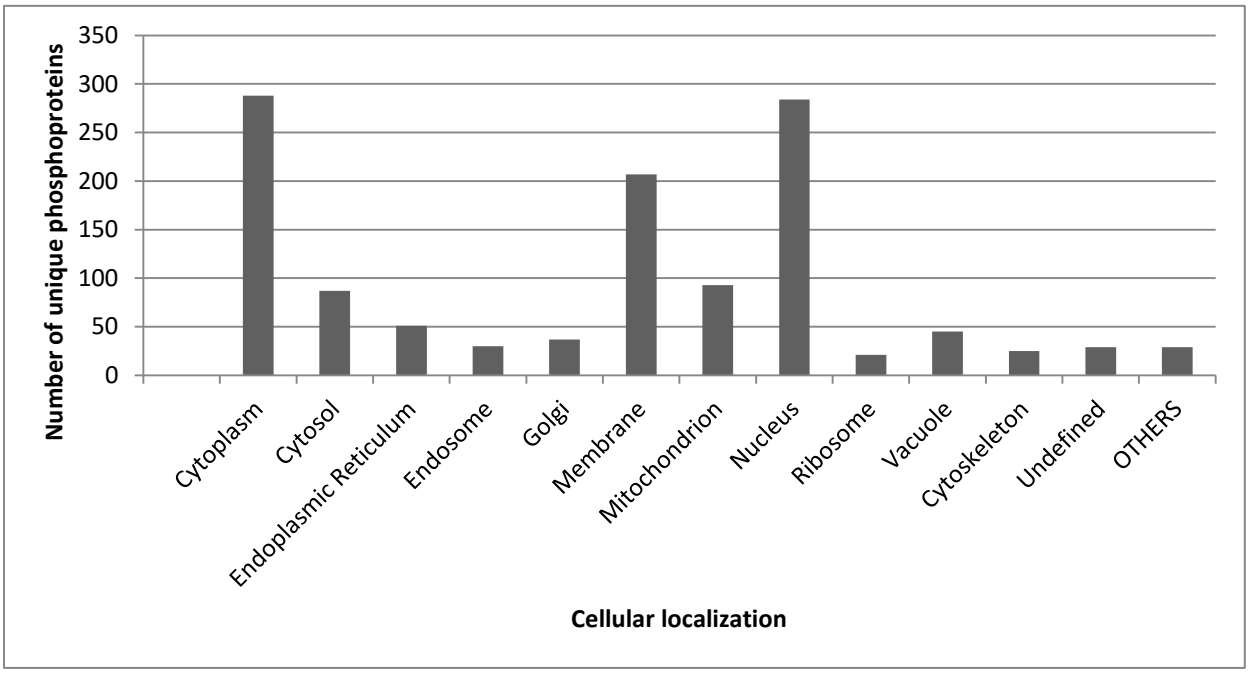

Figure S5. Cellular localization of phosphoproteins found in WT *Saccharomyces cerevisiae* – day 7

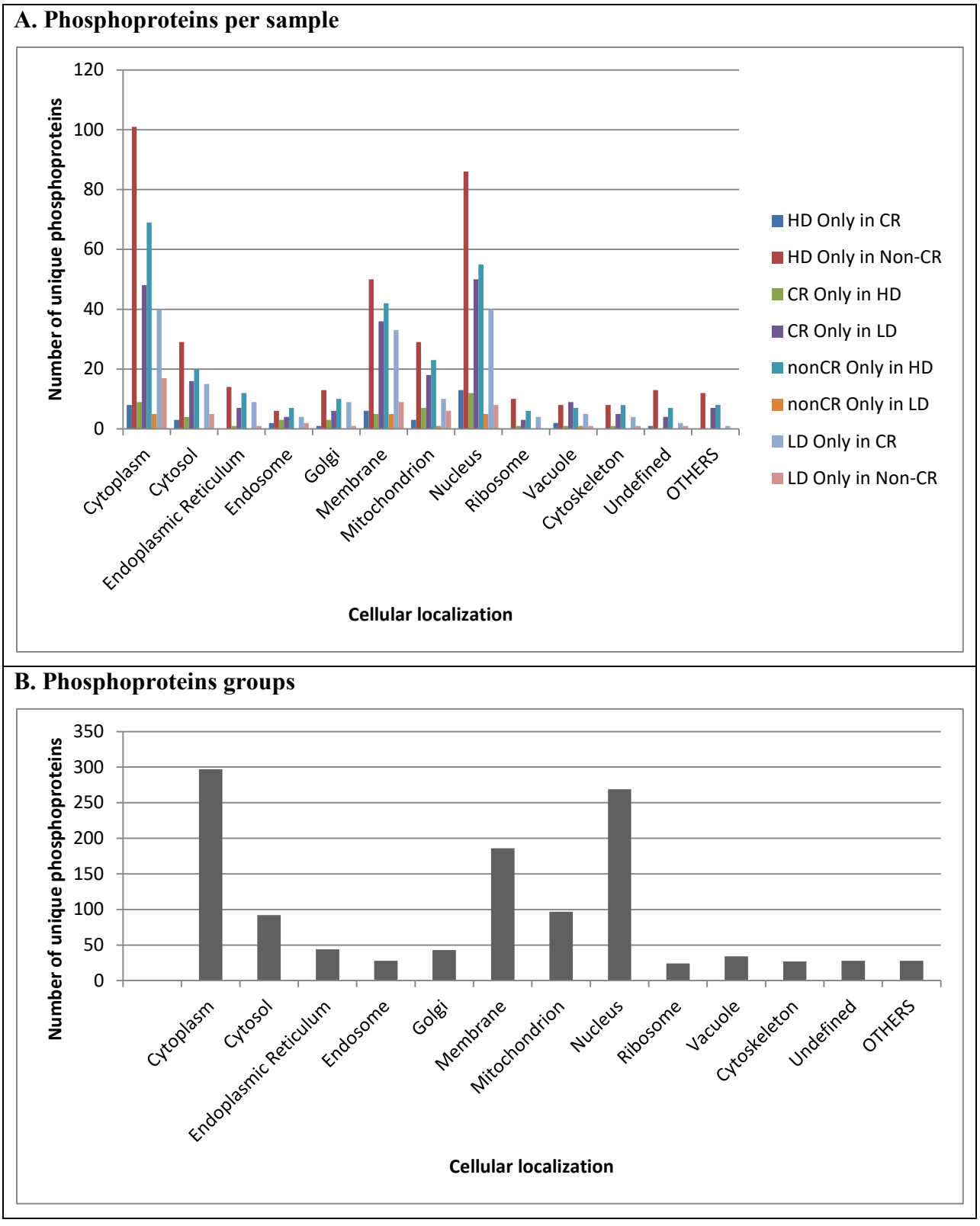

Figure S6 A. Relative sample abundance – WT experiment 1 – peptide groups

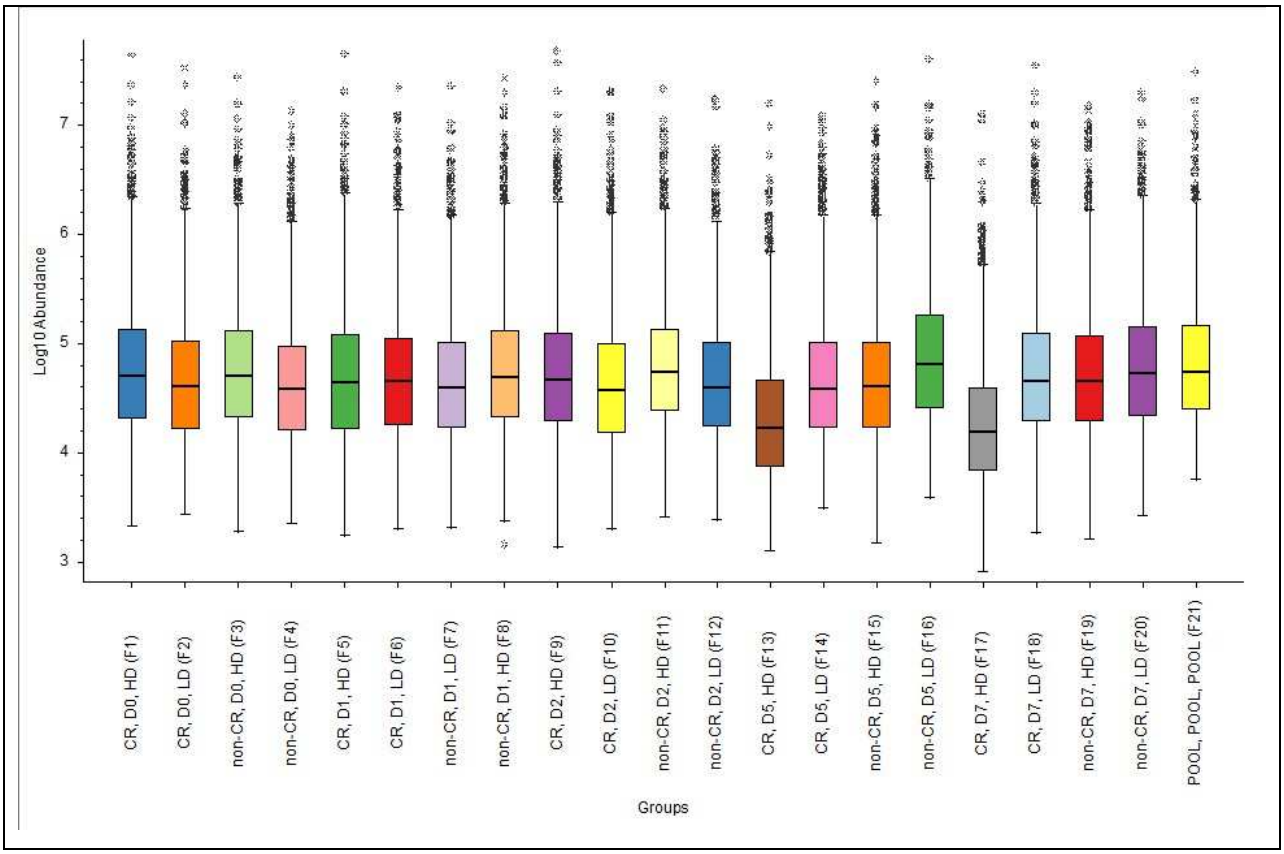

Figure S6 B. Relative sample abundance – WT experiment 1 – proteins

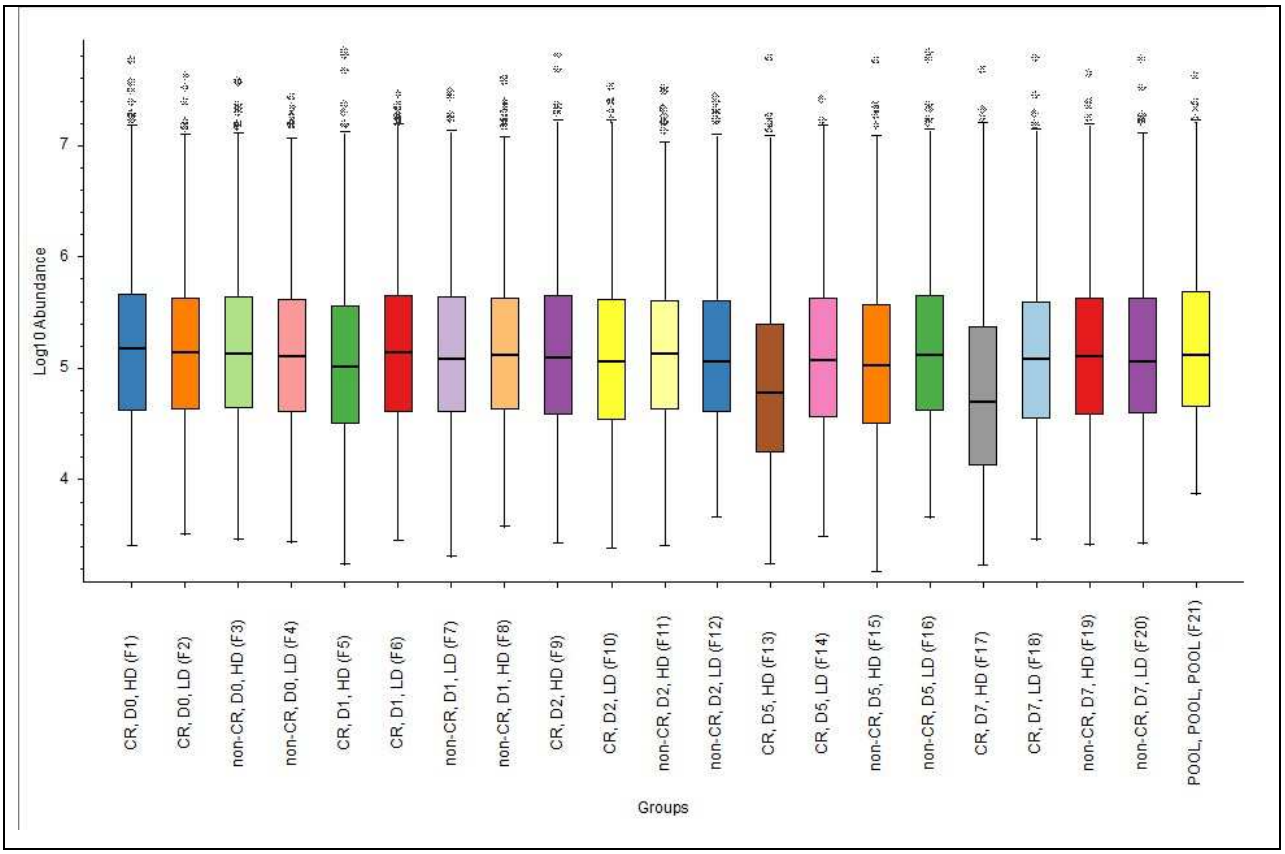

Figure S7 A. Relative sample abundance – WT experiment 2 – peptide groups

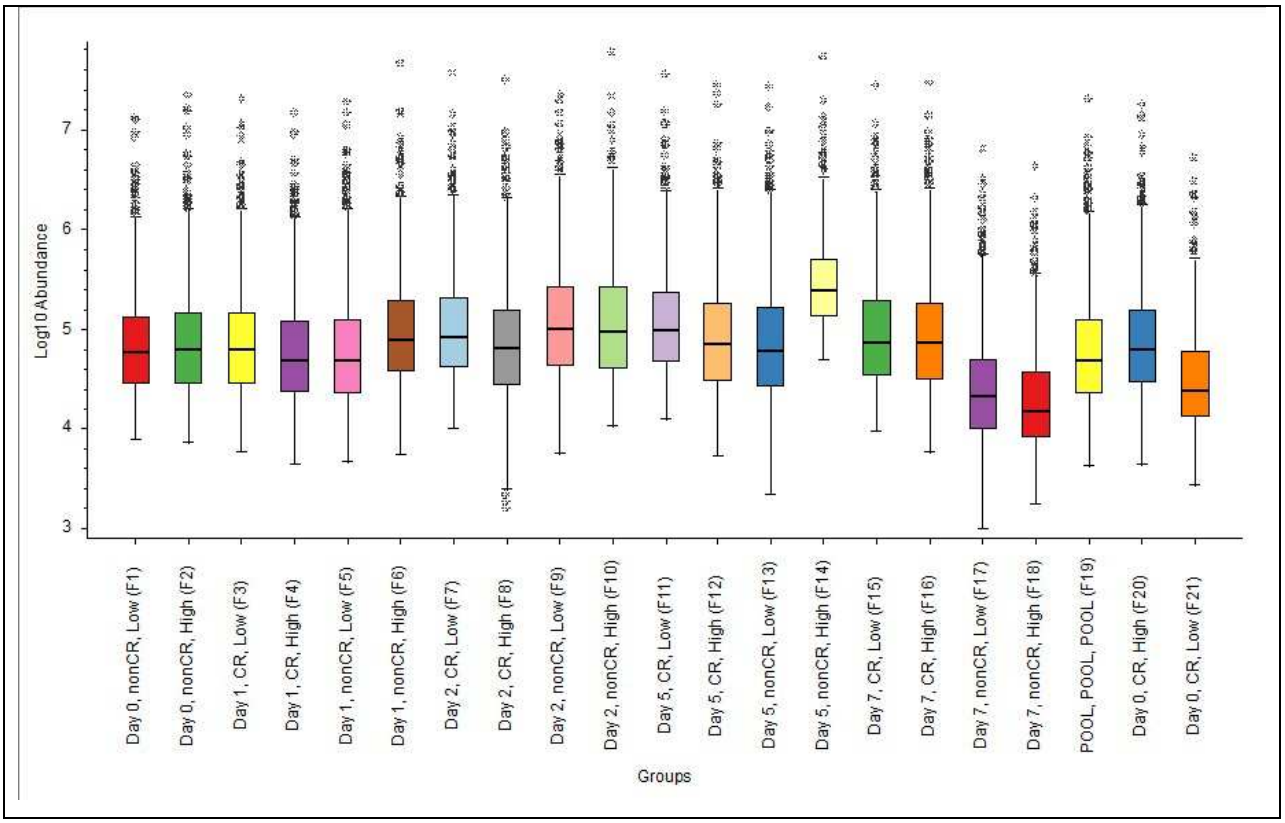

Figure S7 B. Relative sample abundance – WT experiment 2 – proteins

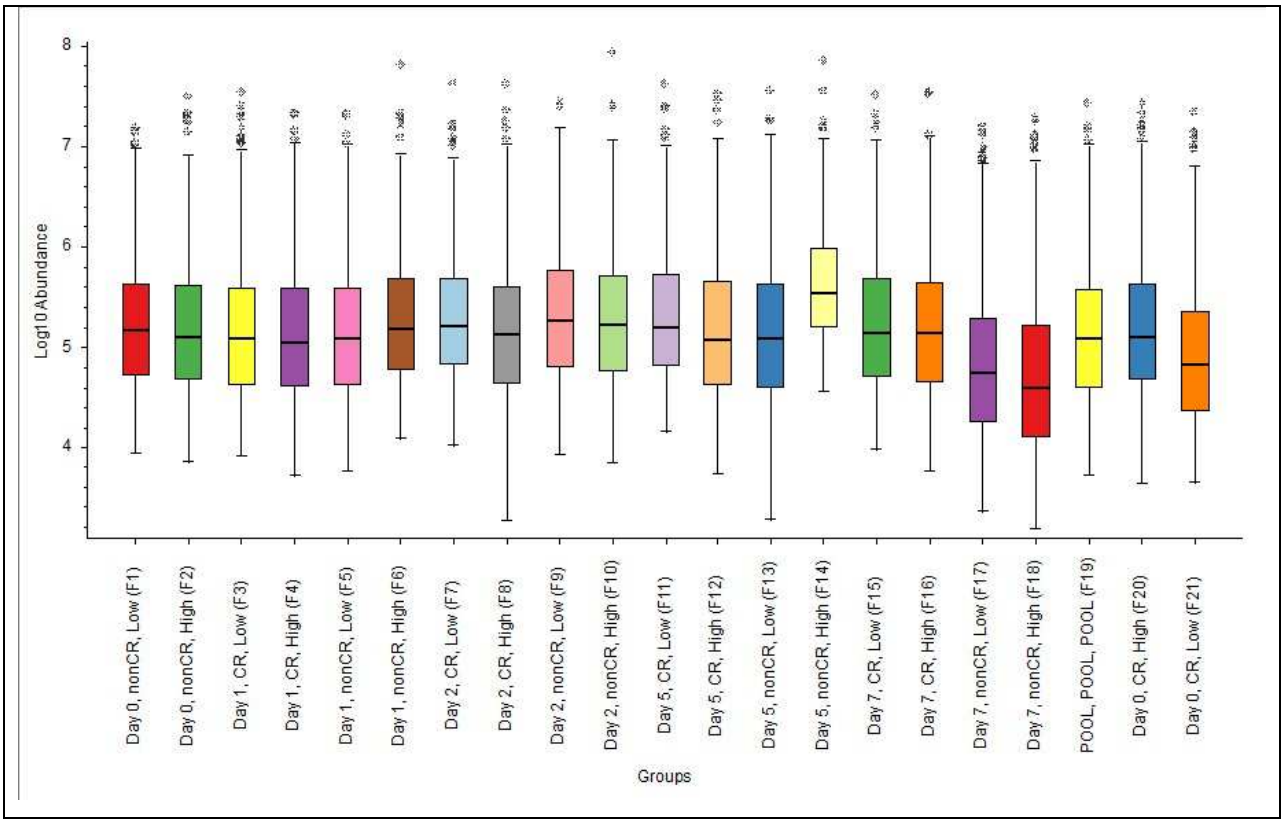

Figure S8A. Relative sample abundance – *tor1*Δ - peptide groups

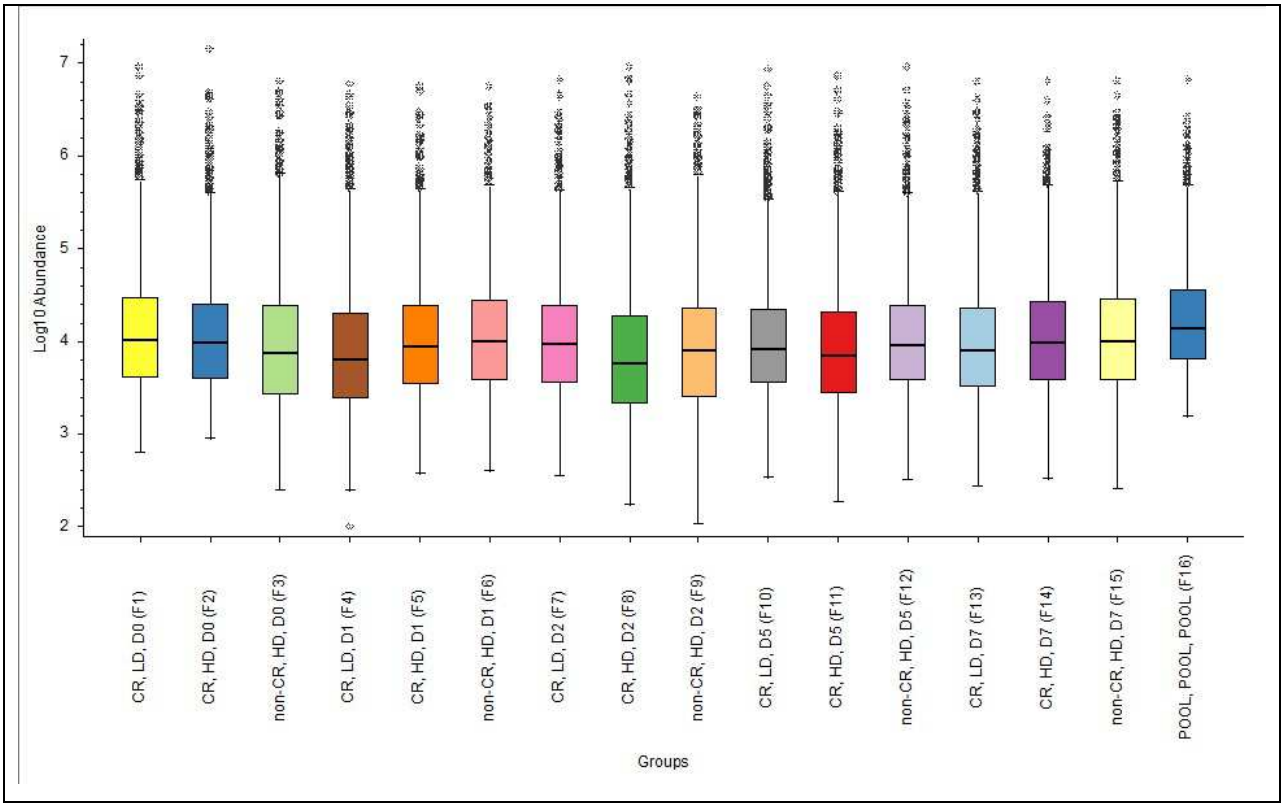

Figure S8B. Relative sample abundance – *tor1*Δ - proteins

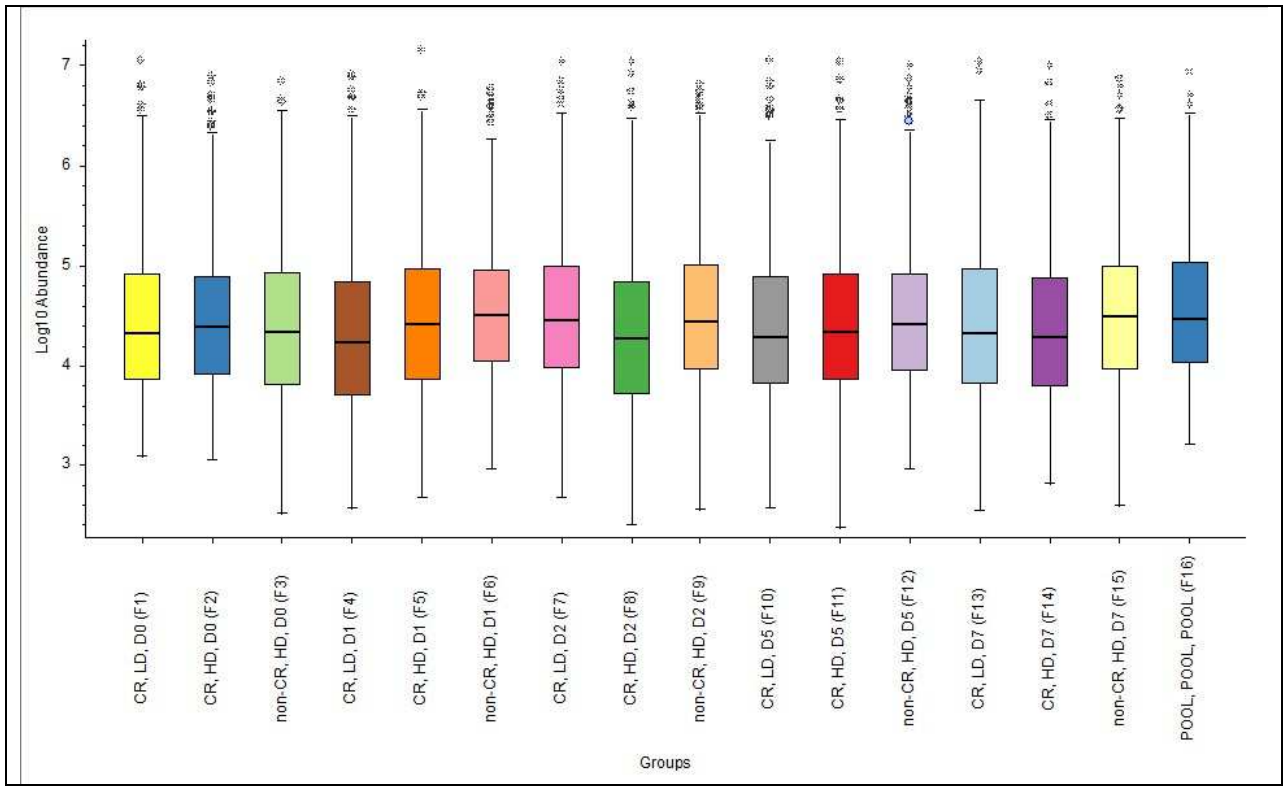

Figure S9. Missed cleavage by trypsin – WT – experiment 1

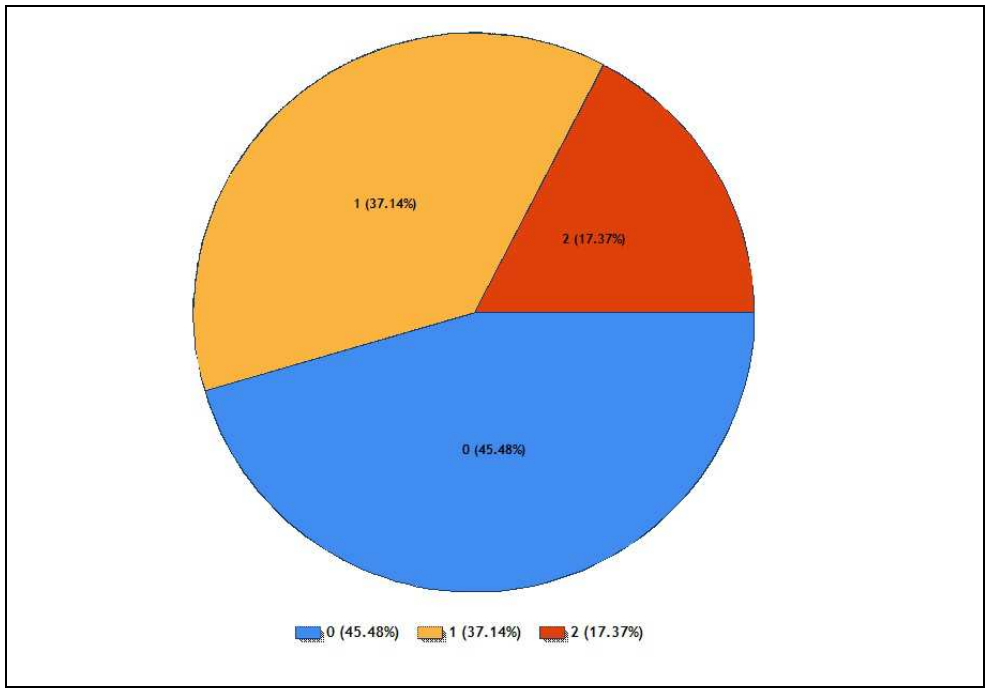

Figure S10. Missed cleavage by trypsin – WT – experiment 2

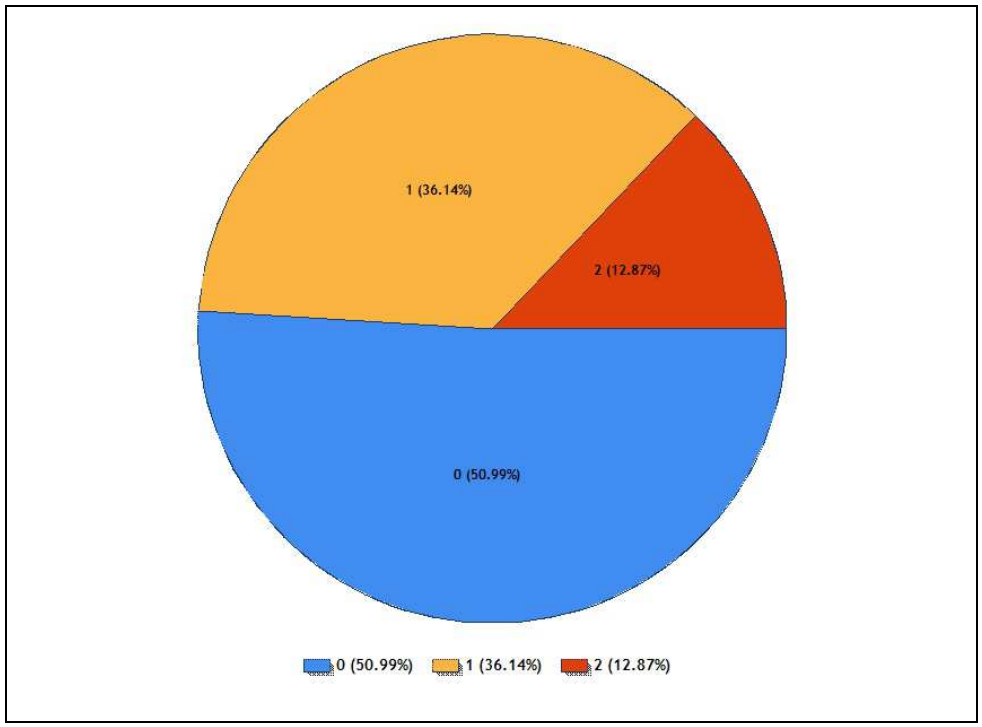

S11. Missed cleavage by trypsin –*tor1Δ*

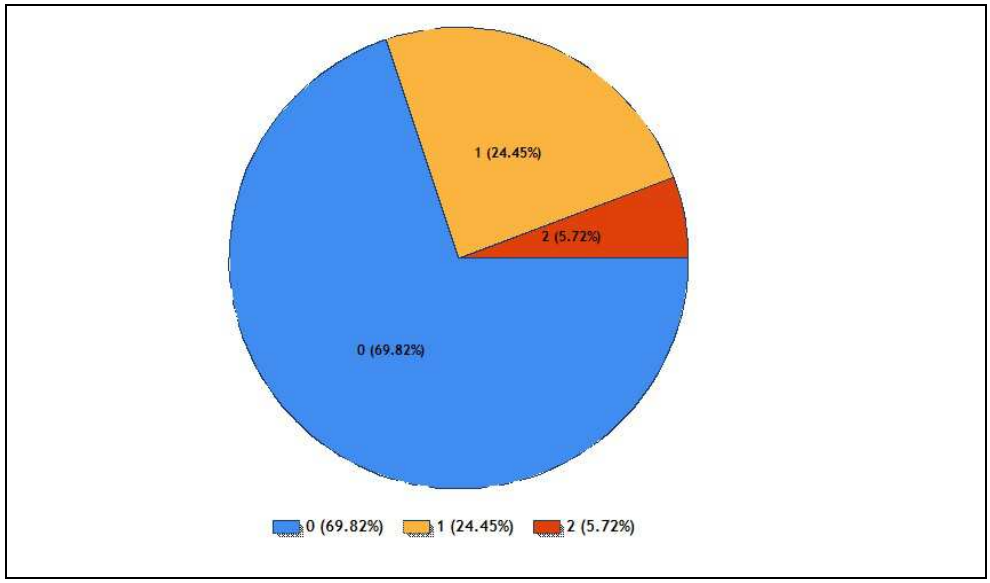

Table S1. Novel phosphosites found in *tor1* mutant *Saccharomyces cerevisiae*, and associated kinases – day 0 CR HD/LD

			All phoshosites found		Phosphosites found in respective sample		Psites in literature		
Accession	Description	Found in day 0 CR:	Phospho (S; T; Y) Count	Phospho (S; T; Y) Positions	Phospho (S; T; Y) Count	Phospho (S; T; Y) Positions	UniProt/BioGrid known Psites	Known kinases	BioGrid Predicted protein kinases
Q07629	Uncharacterized membrane protein YDL218W [OS=Saccharomyces cerevisiae S288C]	HD	15	Phospho [T219; S220; S266; S272; Y279; S280; T281; S284; S288; Y289; T294; S299; S303; S305; T306]	5	Phospho [S272; S288; S303; S305; T306]	None	N/A	N/A
P38682	ADP-ribosylation factor GTPase-activating protein GLO3 [OS=Saccharomyces cerevisiae S288C]	HD	12	Phospho [S164; T165; S166; S281; S282; S283; T284; S306; T312; S389; S390; S398]	2	Phospho [S389; S390]	S2; T165; S166; S170; S183; S185; S216; T278; S282; S306; T324; S389; S390; S398; S419	None	S2 - CKA2; S216 CLA4; T278 - HRR25; S389 - RAD53 and CKA2; S390 - PKA and CKA2; S398 - PKA;
P08456	CDP-diacylglycerol--serine O-phosphatidyltransferase [OS=Saccharomyces cerevisiae S288C]	HD	7	Phospho [Y32; S34; T40; S42; S46; S47; S50]	1	Phospho [S34]	S4; Y32; S34; T40; S42; S46; S47; S50; T53; T54	S46 and S47 - TPK1	None
P40517	Ran-specific GTPase-activating protein 2 [OS=Saccharomyces cerevisiae S288C]	HD	8	Phospho [T123; T124; S125; T126; S128; T170; S179; S181]	3	Phospho [T124; S125; T126]	S14; T19; T31; T123; S125; T126; S179; S181	S14 - RAD53; T31 - CDC28	T19 - CK2; T123 - CKA2; S179 - CKA2/CK2
P40075	Vesicle-associated membrane protein-associated protein SCS2 [OS=Saccharomyces cerevisiae S288C]	HD	2	Phospho [T200; T204]			S2; S106; T145; S153; T200; S201; S203; T204	T204 - CDC28 and CLB2	S2 - CKA2; S106 - CKA2/CK2; T145 - KIC1; T200 - CKA2; S203 - CHK1
P38079	protein YRO2 [OS=Saccharomyces cerevisiae S288C]	HD	4	Phospho [S301; S302; T341; S343]	1	Phospho [S343]	S290; S293; S296; S297; S299; S301; S302; T341; S343	None	S290 - PKA and CDC28; S302 - PLK; T341 - CKA2 (CK2);
Q12236	Serine/threonine-protein kinase PKH2 [OS=Saccharomyces cerevisiae S288C]	HD	11	Phospho [S49; T50; S51; T608; S609; S610; T987; S988; S990; S992; S1009]			S8; S10; S49; T50; S51; T74; S138; S346; T352; T560; S619; S641; T684; S975; T987; S988; S990; S992; S1001; S1009; S1011; S1013; S1016; S1019; S1022	None	S1009 - PKD; S1011 - IPL1; S1013 - CK1 and CK2; S1019 - IPL1 and CK1; S1022 - CK1
Q02724	Ubiquitin-like-specific protease 1 [OS=Saccharomyces cerevisiae S288C]	HD	4	Phospho [S119; S124; S127; S131]			S21; S25; S48; S119; S124; T179; T182; S183; S264; Y551	S21 - CDC28; S25 - CDC28	None
P04821	Cell division control protein 25 [OS=Saccharomyces cerevisiae S288C]	HD	5	Phospho [S150; S151; S154; S596; T597]			S77; S135; S142; S151; S154; S174; S423; S580; S590; S596; S598; T599; S629; S632; T635; T638; S639; S643; S649; S651; S745; S746; S772; S825; S826; S965; T967; S1282; S1585	S77, S135, S142, S151, S174, S825, and S826 under TPK1	S629 - CLA4; T638 - PHO85; S965 - SNF1; T967 - CK2
P11792	serine/threonine-protein kinase SCH9 [OS=Saccharomyces cerevisiae S288C]	HD	3	Phospho [S288; S289; S290]	3	Phospho [S288; S289; S290]	S160; S163; S288; S289; S290; T466; T568; T570; Y577; S711; T723; S726; T737; S758; S765; S801; S803	T570 - PKH (PKH1); S711, T723, S726, T737, S758, and S765 under TOR1;	None
Q04636	FACT complex subunit pob3 [OS=Saccharomyces cerevisiae S288C]	HD	2	Phospho [S194; S195]			S194; S195	None	None
P41810	Coatomer subunit beta [OS=Saccharomyces cerevisiae S288C]	HD	2	Phospho [T563; T570]			S181; S540; T895	None	None
Q08831	Protein VTS1 [OS=Saccharomyces cerevisiae S288C]	HD	4	Phospho [S309; S311; S318; S319]	2	Phospho [S309; S311]	S30; S33; S34; T135; S137; S309; S311; S318; S319;	None	S311 - CAMK2
Q12361	G protein-coupled receptor GPR1 [OS=Saccharomyces cerevisiae S288C]	HD	3	Phospho [T369; T371; S373]	2	Phospho [T369; S373]	T368; T371; S903	None	T369 - PKC1; S903 - PLK
P36010	Nucleoside diphosphate kinase [OS=Saccharomyces cerevisiae S288C]	LD	4	Phospho [T95; T104; S121; S123]	2	Phospho [S121; S123]	T95	None	None

Table S2. Novel phosphosites found in *tor1* mutant *Saccharomyces cerevisiae*, and associated kinases – day 0 HD CR/non-CR

			All phoshosites found		Phosphosites found in respective sample		Psites in literature		
Accession	Description	Found in day 0 HD	Phospho (S; T; Y) Count	Phospho (S; T; Y) Positions	Phospho (S; T; Y) Count	Phospho (S; T; Y) Positions	UniProt/BioGrid known Psites	Known kinases	BioGrid Predicted protein kinases
Q03695	uncharacterized protein YMR206W [OS=Saccharomyces cerevisiae S288C]	CR	5	Phospho [S77; S168; Y169; S221; S229]	1	Phospho [S168]	None	N/A	None
Q06150	Protein BOP2 [OS=Saccharomyces cerevisiae S288C]	CR	2	Phospho [S381; S383]	1	Phospho [S383]	T379; S383	None	None
P34230	Peroxisomal long-chain fatty acid import protein 1 [OS=Saccharomyces cerevisiae S288C]	CR	1	Phospho [S632]	1	Phospho [S632]	None	N/A	None
P41810	Coatomer subunit beta [OS=Saccharomyces cerevisiae S288C]	CR	2	Phospho [T563; T570]			S181; S540; T895	None	None
P10592	Heat shock protein SSA2 [OS=Saccharomyces cerevisiae S288C]	non-CR	3	Phospho [T492; S495; T499]	1	Phospho [T492]	T12; S14; S20; T35; T36; T45; S426; S545; T549; S551	None	T35 - CDC28; S545 - CK1; T549 - AURORA and ALK1/2
P36010	Nucleoside diphosphate kinase [OS=Saccharomyces cerevisiae S288C]	non-CR	4	Phospho [T95; T104; S121; S123]	2	Phospho [T95; T104]	T95	None	None
P37303	Low specificity L-threonine aldolase [OS=Saccharomyces cerevisiae S288C]	non-CR	3	Phospho [S367; S369; T370]	2	Phospho [S367; S369]	S367; S369; T370	S369 - RTK1	None
P41948	ammonium transporter MEP2 [OS=Saccharomyces cerevisiae S288C]	non-CR	4	Phospho [S490; S491; T492; T495]	4	Phospho [S490; S491; T492; T495]	T459; S484; S487; S490; S491	None	None
P31244	DNA repair protein RAD16 [OS=Saccharomyces cerevisiae S288C]	non-CR	2	Phospho [S25; S109]	2	Phospho [S25; S109]	S18; S25; S49; S109; T217; T220	None	S18 - CLA4; S49 - CK2; T217 and T220 under SNF1
Q06631	protein BFR2 [OS=Saccharomyces cerevisiae S288C]	non-CR	1	Phospho [S379]	1	Phospho [S379]	S4; S10; S30; S41; S44; Y46; T54; S366; S372; S379	None	S41 - CKA2; S44 - CK1 and CKA2; S366 - HOG1; S372 - CKA2
P32571	Ubiquitin carboxyl-terminal hydrolase 4 [OS=Saccharomyces cerevisiae S288C]	non-CR	4	Phospho [T413; S414; T500; T502]	2	Phospho [T413; S414]	S414; S443; S498; T502; S646	None	S646 - PKC1
P46995	Histone-lysine N-methyltransferase, H3 lysine-36 specific [OS=Saccharomyces cerevisiae S288C]	non-CR	4	Phospho [S522; S524; S525; S526]	4	Phospho [S522; S524; S525; S526]	S2; S6; S8; S10; S516; S522	None	S2 - RIM11; S10 - CK2; S516 - SNF1
P32486	beta-glucan synthesis-associated protein KRE6 [OS=Saccharomyces cerevisiae S288C]	non-CR	2	Phospho [S134; S136]	2	Phospho [S134; S136]	S69; S73; Y76; S81; S83; S84; S90; S95; S116; T117; S122; S133; S134; S136; S139; Y155; S160; S164	None	S133 - SNF1
P22336	Replication factor A protein 1 [OS=Saccharomyces cerevisiae S288C]	non-CR	1	Phospho [S178]	1	Phospho [S178]	S160; S178	S178 under MEC1 and TEL1	None
P39928	osmosensing histidine protein kinase SLN1 [OS=Saccharomyces cerevisiae S288C]	non-CR	1	Phospho [S833]	1	Phospho [S833]	S118; S469; S473; S483; S502; H576; S758; T766; S767; S770; S775; S833; S962; S980; S981; S1041; S1044	None	T766 and S767 - CK1; S833 - CK2
P53009	Protein kinase-like protein SCY1 [OS=Saccharomyces cerevisiae S288C]	non-CR	1	Phospho [S704]	1	Phospho [S704]	S704; S791; S792	None	S704 - CDC28
P39016	Suppressor protein MPT5 [OS=Saccharomyces cerevisiae S288C]	non-CR	1	Phospho [S176]	1	Phospho [S176]	S138; S139; S148; S150; S156; S176; S662; S672; S674; S675; T677; T756; S820; S834; S838	None	None
P48563	Protein MON2 [OS=Saccharomyces cerevisiae S288C]	non-CR	5	Phospho [S566; S567; T569; T570; S571]	5	Phospho [S566; S567; T569; T570; S571]	S564; T565; S566; S567; T569; S571; S1231	None	S564 - YPK2; S571 - CK1/CK2; S1231 - CDC28
Q01477	Ubiquitin carboxyl-terminal hydrolase 3 [OS=Saccharomyces cerevisiae S288C]	non-CR	1	Phospho [S400]	1	Phospho [S400]	S242; S243; S329; T337; S339; S341; S360; S398; S400; S404	S339 - PTK1; S400 - SNF1	S398 - SNF1

Table S3.1. Novel phosphosites found in *tor1* mutant *Saccharomyces cerevisiae* - day 1 HD CR

			All phoshosites found		Phosphosites found in respective sample	
Accession	Description	Found in day 1 - HD:	Phospho (S; T; Y) Count	Phospho (S; T; Y) Positions	Phospho (S; T; Y) Count	Phospho (S; T; Y) Positions
Q12136	Something about silencing protein 10 [OS=Saccharomyces cerevisiae S288C]	CR	5	Phospho [S336; S339; Y475; S477; S483]	1	Phospho [S477]
P25635	Periodic tryptophan protein 2 [OS=Saccharomyces cerevisiae S288C]	CR	1	Phospho [S232]	1	Phospho [S232]
P53830	Cold sensitive U2 snRNA suppressor 2 [OS=Saccharomyces cerevisiae S288C]	CR	1	Phospho [S163]	1	Phospho [S163]
P53104	Serine/threonine-protein kinase ATG1 [OS=Saccharomyces cerevisiae S288C]	CR	2	Phospho [S647; T656]		
P53335	Protein PXR1 [OS=Saccharomyces cerevisiae S288C]	CR	3	Phospho [S227; S228; S230]	3	Phospho [S227; S228; S230]
P07149	Fatty acid synthase subunit beta [OS=Saccharomyces cerevisiae S288C]	CR	1	Phospho [S1121]		
P38996	Nuclear polyadenylated RNA-binding protein 3 [OS=Saccharomyces cerevisiae S288C]	CR	1	Phospho [T86]	1	Phospho [T86]
P34761	protein WHI3 [OS=Saccharomyces cerevisiae S288C]	CR	2	Phospho [S36; S37]	2	Phospho [S36; S37]
P40457	Protein MLP2 [OS=Saccharomyces cerevisiae S288C]	CR	1	Phospho [S1670]	1	Phospho [S1670]
Q06338	protein BCP1 [OS=Saccharomyces cerevisiae S288C]	CR	2	Phospho [T205; T209]	1	Phospho [T205]
P32643	Trans-aconitate 3-methyltransferase [OS=Saccharomyces cerevisiae S288C]	CR	2	Phospho [S84; T87]	1	Phospho [S84]
P27796	3-ketoacyl-CoA thiolase, peroxisomal [OS=Saccharomyces cerevisiae S288C]	CR	2	Phospho [S169; S170]	2	Phospho [S169; S170]
P33300	mannosyl phosphorylinositol ceramide synthase SUR1 [OS=Saccharomyces cerevisiae S288C]	CR	1	Phospho [S349]	1	Phospho [S349]
Q07528	Autophagy-related protein 20 [OS=Saccharomyces cerevisiae S288C]	CR	2	Phospho [S361; S363]	2	Phospho [S361; S363]
P53836	CCR4-NOT transcriptional complex subunit CAF120 [OS=Saccharomyces cerevisiae S288C]	CR	5	Phospho [S491; S492; S493; S494; S501]	1	Phospho [S494]

Table S3.2. Novel phosphosites found in *tor1* mutant *Saccharomyces cerevisiae* - day 1 HD non-CR

			All phoshosites found		Phosphosites found in respective sample	
Accession	Description	Found in day 1 - HD:	Phospho (S; T; Y) Count	Phospho (S; T; Y) Positions	Phospho (S; T; Y) Count	Phospho (S; T; Y) Positions
P47096	3-hydroxyanthranilate 3,4-dioxygenase [OS=Saccharomyces cerevisiae S288C]	non-CR	1	Phospho [S176]	1	Phospho [S176]
P40075	Vesicle-associated membrane protein-associated protein SCS2 [OS=Saccharomyces cerevisiae S288C]	non-CR	2	Phospho [T200; T204]	1	Phospho [T204]
P37303	Low specificity L-threonine aldolase [OS=Saccharomyces cerevisiae S288C]	non-CR	3	Phospho [S367; S369; T370]		
P46995	Histone-lysine N-methyltransferase, H3 lysine-36 specific [OS=Saccharomyces cerevisiae S288C]	non-CR	4	Phospho [S522; S524; S525; S526]	2	Phospho [S522; S526]
P39016	Suppressor protein MPT5 [OS=Saccharomyces cerevisiae S288C]	non-CR	1	Phospho [S176]	1	Phospho [S176]
P10863	Cold shock-induced protein TIR1 [OS=Saccharomyces cerevisiae S288C]	non-CR	3	Phospho [S116; S120; S121]	3	Phospho [S116; S120; S121]
P41913	Protein gds1 [OS=Saccharomyces cerevisiae S288C]	non-CR	2	Phospho [S386; S388]	2	Phospho [S386; S388]
P38713	Oxysterol-binding protein homolog 3 [OS=Saccharomyces cerevisiae S288C]	non-CR	2	Phospho [T445; S446]	2	Phospho [T445; S446]
P40543	Uncharacterized protein YIL024C [OS=Saccharomyces cerevisiae S288C]	non-CR	2	Phospho [S107; T110]	2	Phospho [S107; T110]
P40449	Uncharacterized protein YIL161W [OS=Saccharomyces cerevisiae S288C]	non-CR	1	Phospho [T25]		
P32896	Protein PDC2 [OS=Saccharomyces cerevisiae S288C]	non-CR	3	Phospho [S679; S684; T685]		
P07213	Mitochondrial import receptor subunit TOM70 [OS=Saccharomyces cerevisiae S288C]	non-CR	3	Phospho [S77; S78; S85]	3	Phospho [S77; S78; S85]
P40028	Holliday junction resolvase YEN1 [OS=Saccharomyces cerevisiae S288C]	non-CR	1	Phospho [S239]	1	Phospho [S239]
Q03361	Uncharacterized protein JIP4 [OS=Saccharomyces cerevisiae S288C]	non-CR	1	Phospho [S708]	1	Phospho [S708]
P53971	FKBP12-associated protein 1 [OS=Saccharomyces cerevisiae S288C]	non-CR	1	Phospho [S958]		
P11484	Ribosome-associated molecular chaperone SSB1 [OS=Saccharomyces cerevisiae S288C]	non-CR	4	Phospho [T441; S508; S515; S516]	2	Phospho [S515; S516]
P22216	Serine/threonine-protein kinase RAD53 [OS=Saccharomyces cerevisiae S288C]	non-CR	3	Phospho [S175; S181; S774]	1	Phospho [S175]

Table S4. Novel phosphosites found in *tor1* mutant *Saccharomyces cerevisiae* - day 1 CR HD/LD

			All phoshosites found		Phosphosites found in respective sample	
Accession	Description	Found in day 1 CR:	Phospho (S; T; Y) Count	Phospho (S; T; Y) Positions	Phospho (S; T; Y) Count	Phospho (S; T; Y) Positions
Q06485	Autophagy-related protein 33 [OS=Saccharomyces cerevisiae S288C]	HD	3	Phospho [S124; S127; S129]	2	Phospho [S127; S129]
P16550	Protein APA1 [OS=Saccharomyces cerevisiae S288C]	HD	1	Phospho [T60]	1	Phospho [T60]
P23201	Protein SPA2 [OS=Saccharomyces cerevisiae S288C]	HD	7	Phospho [S254; S599; S605; S606; S607; S986; S988]	5	Phospho [S254; S606; S607; S986; S988]
P22148	Protein MSN1 [OS=Saccharomyces cerevisiae S288C]	HD	1	Phospho [S238]		
P32862	Glucose transport transcription regulator RGT1 [OS=Saccharomyces cerevisiae S288C]	HD	12	Phospho [S202; S454; T456; T457; S464; S465; S468; S599; S601; T1129; S1130; T1135]	2	Phospho [S202; S599]
P32660	Phospholipid-transporting ATPase DNF1 [OS=Saccharomyces cerevisiae S288C]	HD	7	Phospho [S92; T94; S1506; Y1544; T1551; S1552; T1559]	3	Phospho [T1551; S1552; T1559]
P25628	sterol O-acyltransferase 1 [OS=Saccharomyces cerevisiae S288C]	HD	2	Phospho [S21; S45]	1	Phospho [S21]
P43565	Serine/threonine-protein kinase RIM15 [OS=Saccharomyces cerevisiae S288C]	HD	6	Phospho [S709; S711; S733; S736; S1554; S1557]	1	Phospho [S709]
P38266	Altered inheritance of mitochondria protein 3 [OS=Saccharomyces cerevisiae S288C]	HD	4	Phospho [S843; S847; Y914; S915]	2	Phospho [Y914; S915]
P25568	Autophagy-related protein 22 [OS=Saccharomyces cerevisiae S288C]	HD	2	Phospho [S281; Y283]	2	Phospho [S281; Y283]
P32190	glycerol kinase [OS=Saccharomyces cerevisiae S288C]	HD	2	Phospho [S96; T97]	2	Phospho [S96; T97]
P38628	phosphoacetylglucosamine mutase [OS=Saccharomyces cerevisiae S288C]	HD	3	Phospho [T65; S67; Y71]	2	Phospho [T65; S67]
P53830	Cold sensitive U2 snRNA suppressor 2 [OS=Saccharomyces cerevisiae S288C]	HD	1	Phospho [S163]	1	Phospho [S163]
P53104	Serine/threonine-protein kinase ATG1 [OS=Saccharomyces cerevisiae S288C]	HD	2	Phospho [S647; T656]		
P40457	Protein MLP2 [OS=Saccharomyces cerevisiae S288C]	HD	1	Phospho [S1670]	1	Phospho [S1670]
P33300	mannosyl phosphorylinositol ceramide synthase SUR1 [OS=Saccharomyces cerevisiae S288C]	HD	1	Phospho [S349]	1	Phospho [S349]
Q02799	zinc finger protein LEE1 [OS=Saccharomyces cerevisiae S288C]	HD	3	Phospho [S21; S23; S282]	2	Phospho [S21; S23]
Q06144	Protein ORM2 [OS=Saccharomyces cerevisiae S288C]	HD	4	Phospho [T5; S9; S15; T18]	4	Phospho [T5; S9; S15; T18]
P34909	General negative regulator of transcription subunit 4 [OS=Saccharomyces cerevisiae S288C]	HD	7	Phospho [T370; S374; T379; T380; T383; S542; T543]	6	Phospho [T379; T380; T383; T399; S542; T543]
Q02642	Nascent polypeptide-associated complex subunit beta-1 [OS=Saccharomyces cerevisiae S288C]	HD	1	Phospho [T151]	1	Phospho [T151]
P51601	GTP cyclohydrolase 1 [OS=Saccharomyces cerevisiae S288C]	HD	4	Phospho [T22; S23; Y25; T26]	3	Phospho [T22; S23; Y25]
P38355	uncharacterized transporter YBR287W [OS=Saccharomyces cerevisiae S288C]	HD	1	Phospho [T199]		
Q12265	Ribose-phosphate pyrophosphokinase 5 [OS=Saccharomyces cerevisiae S288C]	HD	8	Phospho [Y119; T120; S123; T127; S130; S131; S132; T135]	1	Phospho [T127]
P53191	Phosphatidylinositol 3-phosphate-binding protein 2 [OS=Saccharomyces cerevisiae S288C]	HD	1	Phospho [S300]	1	Phospho [S300]
P33298	26S proteasome regulatory subunit 6B homolog [OS=Saccharomyces cerevisiae S288C]	HD	1	Phospho [T8]	1	Phospho [T8]
Q12006	palmitoyltransferase PFA4 [OS=Saccharomyces cerevisiae S288C]	HD	1	Phospho [S339]	1	Phospho [S339]
P38352	SCF-associated factor 1 [OS=Saccharomyces cerevisiae S288C]	HD	8	Phospho [S266; S268; S271; T272; Y274; T281; T286; S289]	5	Phospho [S266; S268; S271; T272; T286]
P38825	Protein TOM71 [OS=Saccharomyces cerevisiae S288C]	HD	1	Phospho [S55]	1	Phospho [S55]
Q00362	Protein phosphatase PP2A regulatory subunit B [OS=Saccharomyces cerevisiae S288C]	HD	2	Phospho [S401; S403]	2	Phospho [S401; S403]
P38994	Probable phosphatidylinositol 4-phosphate 5-kinase MSS4 [OS=Saccharomyces cerevisiae S288C]	HD	2	Phospho [T659; S661]	2	Phospho [T659; S661]
P53962	Uncharacterized WD repeat-containing protein YNL035C [OS=Saccharomyces cerevisiae S288C]	HD	1	Phospho [S351]	1	Phospho [S351]
P32916	Signal recognition particle receptor subunit alpha homolog [OS=Saccharomyces cerevisiae S288C]	HD	6	Phospho [S231; S232; S233; S235; S238; S239]	2	Phospho [S238; S239]
Q08484	GTPase-activating protein gyp1 [OS=Saccharomyces cerevisiae S288C]	HD	4	Phospho [S212; S213; S214; S215]	4	Phospho [S212; S213; S214; S215]
P40529	ADP-ribosylation factor GTPase-activating protein effector protein 2 [OS=Saccharomyces cerevisiae S288C]	HD	5	Phospho [S159; S162; S178; S180; T182]	2	Phospho [S180; T182]
Q06636	Glycosylphosphatidylinositol anchor biosynthesis protein 11 [OS=Saccharomyces cerevisiae S288C]	HD	3	Phospho [T14; S16; S18]	3	Phospho [T14; S16; S18]
P07703	DNA-directed RNA polymerases I and III subunit RPAC1 [OS=Saccharomyces cerevisiae S288C]	HD	2	Phospho [S17; T18]	2	Phospho [S17; T18]
P47096	3-hydroxyanthranilate 3,4-dioxygenase [OS=Saccharomyces cerevisiae S288C]	LD	1	Phospho [S176]	1	Phospho [S176]
P20459	eukaryotic translation initiation factor 2 subunit alpha [OS=Saccharomyces cerevisiae S288C]	LD	3	Phospho [S292; S294; S301]	1	Phospho [S292]
Q07825	Putative Xaa-Pro aminopeptidase FRA1 [OS=Saccharomyces cerevisiae S288C]	LD	2	Phospho [S92; S95]	2	Phospho [S92; S95]
P32497	Eukaryotic translation initiation factor 3 subunit C [OS=Saccharomyces cerevisiae S288C]	LD	4	Phospho [Y96; S98; S99; S103]	2	Phospho [S98; S103]
P38219	obg-like ATPase 1 [OS=Saccharomyces cerevisiae S288C]	LD	1	Phospho [S116]	1	Phospho [S116]

Table S5. Novel phosphosites found in *tor1* mutant *Saccharomyces cerevisiae* - day 2 HD CR/non-CR

			All phoshosites found		Phosphosites found in respective sample	
Accession	Description	Found in day 2 HD:	Phospho (S; T; Y) Count	Phospho (S; T; Y) Positions	Phospho (S; T; Y) Count	Phospho (S; T; Y) Positions
P25613	Accumulation of dyads protein 2 [OS=Saccharomyces cerevisiae S288C]	CR	3	Phospho [Y46; T47; Y54]	2	Phospho [Y46; T47]
Q06150	Protein BOP2 [OS=Saccharomyces cerevisiae S288C]	CR	2	Phospho [S381; S383]	2	Phospho [S381; S383]
P04801	Threonine--tRNA ligase, cytoplasmic [OS=Saccharomyces cerevisiae S288C]	CR	3	Phospho [S201; S288; S289]	2	Phospho [S288; S289]
P14180	Chitin synthase 2 [OS=Saccharomyces cerevisiae S288C]	CR	2	Phospho [S462; T473]	2	Phospho [S462; T473]
P40570	Putative uncharacterized protein YIR014W [OS=Saccharomyces cerevisiae S288C]	CR	1	Phospho [S78]	1	Phospho [S78]
Q12499	Nucleolar protein 58 [OS=Saccharomyces cerevisiae S288C]	CR	3	Phospho [S440; S442; S444]	3	Phospho [S440; S442; S444]
P40453	Ubiquitin carboxyl-terminal hydrolase 7 [OS=Saccharomyces cerevisiae S288C]	non-CR	1	Phospho [S193]	1	Phospho [S193]
P32862	Glucose transport transcription regulator RGT1 [OS=Saccharomyces cerevisiae S288C]	non-CR	12	Phospho [S202; S454; T456; T457; S464; S465; S468; S599; S601; T1129; S1130; T1135]	3	Phospho [S465; S599; S601]
P53104	Serine/threonine-protein kinase ATG1 [OS=Saccharomyces cerevisiae S288C]	non-CR	2	Phospho [S647; T656]	2	Phospho [S647; T656]
Q02799	zinc finger protein LEE1 [OS=Saccharomyces cerevisiae S288C]	non-CR	3	Phospho [S21; S23; S282]	3	Phospho [S21; S23; S282]
P34909	General negative regulator of transcription subunit 4 [OS=Saccharomyces cerevisiae S288C]	non-CR	7	Phospho [T370; S374; T379; T380; T383; S542; T543]	3	Phospho [T370; S374; T379]
P38355	uncharacterized transporter YBR287W [OS=Saccharomyces cerevisiae S288C]	non-CR	1	Phospho [T199]	1	Phospho [T199]
P31380	ATP-dependent helicase FUN30 [OS=Saccharomyces cerevisiae S288C]	non-CR	2	Phospho [T450; S451]	2	Phospho [T450; S451]
P47096	3-hydroxyanthranilate 3,4-dioxygenase [OS=Saccharomyces cerevisiae S288C]	non-CR	1	Phospho [S176]	1	Phospho [S176]
P46995	Histone-lysine N-methyltransferase, H3 lysine-36 specific [OS=Saccharomyces cerevisiae S288C]	non-CR	4	Phospho [S522; S524; S525; S526]	3	Phospho [S522; S524; S525]
P39016	Suppressor protein MPT5 [OS=Saccharomyces cerevisiae S288C]	non-CR	1	Phospho [S176]	1	Phospho [S176]
P40449	Uncharacterized protein YIL161W [OS=Saccharomyces cerevisiae S288C]	non-CR	1	Phospho [T25]	1	Phospho [T25]
P32896	Protein PDC2 [OS=Saccharomyces cerevisiae S288C]	non-CR	3	Phospho [S679; S684; T685]	3	Phospho [S679; S684; T685]
P07213	Mitochondrial import receptor subunit TOM70 [OS=Saccharomyces cerevisiae S288C]	non-CR	3	Phospho [S77; S78; S85]	2	Phospho [S77; S78]
Q12513	Translation machinery-associated protein 17 [OS=Saccharomyces cerevisiae S288C]	non-CR	1	Phospho [S68]	1	Phospho [S68]
P05986	cAMP-dependent protein kinase type 3 [OS=Saccharomyces cerevisiae S288C]	non-CR	7	Phospho [T20; T23; S44; T46; T240; Y241; T242]	7	Phospho [T20; T23; S44; T46; T240; Y241; T242]
P36053	transcription elongation factor 1 [OS=Saccharomyces cerevisiae S288C]	non-CR	2	Phospho [S117; S124]	3	Phospho [S117; S124; S142]
P40344	Autophagy-related protein 3 [OS=Saccharomyces cerevisiae S288C]	non-CR	1	Phospho [S111]	1	Phospho [S111]
P40056	Golgi to ER traffic protein 2 [OS=Saccharomyces cerevisiae S288C]	non-CR	2	Phospho [T56; T65]	2	Phospho [T56; T65]
Q06511	Ribosomal RNA-processing protein 15 [OS=Saccharomyces cerevisiae S288C]	non-CR	1	Phospho [S69]	1	Phospho [S69]
Q92331	Vacuolar protein sorting-associated protein 5 [OS=Saccharomyces cerevisiae S288C]	non-CR	5	Phospho [S142; T145; S146; S251; S252]	5	Phospho [S142; T145; S146; S251; S252]
Q06820	mitochondrial distribution and morphology protein 36 [OS=Saccharomyces cerevisiae S288C]	non-CR	3	Phospho [S42; S137; S141]	3	Phospho [S42; S137; S141]
P38695	Probable glucose transporter HXT5 [OS=Saccharomyces cerevisiae S288C]	non-CR	2	Phospho [S51; S52]	2	Phospho [S51; S52]
P33441	THO complex subunit MFT1 [OS=Saccharomyces cerevisiae S288C]	non-CR	1	Phospho [S266]	2	Phospho [Y264; S266]
P18851	Guanine nucleotide-binding protein subunit beta [OS=Saccharomyces cerevisiae S288C]	non-CR	4	Phospho [Y314; T318; T320; Y323]	4	Phospho [Y314; T318; T320; Y323]

Table S5. Novel phosphosites found in *tor1* mutant *Saccharomyces cerevisiae* - day 2 HD CR/non-CR (continued 1/2)

			All phoshosites found		Phosphosites found in respective sample	
Accession	Description	Found in day 2 HD:	Phospho (S; T; Y) Count	Phospho (S; T; Y) Positions	Phospho (S; T; Y) Count	Phospho (S; T; Y) Positions
Q12395	Defective in cullin neddylation protein 1 [OS=Saccharomyces cerevisiae S288C]	non-CR	1	Phospho [S12]	1	Phospho [S12]
Q12446	Proline-rich protein LAS17 [OS=Saccharomyces cerevisiae S288C]	non-CR	3	Phospho [S586; S588; T598]	2	Phospho [S586; S588]
Q06247	putative uncharacterized protein YLR173W [OS=Saccharomyces cerevisiae S288C]	non-CR	2	Phospho [T24; S27]	2	Phospho [T24; S27]
P38890	putative protein lysine methyltransferase set5 [OS=Saccharomyces cerevisiae S288C]	non-CR	2	Phospho [S458; S461]	2	Phospho [S458; S461]
Q12481	rRNA biogenesis protein rrp36 [OS=Saccharomyces cerevisiae S288C]	non-CR	2	Phospho [S41; S42]	2	Phospho [S41; S42]
P47030	Protein TAX4 [OS=Saccharomyces cerevisiae S288C]	non-CR	2	Phospho [S114; S117]	2	Phospho [S114; S117]
P53197	APC/C activator protein CDH1 [OS=Saccharomyces cerevisiae S288C]	non-CR	5	Phospho [S156; T157; S169; S172; T173]	5	Phospho [S156; T157; S169; S172; T173]
P38810	SED5-binding protein 3 [OS=Saccharomyces cerevisiae S288C]	non-CR	1	Phospho [T48]	1	Phospho [T48]
Q08979	Kelch repeat-containing protein 3 [OS=Saccharomyces cerevisiae S288C]	non-CR	1	Phospho [S47]	1	Phospho [S47]
P53114	Mediator of RNA polymerase II transcription subunit 5 [OS=Saccharomyces cerevisiae S288C]	non-CR	6	Phospho [S257; S259; T261; S262; S268; T273]	6	Phospho [S257; S259; T261; S262; S268; T273]
P46944	Trafficking protein particle complex III-specific subunit 85 [OS=Saccharomyces cerevisiae S288C]	non-CR	3	Phospho [S95; T96; S98]	3	Phospho [S95; T96; S98]
Q03388	Vacuolar protein sorting-associated protein 72 [OS=Saccharomyces cerevisiae S288C]	non-CR	1	Phospho [S396]	1	Phospho [S396]
P53978	Elongation factor 3B [OS=Saccharomyces cerevisiae S288C]	non-CR	2	Phospho [S1039; S1040]	2	Phospho [S1039; S1040]
P43609	Chromatin structure-remodeling complex protein RSC8 [OS=Saccharomyces cerevisiae S288C]	non-CR	2	Phospho [S379; S383]	2	Phospho [S379; S383]
P48365	GTPase-activating protein GYP7 [OS=Saccharomyces cerevisiae S288C]	non-CR	1	Phospho [S265]	1	Phospho [S265]
P53091	DNA replication licensing factor MCM6 [OS=Saccharomyces cerevisiae S288C]	non-CR	2	Phospho [S1016; S1017]	2	Phospho [S1016; S1017]

Table S5. Novel phosphosites found in *tor1* mutant *Saccharomyces cerevisiae* - day 2 HD CR/non-CR (continued 2/2)

			All phoshosites found		Phosphosites found in respective sample	
Accession	Description	Found in day 2 HD:	Phospho (S; T; Y) Count	Phospho (S; T; Y) Positions	Phospho (S; T; Y) Count	Phospho (S; T; Y) Positions
Q08773	iswi chromatin-remodeling complex atpase isw2 [OS=Saccharomyces cerevisiae S288C]	non-CR	1	Phospho [S831]	1	Phospho [S831]
P23255	Transcription initiation factor TFIID subunit 2 [OS=Saccharomyces cerevisiae S288C]	non-CR	1	Phospho [S318]	1	Phospho [S318]
P32333	TATA-binding protein-associated factor MOT1 [OS=Saccharomyces cerevisiae S288C]	non-CR	1	Phospho [S93]	1	Phospho [S93]
Q05022	rRNA biogenesis protein RRP5 [OS=Saccharomyces cerevisiae S288C]	non-CR	3	Phospho [Y185; S187; S188]	3	Phospho [Y185; S187; S188]
Q04958	Lysophospholipase NTE1 [OS=Saccharomyces cerevisiae S288C]	non-CR	2	Phospho [S632; S634]	2	Phospho [S632; S634]
P41948	ammonium transporter MEP2 [OS=Saccharomyces cerevisiae S288C]	non-CR	4	Phospho [S490; S491; T492; T495]	2	Phospho [S491; T492]
P53852	Cysteine--tRNA ligase [OS=Saccharomyces cerevisiae S288C]	non-CR	1	Phospho [S326]	1	Phospho [S326]
P49573	Copper transport protein CTR1 [OS=Saccharomyces cerevisiae S288C]	non-CR	1	Phospho [S344]	1	Phospho [S344]
P37303	Low specificity L-threonine aldolase [OS=Saccharomyces cerevisiae S288C]	non-CR	3	Phospho [S367; S369; T370]	2	Phospho [S367; S369]
P22216	Serine/threonine-protein kinase RAD53 [OS=Saccharomyces cerevisiae S288C]	non-CR	3	Phospho [S175; S181; S774]	2	Phospho [S774; T780]
P40473	Transcriptional activator POG1 [OS=Saccharomyces cerevisiae S288C]	non-CR	3	Phospho [S152; T155; T156]	2	Phospho [S152; T156]
P40489	Transcriptional repressor XBP1 [OS=Saccharomyces cerevisiae S288C]	non-CR	4	Phospho [S498; T500; S501; S502]	3	Phospho [S498; S501; S502]
Q02884	Elongator complex protein 4 [OS=Saccharomyces cerevisiae S288C]	non-CR	1	Phospho [S222]	1	Phospho [S222]
P12383	Transcription factor PDR1 [OS=Saccharomyces cerevisiae S288C]	non-CR	3	Phospho [S939; S942; S948]	3	Phospho [S939; S942; S948]
Q12221	mRNA-binding protein PUF2 [OS=Saccharomyces cerevisiae S288C]	non-CR	2	Phospho [S198; T199]	2	Phospho [S198; T199]
P22336	Replication factor A protein 1 [OS=Saccharomyces cerevisiae S288C]	non-CR	1	Phospho [S178]	1	Phospho [S178]
Q06680	Condensin complex subunit 3 [OS=Saccharomyces cerevisiae S288C]	non-CR	1	Phospho [S198]	1	Phospho [S198]
P32591	SWI/SNF complex subunit SWI3 [OS=Saccharomyces cerevisiae S288C]	non-CR	2	Phospho [S185; T191]	2	Phospho [S185; T191]
P10862	postreplication repair E3 ubiquitin-protein ligase RAD18 [OS=Saccharomyces cerevisiae S288C]	non-CR	1	Phospho [S431]	1	Phospho [S431]
P53940	J domain-containing protein APJ1 [OS=Saccharomyces cerevisiae S288C]	non-CR	4	Phospho [Y513; S514; S515; S518]	3	Phospho [Y513; S514; S515]
Q07351	Zinc finger protein STP4 [OS=Saccharomyces cerevisiae S288C]	non-CR	2	Phospho [S360; S363]	2	Phospho [S360; S363]
P53685	NAD-dependent protein deacetylase hst1 [OS=Saccharomyces cerevisiae S288C]	non-CR	2	Phospho [S137; S138]	2	Phospho [S137; S138]
Q06525	Pre-mRNA-splicing factor URN1 [OS=Saccharomyces cerevisiae S288C]	non-CR	1	Phospho [T453]	1	Phospho [T453]
Q01560	Nucleolar protein 3 [OS=Saccharomyces cerevisiae S288C]	non-CR	2	Phospho [S224; T228]	1	Phospho [S224]
P28000	DNA-directed RNA polymerases I and III subunit RPAC2 [OS=Saccharomyces cerevisiae S288C]	non-CR	1	Phospho [T33]	1	Phospho [T33]
Q04835	Uncharacterized membrane protein YMR253C [OS=Saccharomyces cerevisiae S288C]	non-CR	4	Phospho [S36; S38; S42; S44]	2	Phospho [S38; S42]
P18961	Serine/threonine-protein kinase YPK2/YKR2 [OS=Saccharomyces cerevisiae S288C]	non-CR	4	Phospho [T63; T66; T499; T501]	4	Phospho [T63; T66; T499; T501]

Table S6. Novel phosphosites found in *tor1* mutant *Saccharomyces cerevisiae* - day 2 CR HD/LD

			All phoshosites found		Phosphosites found in respective	
Accession	Description	Found in day 2 CR:	Phospho (S; T; Y) Count	Phospho (S; T; Y) Positions	Phospho (S; T; Y) Count	Phospho (S; T; Y) Positions
P38352	SCF-associated factor 1 [OS=Saccharomyces cerevisiae S288C]	HD	8	Phospho [S266; S268; S271; T272; Y274; T281; T286; S289]	3	Phospho [S266; S268; S271]
P40570	Putative uncharacterized protein YIR014W [OS=Saccharomyces cerevisiae S288C]	HD	1	Phospho [S78]	1	Phospho [S78]
P40453	Ubiquitin carboxyl-terminal hydrolase 7 [OS=Saccharomyces cerevisiae S288C]	LD	1	Phospho [S193]	3	Phospho [S274; Y275; S277]
P31380	ATP-dependent helicase FUN30 [OS=Saccharomyces cerevisiae S288C]	LD	2	Phospho [T450; S451]	1	Phospho [S451]
P47096	3-hydroxyanthranilate 3,4-dioxygenase [OS=Saccharomyces cerevisiae S288C]	LD	1	Phospho [S176]	1	Phospho [S176]
P40473	Transcriptional activator POG1 [OS=Saccharomyces cerevisiae S288C]	LD	3	Phospho [S152; T155; T156]		
P53214	Protein MTL1 [OS=Saccharomyces cerevisiae S288C]	LD	2	Phospho [S494; T496]		

Table S7. Novel phosphosites found in *tor1* mutant *Saccharomyces cerevisiae* - day 5 HD CR/non-CR

			All phoshosites found		Phosphosites found in respective sample	
Accession	Description	Found in day 5 HD:	Phospho (S; T; Y) Count	Phospho (S; T; Y) Positions	Phospho (S; T; Y) Count	Phospho (S; T; Y) Positions
P40187	GSY2-interacting protein PIG2 [OS=Saccharomyces cerevisiae S288C]	CR	5	Phospho [S141; S162; T166; S296; S304]	2	Phospho [S162; T166]
P48510	Ubiquitin domain-containing protein DSK2 [OS=Saccharomyces cerevisiae S288C]	CR	2	Phospho [S357; S360]	2	Phospho [S357; S360]
P0CX29	40S ribosomal protein S23-A [OS=Saccharomyces cerevisiae S288C]	CR	1	Phospho [S128]	1	Phospho [S128]
P20676	nucleoporin NUP1 [OS=Saccharomyces cerevisiae S288C]	CR	2	Phospho [S765; S767]	2	Phospho [S765; S767]
P53830	Cold sensitive U2 snRNA suppressor 2 [OS=Saccharomyces cerevisiae S288C]	CR	1	Phospho [S163]	1	Phospho [S163]
P36143	Glycogenin-1 [OS=Saccharomyces cerevisiae S288C]	CR	4	Phospho [S477; S480; S481; S483]	2	Phospho [S481; S483]
P41818	protein GLC8 [OS=Saccharomyces cerevisiae S288C]	CR	2	Phospho [S12; S184]		
Q12006	palmitoyltransferase PFA4 [OS=Saccharomyces cerevisiae S288C]	CR	1	Phospho [S339]	1	Phospho [S339]
Q03337	Trafficking protein particle complex subunit 31 [OS=Saccharomyces cerevisiae S288C]	CR	2	Phospho [S125; S126]	1	Phospho [S126]
P34233	Transcriptional regulatory protein ASH1 [OS=Saccharomyces cerevisiae S288C]	CR	1	Phospho [S56]	1	Phospho [S56]
P47089	Translation machinery-associated protein 22 [OS=Saccharomyces cerevisiae S288C]	CR	2	Phospho [Y43; T45]	2	Phospho [Y43; T45]
P33419	Spindle pole component 29 [OS=Saccharomyces cerevisiae S288C]	CR	2	Phospho [S189; S191]	2	Phospho [S189; S191]
P40543	Uncharacterized protein YIL024C [OS=Saccharomyces cerevisiae S288C]	non-CR	2	Phospho [S107; T110]	1	Phospho [S107]
Q04183	Trafficking protein particle complex II-specific subunit 120 [OS=Saccharomyces cerevisiae S288C]	non-CR	2	Phospho [S358; S387]	1	Phospho [S387]
P32488	Increasing suppression factor 1 [OS=Saccharomyces cerevisiae S288C]	non-CR	4	Phospho [S119; T121; S276; T280]	1	Phospho [S119]
P38691	Serine/threonine-protein kinase ksp1 [OS=Saccharomyces cerevisiae S288C]	non-CR	1	Phospho [S884]		

Table S8. Novel phosphosites found in *tor1* mutant *Saccharomyces cerevisiae* - day 5 CR HD/LD

			All phoshosites found		Phosphosites found in respective	
Accession	Description	Found in day 5 CR	Phospho (S; T; Y) Count	Phospho (S; T; Y) Positions	Phospho (S; T; Y) Count	Phospho (S; T; Y) Positions
P40453	Ubiquitin carboxyl-terminal hydrolase 7 [OS=Saccharomyces cerevisiae S288C]	HD	1	Phospho [S193]		
P31384	glucose-repressible alcohol dehydrogenase transcriptional effector [OS=Saccharomyces cerevisiae S288C]	HD	6	Phospho [T266; S269; T270; S272; T274; T276]	3	Phospho [S269; T270; S272]
P53236	Chromatin structure-remodeling complex subunit RSC1 [OS=Saccharomyces cerevisiae S288C]	HD	4	Phospho [S655; S656; S670; S672]	2	Phospho [S670; S672]
P48510	Ubiquitin domain-containing protein DSK2 [OS=Saccharomyces cerevisiae S288C]	HD	2	Phospho [S357; S360]	2	Phospho [S357; S360]
P0CX29	40S ribosomal protein S23-A [OS=Saccharomyces cerevisiae S288C]	HD	1	Phospho [S128]	1	Phospho [S128]
P20676	nucleoporin NUP1 [OS=Saccharomyces cerevisiae S288C]	HD	2	Phospho [S765; S767]	2	Phospho [S765; S767]
Q12006	palmitoyltransferase PFA4 [OS=Saccharomyces cerevisiae S288C]	HD	1	Phospho [S339]	1	Phospho [S339]
P47089	Translation machinery-associated protein 22 [OS=Saccharomyces cerevisiae S288C]	HD	2	Phospho [Y43; T45]	2	Phospho [Y43; T45]
P41058	40S ribosomal protein S29-B [OS=Saccharomyces cerevisiae S288C]	HD	1	Phospho [S26]	1	Phospho [S26]
Q03758	Ubiquitin ligase-binding protein BUL2 [OS=Saccharomyces cerevisiae S288C]	HD	3	Phospho [S66; S68; T69]	1	Phospho [S68]
P09959	regulatory protein SWI6 [OS=Saccharomyces cerevisiae S288C]	HD	2	Phospho [S176; S178]	2	Phospho [S176; S178]

Table S9. Novel phosphosites found in *tor1* mutant *Saccharomyces cerevisiae* - day 7 HD CR/non-CR

			All phoshosites found		Phosphosites found in respective sample	
Accession	Description	Found in day 7 HD:	Phospho (S; T; Y) Count	Phospho (S; T; Y) Positions	Phospho (S; T; Y) Count	Phospho (S; T; Y) Positions
P0C2J1	Transposon Ty1-PR3 Gag-Pol polyprotein [OS=Saccharomyces cerevisiae S288C]	CR	13	Phospho [S20; S47; T48; S365; T405; S406; S409; S411; T412; S416; S418; S1093; S1095]		
P53836	CCR4-NOT transcriptional complex subunit CAF120 [OS=Saccharomyces cerevisiae S288C]	CR	5	Phospho [S491; S492; S493; S494; S501]	5	Phospho [S491; S492; S493; S494; S501]
P28834	Isocitrate dehydrogenase [NAD] subunit 1, mitochondrial [OS=Saccharomyces cerevisiae S288C]	CR	2	Phospho [S343; T346]		
P23248	40S ribosomal protein S1-B [OS=Saccharomyces cerevisiae S288C]	CR	1	Phospho [T37]		
Q04214-1	Transposon Ty1-MR1 Gag-Pol polyprotein [OS=Saccharomyces cerevisiae S288C]	CR	8	Phospho [S7; S10; S13; S16; S20; T22; S23; S960]	2	Phospho [S7; S10]
P36010	Nucleoside diphosphate kinase [OS=Saccharomyces cerevisiae S288C]	CR	4	Phospho [T95; T104; S121; S123]		
P24000	60S ribosomal protein L24-B [OS=Saccharomyces cerevisiae S288C]	CR	3	Phospho [S7; S9; S95]		
P53978	Elongation factor 3B [OS=Saccharomyces cerevisiae S288C]	CR	2	Phospho [S1039; S1040]		
P33442	40S ribosomal protein S1-A [OS=Saccharomyces cerevisiae S288C]	CR	1	Phospho [T37]		
P48164	40S ribosomal protein S7-B [OS=Saccharomyces cerevisiae S288C]	CR	1	Phospho [S14]		
P32639	Pre-mRNA-splicing helicase BRR2 [OS=Saccharomyces cerevisiae S288C]	non-CR	1	Phospho [S403]	1	Phospho [S403]
P32660	Phospholipid-transporting ATPase DNF1 [OS=Saccharomyces cerevisiae S288C]	non-CR	7	Phospho [S92; T94; S1506; Y1544; T1551; S1552; T1559]	3	Phospho [S1506; T1551; S1552]
P40543	Uncharacterized protein YIL024C [OS=Saccharomyces cerevisiae S288C]	non-CR	2	Phospho [S107; T110]	2	Phospho [S107; T110]
P32488	Increasing suppression factor 1 [OS=Saccharomyces cerevisiae S288C]	non-CR	4	Phospho [S119; T121; S276; T280]		
P22696	Peptidyl-prolyl cis-trans isomerase ESS1 [OS=Saccharomyces cerevisiae S288C]	non-CR	1	Phospho [S161]	1	Phospho [S161]
Q12057	[PSI+] induction protein 2 [OS=Saccharomyces cerevisiae S288C]	non-CR	2	Phospho [S193; S194]	2	Phospho [S193; S194]
P38352	SCF-associated factor 1 [OS=Saccharomyces cerevisiae S288C]	non-CR	8	Phospho [S266; S268; S271; T272; Y274; T281; T286; S289]	1	Phospho [S266]
P53316	Uncharacterized RNA-binding protein YGR250C [OS=Saccharomyces cerevisiae S288C]	non-CR	9	Phospho [S482; S485; T486; S589; S590; S643; S644; S645; S651]	2	Phospho [S644; S645]
Q06680	Condensin complex subunit 3 [OS=Saccharomyces cerevisiae S288C]	non-CR	1	Phospho [S198]		
P25333	Serine/threonine-protein kinase HAL4/SAT4 [OS=Saccharomyces cerevisiae S288C]	non-CR	1	Phospho [T162]	1	Phospho [T162]
P53214	Protein MTL1 [OS=Saccharomyces cerevisiae S288C]	non-CR	2	Phospho [S494; T496]	1	Phospho [S494]
P34909	General negative regulator of transcription subunit 4 [OS=Saccharomyces cerevisiae S288C]	non-CR	7	Phospho [T370; S374; T379; T380; T383; S542; T543]	2	Phospho [S542; T543]
Q06178	Nicotinamide/nicotinic acid mononucleotide adenylyltransferase 1 [OS=Saccharomyces cerevisiae S288C]	non-CR	1	Phospho [S13]	1	Phospho [S13]
P32849	DNA repair protein RAD5 [OS=Saccharomyces cerevisiae S288C]	non-CR	2	Phospho [S129; S130]	2	Phospho [S129; S130]
P53107	Ran-specific GTPase-activating protein 30 [OS=Saccharomyces cerevisiae S288C]	non-CR	1	Phospho [T272]	1	Phospho [T272]
P38266	Altered inheritance of mitochondria protein 3 [OS=Saccharomyces cerevisiae S288C]	non-CR	4	Phospho [S843; S847; Y914; S915]	2	Phospho [Y914; S915]
P32190	glycerol kinase [OS=Saccharomyces cerevisiae S288C]	non-CR	2	Phospho [S96; T97]	1	Phospho [S96]
Q04233	protein GIS4 [OS=Saccharomyces cerevisiae S288C]	non-CR	3	Phospho [S642; S729; S731]	1	Phospho [S642]
P04821	Cell division control protein 25 [OS=Saccharomyces cerevisiae S288C]	non-CR	5	Phospho [S150; S151; S154; S596; T597]	4	Phospho [S150; S151; S154; S158]
Q02648	tRNA (uracil-O(2)-)-methyltransferase [OS=Saccharomyces cerevisiae S288C]	non-CR	1	Phospho [S107]	1	Phospho [S107]
P53121	Putative flavin carrier protein 3 [OS=Saccharomyces cerevisiae S288C]	non-CR	2	Phospho [S687; T688]	2	Phospho [S687; T688]
Q06407	Rho-type GTPase-activating protein 2 [OS=Saccharomyces cerevisiae S288C]	non-CR	4	Phospho [S141; S142; S770; S772]		

Table S10. Novel phosphosites found in *tor1* mutant *Saccharomyces cerevisiae* - day 7 CR HD/LD

			All phoshosites found		Phosphosites found in respective sample	
Accession	Description	Found in day 7 CR:	Phospho (S; T; Y) Count	Phospho (S; T; Y) Positions	Phospho (S; T; Y) Count	Phospho (S; T; Y) Positions
P04821	Cell division control protein 25 [OS=Saccharomyces cerevisiae S288C]	LD	5	Phospho [S150; S151; S154; S596; T597]	N/A	N/A
P48510	Ubiquitin domain-containing protein DSK2 [OS=Saccharomyces cerevisiae S288C]	LD	2	Phospho [S357; S360]	N/A	N/A
P47025	Mitochondrial division protein 1 [OS=Saccharomyces cerevisiae S288C]	LD	1	Phospho [S376]	N/A	N/A